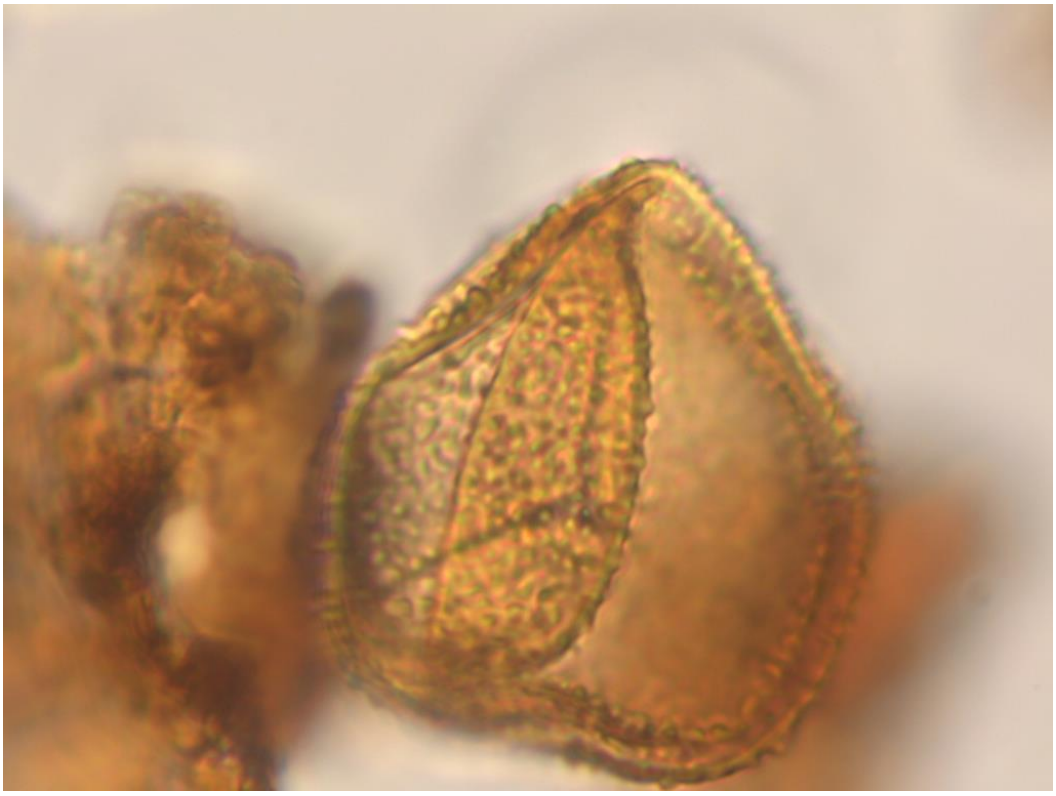

VEGETATION AND MARINE ECOSYSTEM CHANGE

Early Pleistocene in the Netherlands

Lisanne Jeannette Krom
University of Utrecht, in cooperation with TNO

Vegetation and Marine ecosystem change during the Early Pleistocene in the Netherlands

Lisanne Jeanette Krom
4250419

In partial fulfilment of the degree of Master of Science in the Earth Science

Department of Physical Geography
Utrecht University

Supervisors:
Dr. Timme Donders
Dr. Alexander Houben

August 3, 2020

Image on the front page is an Osmunda spore, found multiple times in the Petten BH-1 core

I declare that:

1. This is an original report, which is entirely my own work,
2. where I have made use of the ideas of other writers, I have acknowledged the source in all instances,
3. where I have used any diagram or visuals, I have acknowledged the source in all instances,
4. this report has not and will not be submitted elsewhere for academic assessment in any other academic course.

Student data:

Name: Lisanne Jeanette Krom
Registration number: 4250419
Date: August 3, 2020

Signature:

Preface and Acknowledgements

This thesis about vegetation and marine ecosystem change during the Early Pleistocene in the Netherlands has been written as part of the Master Science degree in Earth Science, programme Marine Science, at Utrecht University. The research was performed under the supervision of Dr. Timme Donders and Dr. Alexander Houben. The aim of the thesis is to reconstruct paleo-environmental changes and to observe the alternation of the terrestrial and marine environment during the Early Pleistocene. The BH-1 core, recovered in Petten (Noord-Holland), is used to make reconstruction of the environment with the use of pollen and dinoflagellate cysts.

The good recovery of the lower part of the borehole allowed a combined palynological and sedimentary study, this allows to link the fluvial records to the shallow marine environment. The same core is used for the parallel thesis of Ding (2020), who focuses on the mineralogical and sedimentological observations. The palynology, mineralogy and sedimentology are used to make a combined reconstruction of the environment for the Early Pleistocene for the Netherlands.

First, I would like to thank my supervisors Timme Donders and Alexander Houben for their great effort and enthusiasm to complete my thesis. I would also like to thank Kim Cohen, Wim Hoek and Hao Ding for the discussions we did online, these discussions helped me to finish my thesis and I have learned a lot about the subject. For the short period at the office of TNO, which was ended quite abruptly due to the Covid-19 pandemic, I would like to thank Roel Verreussel, Dirk Munsterman and Frans Bunnik for their help during the endless periods of microscopic analysing. They were very interested in the core and told me a lot of stories about their work experience and their knowledge about pollen and dinoflagellate cysts.

Furthermore, I would also like to thank my roommates and boyfriend for their encouragement while working at home during the Covid-19 pandemic. Their sweet gifts and talks have ensured me that I had enough confidence and motivation to finish my thesis on time. I also would like to thank my friend Lonneke Roelofs for her help to get a good structure in my thesis and to add some good suggestions. Last and foremost as a sign of appreciations, I would like to thank my parents and my sister for always being there when I need them.

Abstract

This thesis aims to make a reconstruction for the paleo-environmental changes and the alternation of the terrestrial and marine environments during the Early Pleistocene in the Southern North Sea Basin. The cored section contains both terrestrial and marine material, which allows to link the fluvial records to the shallow marine environment. Terrestrial signals may have been derived from two river catchments in Europe during the Early Pleistocene, the Eridanos paleo-river from the northeast and the Rhine-Meuse river from the southeast. The age of the base of the core is interpreted as Early Pleistocene, Middle-Gelasian (2.1 – 2.3 Ma). The Early Pleistocene is an important Sub-epoch because it covers the intensification of large scale glaciation on the Northern Hemisphere. Lisiecki and Raymo used stable oxygen isotope ratios to indicate global temperature and ice-sheet evolution, this has resulted in Marine Isotope Stages (MISs).

The standard chronostratigraphic subdivision for the Netherlands, largely based on the work of Waldo Zagwijn, is primarily based on pollen data. The records had been constructed in the Eastern part of the Netherlands, this had as complication that no marine influence is recorded in the cores. Furthermore, the records had been constructed using data from different sites, this makes the sites incomplete and hard to data with the isotopic records obtained from the deep sea. Different key-aspects are used to achieve the aim, those key-aspects are alternation between marine- and terrestrial environments; identify the characteristics of the Early Pleistocene glacial/interglacial cycles; recognize patterns in the vegetation assemblages; correlate with the MISs stack of Lisiecki and Raymo (2005); recognize different hiatus and reworking events and to find trends to correlate with regional data.

A palynological data set based on pollen and organic-walled dinoflagellate cysts are used to achieve the aim of the thesis. In the laboratory, 70 samples are prepared by removing carbonates, silicates and sieving to bring the sediment size to 250 – 10 µm. Microscopic analysis are performed by using a Leica DM 2500 microscope, palynomorph taxa are scored until a minimum of 200 pollen is achieved. The palynological analysis can be subdivided into three groups: Pollen&Spores, Algae and Dinoflagellate cysts. Together with the lithological and mineralogical data of Ding (2020) the paleo-environment is determined.

Based on quantitative palynological data, the section is subdivided into three intervals: Interval 1 dominated by marine palynomorphs, Interval 2 dominated by a tidal environment and Interval 3 by terrestrial palynomorphs. The marine dominance declines when going upwards in the core, Interval 3 consists almost no dinoflagellate cysts anymore. The change from a marine to a more terrestrial environment is also observed in the estimated water depth. The estimated water depth indicate a change from deep water to a fluvial environment. Interval 1 shows a continuous sedimentation pattern, while for the upper part more erosion is observed. The erosion is proved by the sharp grass peaks and the relative low sedimentation rate (0.02 cm/year) calculated by the $\delta^{18}O$ – stack.

Five glacial/interglacial cycles are observed in the vegetational data, the cycles start with a high amount of grasses and some forest vegetation, typical vegetation for a glacial environment in the Early Pleistocene. The vegetational change towards an interglacial environment is to ferns, deciduous forest and Tsuga&Taxodium domination. Not every detail is studied, due to the high amount of possible erosion and reworking events a lot of material is missing. For future research it is good to make a good dating for the core and to do palynological research on a higher resolution to find more details.

Contents

1. Introduction

The Pleistocene (2.588 Million years ago (Ma) – 11.7 kyr) is an important period in Earth's history as at the start of the Pleistocene is marked by the intensification of large scale glaciation on the Northern Hemisphere (e.g. Zagwijn (1992), Gibbard & Cohen (2008)). The Early Pleistocene (2.588 – 0.774 Ma) is characterised by intensified glaciation cycles together with the subsidence of the North Sea Basin (Kooi et al., 1991) and the development of deltas from the Eridanos paleo- and Rhine-Meuse rivers. Ottensen et al., 2018 mentioned the sediments preserved in the North Sea Basin, contain important information about past environmental conditions, such as the timing and magnitude of ice-sheet build-up and decay and the changing configuration and activity of adjacent fluvial systems.

The Pleistocene Epoch is subdivided into different Sub-epochs and Stages. The local Sub-stages for the Netherlands are described by Zagwijn (1992) and are used as a regional for North-West Europe (Table 1). The foundation of these Sub-stages lies in pollen data. However, the link between the terrestrial and the marine realm remains uncertain, largely due to an overall absence of available sedimentary sections containing both a marine- as well as terrestrial fossil record. Most of the terrestrial boreholes are discontinuous and influenced by local variations in the depositional environment (e.g. Donders et al., 2007; Westerhoff, 2009), causing the possibility of missing multiple periods in the current climatic record for the Netherlands. Donders et al., (2007) described that these subdivisions are originally proposed as regional zones, however, they have been applied and correlated to continental sites over a wide range of regions across Europe. Despite the wide use of the continental correlation schemes for the Pliocene and Pleistocene (Donders et al., 2007), it is never been tested in an area where both terrestrial and marine palynomorphs are found. Different authors (Kuhlmann et al., 2004; Donders et al., 2018; Noorbergen et al., 2016) have studied different cores in the North Sea Basin. Donders et al., 2007 mentioned that these climate reconstructions include fluctuations based on local zonation's.

In 2018, two cores were recovered in the North-Western part of the Netherlands (Petten) by GeoSconic Drilling Ltd, BH-1 and BH-2, reaching 385 m. The used core BH-1 reached a terminal depth of 381.85 m and the top of the core was at an elevation of 3.16 m NAP. Down to 101.50 m depth, sonic drilling was performed, below that wireline rotary coring was performed. The cores were recovered in an unconsolidated, dominantly sandy Pleistocene sequence. The lower part (385 – 195 m) of the first borehole allowed a combined palynological and sedimentary study. Dr. Alexander Houben (TNO – *Geological Survey of the Netherlands* (TNO – GSN)) did the first analysis on the core. Houben (2019) did palynological and magnetostratigraphic analysis on the core and found an age of Middle Gelasian to Calabrian (2.3 – 0.8 Ma) which is characterised by reversed or possibly reversed polarities (220 – 385 m), corresponding to Matuyama reversed phase. At a depth of 380.91 – 376.72 m the normal Reunion sub-chron (2.13 – 2.15 Ma) and at a depth of 321.70 – 357.12 m the Olduvai event (1.78 – 1.94 Ma) is observed (Houben, 2019).

TNO – *Geological Survey of the Netherlands* (TNO – GSN), in cooperation with Utrecht University, aimed to perform a detailed research on the lower part of the first borehole, of which this MSc thesis is a first result. The aim of the overarching project is to reconstruct a new stratigraphic reference section for the Early Pleistocene of the shallow to deltaic deposits of the North-Western Netherlands and to reconstruct the regional response to glacio-eustatic and paleo-climatic change. The project consists of two MSc theses in 2019 – 2020, this thesis (Krom: Palaeontology) and a parallel thesis (Ding: Sedimentology).

The aim of this thesis is to reconstruct paleo-environmental changes and the alternation of the terrestrial and marine environments during the Early Pleistocene in the Southern North Sea Basin. Different key-aspects are used to achieve this aim:

- To indicate the alternation between marine- and terrestrial environments
- To identify and observe the characteristics of the Early Pleistocene glacial/interglacial – cycle for marine and terrestrial environments
- To recognize patterns in the vegetation assemblages
- To correlate the glacial/interglacial - cycle with the Marine Isotope Stages of Lisiecki and Raymo (2005)
- To recognize different hiatus and reworking events
- To find trends or events to correlate with regional data

This will be executed by creating a high-resolution palynological dataset based on pollen and organic-walled dinoflagellate cysts (dinocysts). The parallel thesis (Ding, 2020) provided information about relative sea-levels and depositional environments, the provenance of sediments and the reworking and hiatuses in the sedimentary sequence. Ding (2020) generated a high-resolution sedimentological and lithological log, with which the past water depths and the past conditions of waterflow can be reconstructed. Data about the heavy minerals percentage of the total minerals can help to better understand the evolution of the Eridanos paleo-river and Rhine-Meuse river.

The co-occurrence of terrigenous (pollen and spores) and marine (dinocysts) palynomorphs in deposits provides a means for making land-sea correlations of climate change and its impact on marine environments (Scott et al., 1984; Mudie, 1989; Versteegh, 1994, 1997; Zonneveld, 1996). Pollen and spores provide a reliable source of terrestrial paleo-environmental and -climatic information (Birks and Birks, 1980), they complement the temperate changes derived from the marine biota (Meijer et al., 2006). Dinoflagellate cysts are widely accepted as reliable proxies for reconstructing marine paleo-environments in the Quaternary (e.g. de Vernal et al., 2005; Radi & de Vernal, 2008; van Nieuwenhove et al., 2008; Verleye and Louwve, 2010). The distribution of the cyst taxa through time reflect the changes in sea surface water properties and these changes can be used to reconstruct the past environment in the Quaternary.

The palynological data discussed in this thesis will be integrated with detailed sedimentological and mineralogical analysis from Ding (2020). Together, these theses aimed a new pre-liminary marine- and terrestrial palyno-stratigraphical framework for the Early Pleistocene of the Netherlands. It interprets quantitative trends of the assemblages in terms of climate, sea-level and sediment provenance. In general, a strong coupling of marine and terrestrial ecosystems in response to glacial-interglacial forcing is expected. I expect a more continuous palynological result, which allows me to integrate marine- and continental signals and tie the terrestrial pollen-based stages to marine timescales.

Table 1 Division of the Pliocene and the Pleistocene described by Zagwijn (1957, 1960, 1963)

International			**The Netherlands**		
Epoch	**Sub-Epoch**	**Stage**	**Local Dutch sub-stage**	**Glacial/Interglacial**	**Stadials/Climate stages**
Pleistocene (2.58 – 0.0117 Ma)	Late (0.129 – 0.0117 Ma)	Upper (0.129 – 0.0117 Ma)		Weichselian (0.116 – 0.0117 Ma)	Mainly cold
					Amersfoort – Brorup – Odderade – interstadials (temperate)
				Eemian (0.126 – 0.116 Ma)	Mainly warm – temperate
	Middle (0.773 – 0.129 Ma)	Chibanian (0.781 – 0.129 Ma)		Saalian (0.238 – 0.126 Ma)	Glaciation (northern Netherlands)
					Bantega interstadial (cool)
					Cold
					Hoogeveen interstadial (temperate)
					Cold
				Holsteinian (0.418 – 0.386 Ma)	Mainly warm – temperate
				Elsterien (0.465 – 0.418 Ma)	Glaciation (cold)
	Early (2.58 – 0.773 Ma)	Calabrian (1.80 – 0.781 Ma)	Cromerian (0.850 – 0.465 Ma)	Interglacial IV (Noordbergum)	
				Glacial C	
				Interglacial III (Rosmalen)	
				Glacial B	
				Interglacial II (Westerhoven)	
				Glacial A	
				Interglacial I (Waardenburg)	
			Bavelian (1.07 – 0.85 Ma)	Dorst glacial	
				Leerdam interglacial	
				Linge glacial	
				Bavel interglacial	
			Menapian (1.20 – 1.07 Ma)	Cold (one interstadial)	
			Waalian (1.45 – 1.20 Ma)	C – warm temperate	
				B – cool	
				A – warm temperate	
			Eburonian (1.80 – 1.45 Ma)	Cold complex (3 interstadial)	
		Gelasian (2.58 – 1.80 Ma)	Tiglian (2.50 – 1.80 Ma)	T - C	6 cool 5 warm temperate 4c cool 4ab temperate 1 – 3 warm temperate
				T - B	Cool
				T- A	Warm – temperate
			Praetiglian (2.58 – 2.40 Ma)	PT (cold)	
Pliocene (5.33 – 2.58 Ma)		Piacenzien (3.60 – 2.58 Ma)	Reuverien (3.60 – 2.58 Ma)	R – A	
				R – B	
				R - C	

2. Background information

The North Sea is a mid- to high-latitude epicontinental sea located between the British, Scandinavian and Northern European landmass. To the north the North Sea is connected to the North-Atlantic Ocean and in the south with the English Channel (Lamb et al., 2016). Ottensen et al., 2018 describes that the North Sea is a failed rift basin that formed during the Late Palaeozoic and Mesozoic, and mostly filled to the onset of the Pleistocene. The basin is a 600 kilometre long, elongated basin which was enclosed by different landmasses. The shallow North Sea basin experienced profound changes during subsequent glacial and interglacial cycles. During the Pleistocene, ice sheets have transgressed into the North Sea at several stages (Graham et al., 2010). The ice volume of the ice sheet is coupled to the Northern Hemisphere climate, during cold periods the ice sheet grow and during warm periods the ice sheet shrinks (Arz et al., 2007). The North Sea Basin is influenced by the ice sheets during the Pleistocene (Lamb et all., 2018) (see Chapter 2.2). Figure 1 represents the situation of the North Sea Basin during the onset of the Pleistocene (~2.58 Ma), during this period still a small connection to the North-Atlantic Ocean existed. In the north, the ice sheet started to grow and expanded further north during the Pleistocene.

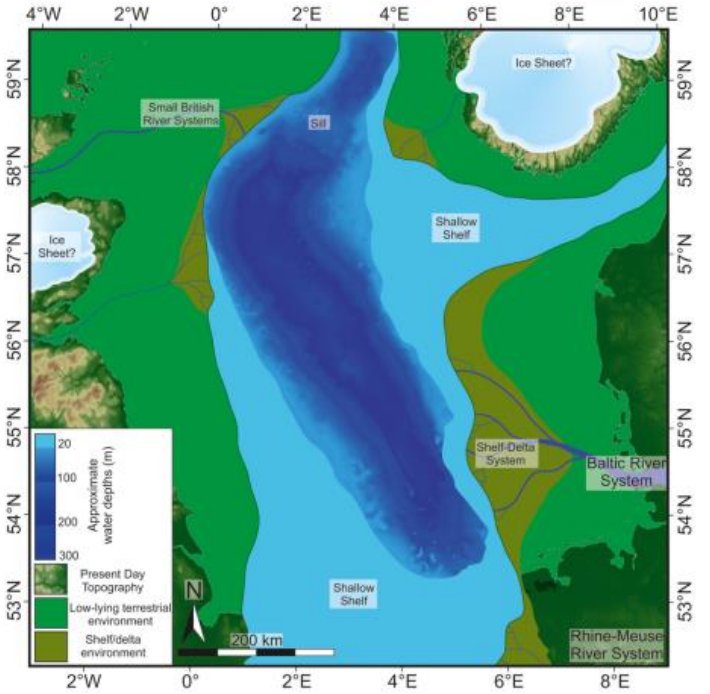

Figure 1 Reconstructed paleo-environmental map of the North Sea at the base of the Pleistocene (2.58 Ma). The map is based on data of Overeem et al., (2001), McMillan et al., (2005), Busschers et al., (2007), Rose (2009) and Noorbergen et al., (2015). Large parts of the present-day North Sea have been flooded under the high stand conditions at the onset of the Pleistocene, creating a very shallow shelf, but where otherwise terrestrial. Important to mention, the Baltic River System is names as Eridanos paleo-river for this thesis. (Lamb et al., 2018)

The focus lies on the southern part of the basin, part of the North-West European Basin which includes the present-day offshore and onshore parts of the Netherlands, Germany and Denmark (Kuhlmann et al., 2006). Lamb et al., 2018 describes that during high-stand conditions at the onset of the Pleistocene, large parts of the present-day North Sea have been flooded. Those high-stands are also marked by Miller et al., (2011), who observed a peak in sea-level at 2.58 Ma in the global sea-level curve. These high-stands created the shallow marine environment presented in Figure 1. During those high-stands large parts of the Netherlands were inundated, during low-stands large shelfs were presented (Lamb et al., 2018). The figure shows the inflow of the different rivers from the east and west, that delivered sediments into the basin.

2.1 River influence

The dominant type of deposition during the Pleistocene was fluvial sediment from a terrestrial low-land environment, other forms were from coastal and glacio-genic depositions (Hijnma et al., 2012). Figure 2 shows the different rivers which flowed into the basin, from the east the Eridanos paleo-river and Rhine-Meuse river and from the west a small British River system. The flow patterns show a north and south dividing watershed, indicated with a black dotted line. The Eridanos paleo-river had a much larger catchment area in comparison with the Rhine-Meuse river. The Eridanos paleo-river originates from the Baltic region (Westerhoff et al., 2009) and had a drainage area in the order of 1.1×10^6 km^2 (Kuhlmann et al., 2004). Due to glacial erosion

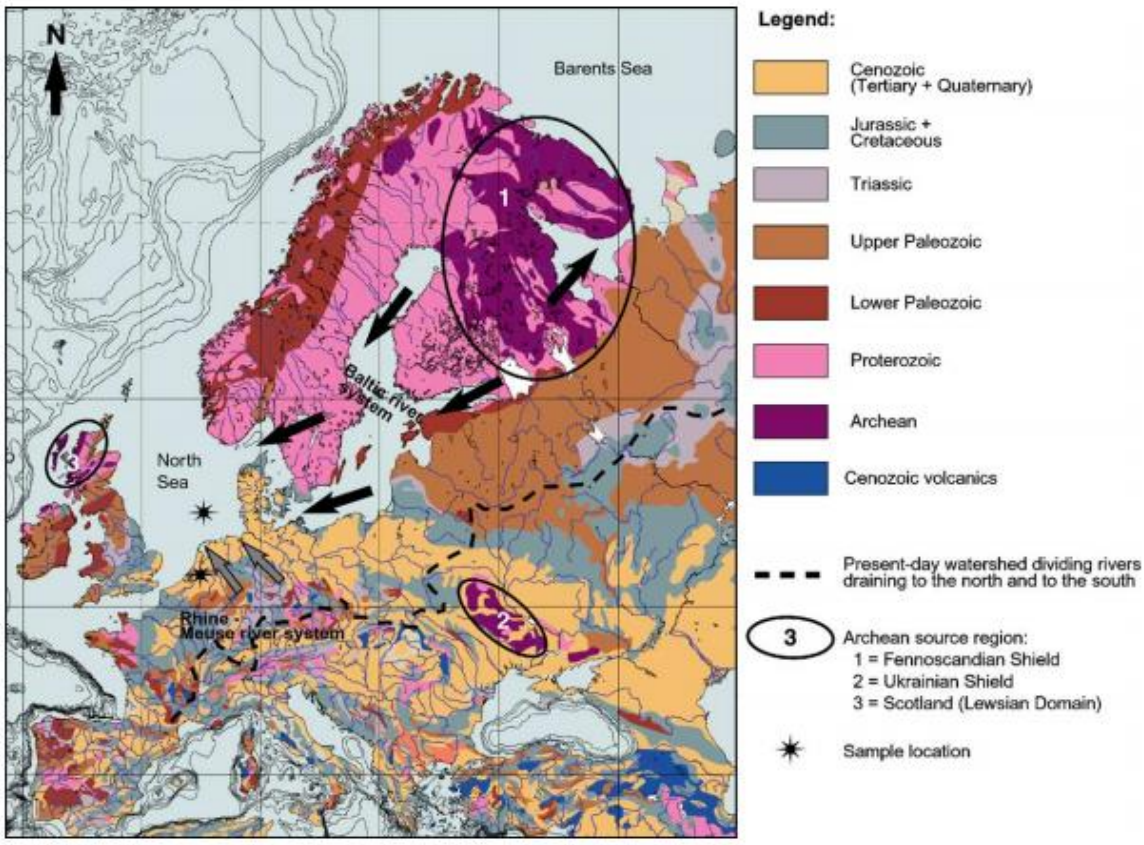

Figure 2 Geological map of Europe with river systems and the north-south dividing watershed. Indicated are the Eridanos paleo river (Baltic river system) with black arrows and the Rhine Meuse river system with grey arrows. The numbers indicate the different Archean source regions. (Kuhlmann et al., 2004)

in Scandinavia during the Pleistocene, the Eridanos paleo-river is no longer existing (Gibbard et al., 1988).

The main source of the terrestrial deposits in the Central North Sea during the Early Pleistocene are from the Eridanos paleo-river (Kuhlmann et al., 2004). Kuhlmann et al., 2004 gave as option that the principal mechanism of sediment delivery in the Southern Basin during the onset of the Pleistocene was from the Eridanos paleo-river, however, with a small component of the Rhine-Meuse river. During the earliest part of the Pleistocene, rapid northward progradation is observed in the Southern North Sea (Lamb et al., 2018). This progradation is linked with climatic cooling and increased sediment supply owing to glacial activity in the sediment source area (Lamb et al., 2018).

2.2 Overview of basin morphology and processes of sedimentation in the North Sea Basin

An increase in sedimentation rates into the North Sea Basin was recorded around 2.6 Ma due to river inflow and the intensification of the Northern Hemisphere glaciation (Dodweswell et al., 2010). Major increase in progradation rates (Patruno et al., 2018) influenced basin morphology. The change of the basin morphology and the processes of sedimentation during the Pleistocene are presented in Figure 3.

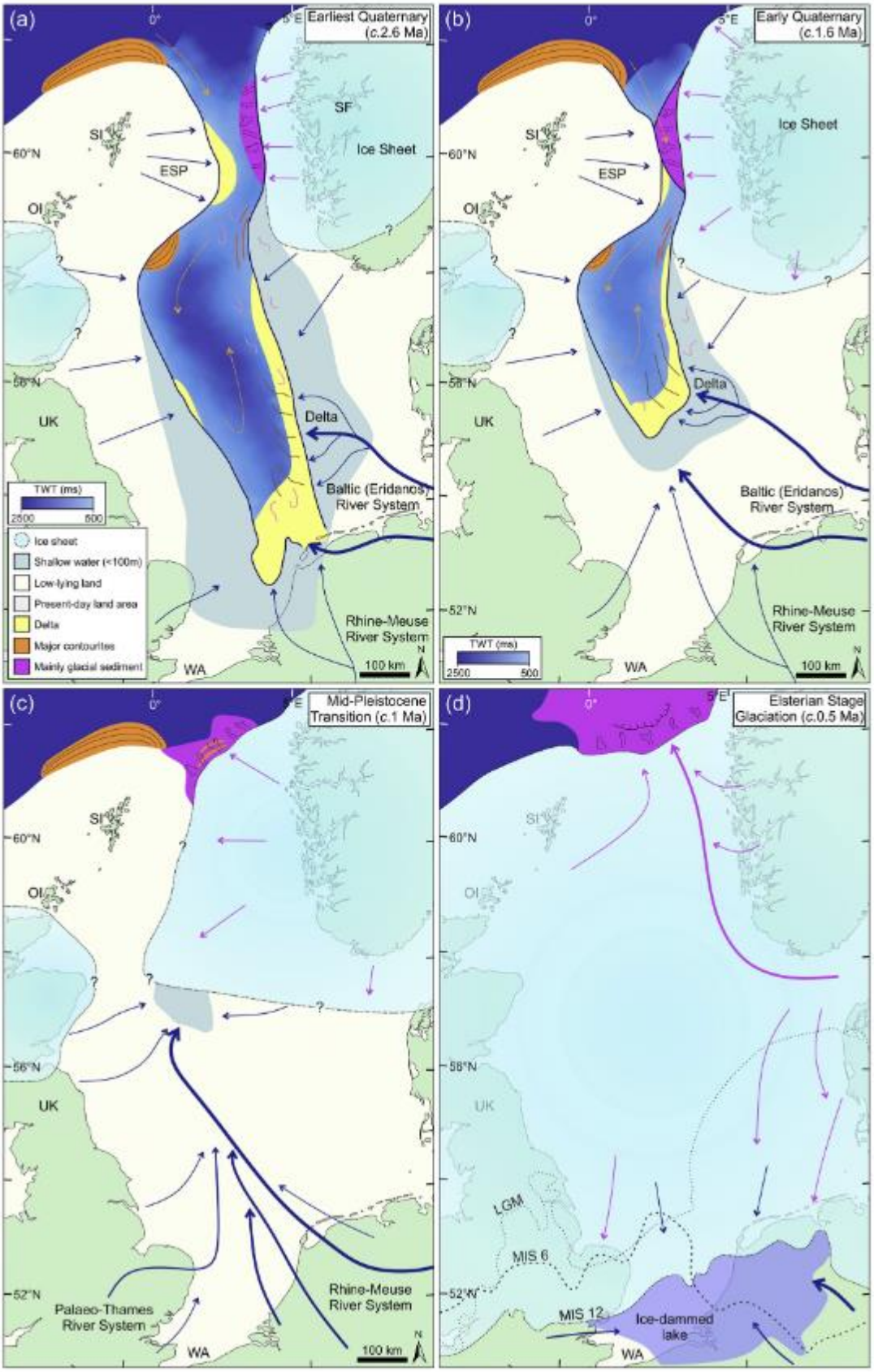

Figure 3 Overview of schematic maps of basin morphology and processes of sedimentation in the North Sea Basin at four time stages through the Pleistocene. A) Earliest Quaternary (~2.6 Ma), B) Early Quaternary (~1.66 Ma), C) Mid-Pleistocene Transition (~1 Ma), D) Elsterian Stage (0.5 Ma). (Ottensen et., 2018)

Since the onset of the Pleistocene (2.58 Ma) (Figure 3A), the North Sea filled up to 1100 m of Early Pleistocene sediments (Ottensen et al., 2018). The Eridanos paleo-river was the dominant river system in the area, the Rhine-Meuse and the Thames had a smaller influence in the area. The northern ice sheet was relatively small and was growing toward the west. At the coast of the Netherlands, a delta formed which expanded to the north. During the Pleistocene (1.6 Ma), most of the Southern basin had been infilled (Figure 3B). The delivery of the fluvio-deltaic sediments from the Eridanos paleo-river and the Rhine-Meuse river continued, however, the Eridanos paleo-river stayed the dominant river (Ottensen et al., 2018) and flows into the middle of the basin during this period. The shared delta, from both rivers, moved to the middle of the basin, causing the Southern North Sea basin to become low lying land. The ice sheet kept growing to the west during this period and delivered even more glacial sediments into the channel that connects the North Sea Basin with the Atlantic Sea. During the Mid-Pleistocene Transition (MPT) (~1 Ma), the ice sheet probably expanded far enough to block the connection to the Atlantic and the whole North Sea Basin became a low-lying land with sediment input of rivers (Figure 3c). Ottensen et al., (2018) describes that during this period the Eridanos paleo-river became the main source of sediments for the basin. During the Elsterian (0.5 Ma) (Figure 3D), the whole basin became covered by the ice sheet. An ice dammed lake is located at the current position of the Netherlands. The Rhine-Meuse river and the Paleo-Thames continued to transfer water and sediments towards the lake (Ottensen et al., 2018).

2.3 Paleoclimatic context

At the onset of the Pleistocene, ice sheets rapidly expanded and gave rise to glacial cycles oscillating on a prominent obliquity (41 kyr) pacing. The period during the 41 kyr pacing is characterised by relative thin ice sheets. Maslin and Brierley (2005) mentioned that after 900 kyr, the cycles start to occur with longer duration and a marked increase in the amplitude of global ice volume variations. This switch to a 100 kyr pacing with thick ice sheets and long periods of cooling is called the Mid-Pleistocene Transition (1.25 – 0.7 Ma). These rhythmic changes in ice volume had a major influence on the depositional system in the Southern North Sea, as it can be recognized in the deposition of the sediments.

One of the hypotheses to explain the change from a 40 to a 100 kyr world is assumed by Clark & Pollard (1998). They proposed that the character of the substrate over which ice moved and its friction with the basal ice layers had caused the change. Ruddiman (2014) describes the change to thicker ice sheets is caused by the slip and slides of the base of the ice sheets. If the sediments are saturated with water, they are more easily deformed by the overlying ice in comparison with sediments without water. The ice lobe, that kept sliding south, melted due to high ablation in the lower latitude (Ruddiman, 2014). The sliding and melting have kept the ice sheet slow, thin and small in volume during the 40 kyr world (Figure 4A). The sliding and melting causes glacial erosion and after million years, just a little of the organic soil and sedimentary cover was left. The erosion caused that the ice sheets do not slide that far south anymore and can grow thicker. Those thicker ice sheets stand a better chance of surviving during relatively weak insolation maxima (Ruddiman, 2014), this can explain the longer cycles (Figure 4B).

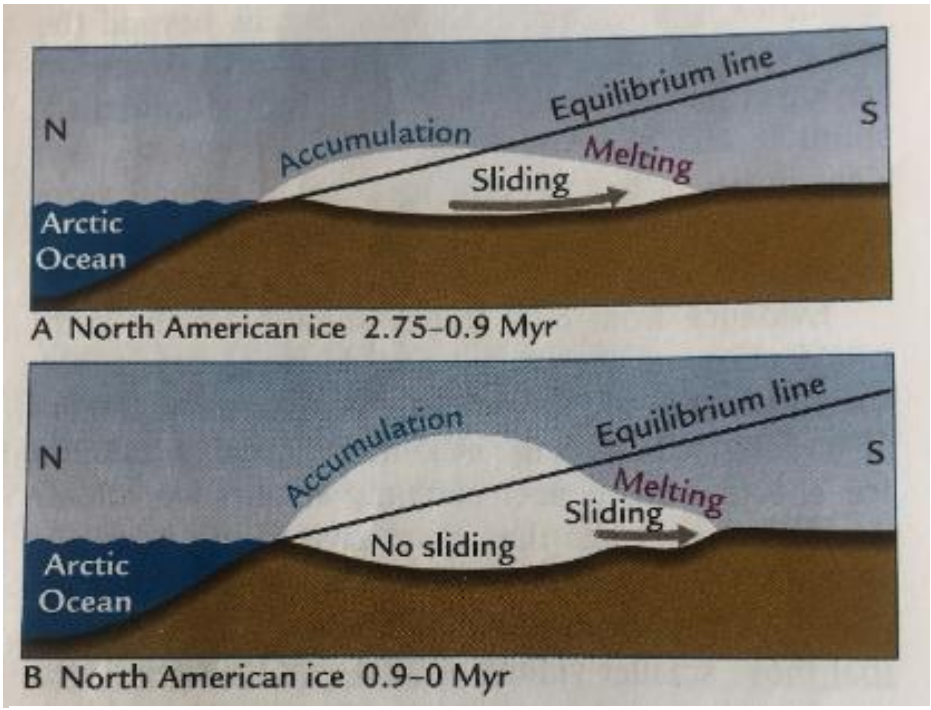

Figure 4 Explanation why ice slipping control ice sheet volume. A) During earlier glaciations, ice sheets have been thin because they slide on water-saturated soils towards lower elevations and warmer temperatures. B) After the ice sheets tripped of most of the softer underlying substrate, their central region could grow higher because they do not longer slide. (Ruddiman, 2004)

2.4 Stratigraphic context

Chrono-stratigraphic subdivision has been made on basis of palynological data. Van der Vlerk & Florschütz (1950, 1953) started with the subdivision of the Early and Early-Middle Pleistocene of the Netherlands based on palynological research, the research is continued by Zagwijn (1957, 1960, 1963, 1975, 1985, 1996 and 1998) and Zagwijn & de Jong (1985) (Drees, 2005). Their research resulted in a detailed chrono stratigraphy (Drees, 2005) and is used as a standard for the Netherlands. Drees (2005) indicated most of the pollen diagrams of the Netherlands were derived from short sections, however, most of these sections contain no other information beside the presence or absence of some pollen taxa. Most of these sections were incomplete when they were compared with the isotopic record obtained from the deep sea (Gibbard et al., 1991).

Zagwijn (1957, 1960) outlined the structure through the recognition of glacials and interglacials (Drees, 2005). However, later it became clear that more climatic variation is observed than just a warm and cold classification. Vlerk and Florschütz (1953) introduced the Praetiglian and Tiglian stages, based on pollen analysis in non-marine facies in boreholes and clay pits in the Tegelen area (Zagwijn, 1957, 1960, 1963). The Praetiglian is considered as the base of the Pleistocene, this coincides with the Gauss-Matuyama boundary with an age of 2.6 Ma (Meijer et al., 2006). The Tiglian stage was first considered as a warm stage, however, it became clear that the climate varied during this interval (Gibbard et al., 1991). The subdivision into warmer and cooler phases is performed by Zagwijn (1963) based on a palynological study (Drees, 2005; Zagwijn, 1992). The Tiglian is subdivided into three substages: Tiglian A (TA), with an interglacial character, Tiglian B (TB), a cool character and Tiglian C (TC) again an interglacial character (Drees, 2005) (Table 2). TC is further subdivided into 6 stages, with a more detailed subdivision of TC4 (Drees, 2005). TA-substage is characterised by high values of *Fagus* (Beech), TB-substage by high values of *Artemisia* and a low content of trees and TC-substage by *Pterocarya* (Wingnut) (Meijer et al.,

2006). The *Fagus*, dominant in TA, do not occur in the other two substages again (Meijer et al., 2006). The Tiglian is an important sub-stage for this thesis because it is based on pollen-analytical investigations and it is likely that the upper part of the TC is included in the core. The BH-1 core is important because it consists pollen and marine deposits, whereby a link can be made between both deposits and maybe a better stratigraphic subdivision for North-West Europe. As Westerhoff, 2009 mentioned, probably multiple TB/TC type transitions are present in more expanded sedimentary records, just like this one.

Table 2 Subdivision Tiglian with corresponding pollen

Glacial / interglacial	**Stadials / Climate stage**	**Dominated pollen species**
T – C	6 cool 5 warm – temperate 4c cool 4ab temperate 1 – 3 warm – temperate	*Pterocarya*
T – B	Cool	*Artemisia*
T- A	Warm - temperate	*Fagus*

2.5 Mineralogical and lithological study

The results of the parallel thesis of Ding (2020) are used as background information for this thesis. More information about the results are represented in the thesis of Ding (2020). Figure 5 indicates the sedimentological log and the water depth based on the detailed logging, sediment size and element concentrations. Ding (2020) have indicated three intervals for the core: marine, littoral/deltaic/tidal and fluvial/lowland. At the deepest part, a full marine environment with deep water is indicated. The second interval shows a lot of variety in water depth, from deep water to supratidal. The alternation in water depth is also indicated by the lithological log, this log indicates a lot of variety in the grain size and material. The upper part is dominated by a fluvial system and the water depth is indicated as supratidal with a water depth of almost zero.

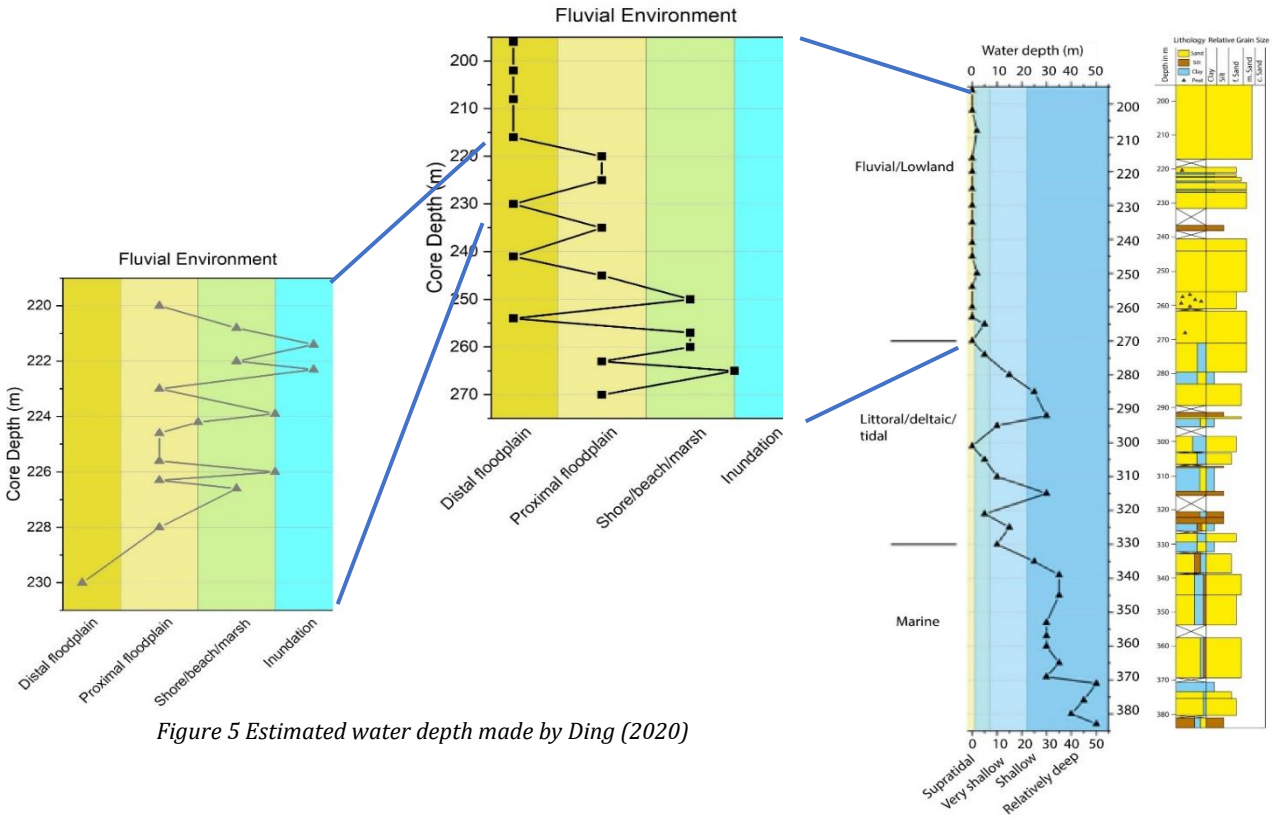

Figure 5 Estimated water depth made by Ding (2020)

Ding (2020) had made a water depth indication for the upper part in more detail (Figure 5). One of the reasons why the first indication was a water depth of almost zero is caused by the fact of fast basin filling with sediments. During periods with very low water, the basin is very fast filled up with sediments.

2.5.1 Mineralogical results

The results of the mineralogical data are presented in a graph in. Not all results are discussed in this thesis because they do not have relevance on the results of this thesis, the other results are described in the parallel thesis of Ding (2020). The minerals important for this thesis are (Table 3):

- Ca/Sr – ratio (Calcium / Strontium): The ratio indicates the productivity of the area, to determine the content of detrital or biogenic carbonate. A high ratio indicates more detrital calcium in the area. Detrital calcium is calcium what is obtained by weathering from the land. A peak in the graph indicates a high amount of weathering on land. These peaks can correlate with periods of open environments, with high erosion rates.
- Sr/Ti – ratio (Strontium / Titanium): Titanium is enriched in coarse-grained fractions and indicates terrigenous sediments. Sr/Ti is a ratio between biology (marine) and lithology (terrigenous). It indicates the productivity for the marine part of the area. A high ratio indicates a high productivity in the ocean.
- Fe/K – ratio (Iron / Potassium): Potassium is enriched in fine sediment fractions and Fe is a terrigenous indicator. A high ratio indicates high humid conditions with fluvial sediments. This ratio can indicate flood events with possibly erosion contacts.
- Zr/Rb – ratio (Zirkonium / Rubidium): Indicates the size of the sediment , a higher ratio indicates more coarse sediment. This sediment can explain about the energy of the system, coarser sediment is deposited by a high energy environment.
- Ba (Barium): Indicates the productivity in the area, higher values indicate a high productivity in the area.
- Heavy minerals: During periods with high values in heavy minerals, the lighter minerals are removed from the area. This could indicate a hiatus, because all the other material is removed from the area.

Table 3 Summary of the mineralogical data

Ratio/Value	**Indicates**	**Peaks (m)**
Ca/Sr	Terrestrial calcium	360 310 = highest peak 270
Sr/Ti	Productivity	320 260 = highest peak 210
Fe/K	Humid conditions	320 290 = highest peak
Zr/Rb	Coarser sediment	290
Ba	Productivity	265
Heavy minerals	Hiatus	290

3. Materials and Methods

3.1 Sample preparation

The core was collected in sediment boxes, in meter long parts, 200 m in total and stored under cooled conditions. A sample was taken approximately every 20 cm, so that no details were missed, and a good paleo-environmental overview can be made later. A selection of 70 samples were used for palynological analysis (Appendix A), analysed by Krom, Donders and Houben. The selection of the samples is based on the lithological data and the results of the first palynological analysis. The lithological description was made earlier together with Hao Ding. Houben (2019) mentioned that the sample taken above 200 m are from the fluvial-littoral Peize Formation (Fm), Appelscha Fm. and Urk Fm. sediments and yield not enough palynomorphs, so these samples are unsuitable for further interpretation.

3.1.1 Removing of carbonates, silicates and sieving

For each sample, 10 grams was crushed in the laboratory and a *Lycopodium-clavatum* (Club moss) tablet was added. The *Lycopodium-clavatum* tablet has a known amount of *Lycopodium*, which can be used later to calculate the absolute amount of pollen in the sample. The known amount of *Lycopodium clavatum* is added to every sample according to the method described by Stockmar (1971) (Mertens et al., 2009). Hydrochloric acid (HCL) with a concentration of 10% was added for removal of carbonates. The amount of HCL was depended on the intensity of the reaction. If the reaction stopped, the residues were topped-off with tap-water and the residues were left to settle (~1 night). After decanting, the samples were filled with tap-water and placed in the centrifuging.

The siliciclastic component of the samples was removed by adding Hydrofluoric acid (HF) with a concentration of 30%. A small amount of HF was added until the reaction had reached a temperature of ~38 degrees. After reaching the temperature, the samples were placed on a shaking machine for 2 hours. The samples were topped-off with tap-water and were again left to settle (~1 night). This process was repeated twice, the third day, three times the amount of residue HCL 30% was added. The HCL 30% was added for the removal of formed fluorosilicates.

The sample needs a size between 250 and 10 µm, the 250 µm sieve was used to remove the largest fines and 10 µm sieve was used to remove the smaller fines. The samples were rinsed with tap-water to make it neutral. The sieved samples were placed in test-tubes and centrifuged for 5 minutes. A small fraction of the residues was pipetted into a clean glass and topped off with a cover glass and embedded in glycerine.

3.2 Sample analysis

The 70 samples are made in the laboratory and used for the analysis (40 (Krom), 24 (Houben) and 6 samples (Donders)). The microscopic analysis are performed by using a Leica DM 2500 microscope. The microscope identifications were performed using 500/787,50x magnification. Palynomorph taxa are scored until a minimum of 200 pollen is achieved or a maximum of 300 added *Lycopodium*. The choice to stop with a maximum of 300 *Lycopodium* is made because this indicates a too low amount of pollen in the sample, this is not worth to count further. The palynological analysis can be subdivided into three classes: Pollen and Spores, Algae and Dinoflagellate cysts (Figure 6 Subdivision of palynological analysis (Houben, 2019)). The three classes are important to investigate differently because they all give information, which can be used to reconstruct the paleo-environment. The pollen and spores indicate the terrestrial signal and represent the terrestrial climate, indicate the relative distance from the shore and can be used for dating by known of Last occurrences (LO) (Houben, 2019). The algae represents the freshwater influx in the area and indicates the depositional environment (Morzadec – Kerfourn (1997). Dinoflagellate cysts indicates the marine signal (Houben, 2019), they can be used for dating, indicating fresh or salt water signal, and it indicates the level of productivity.

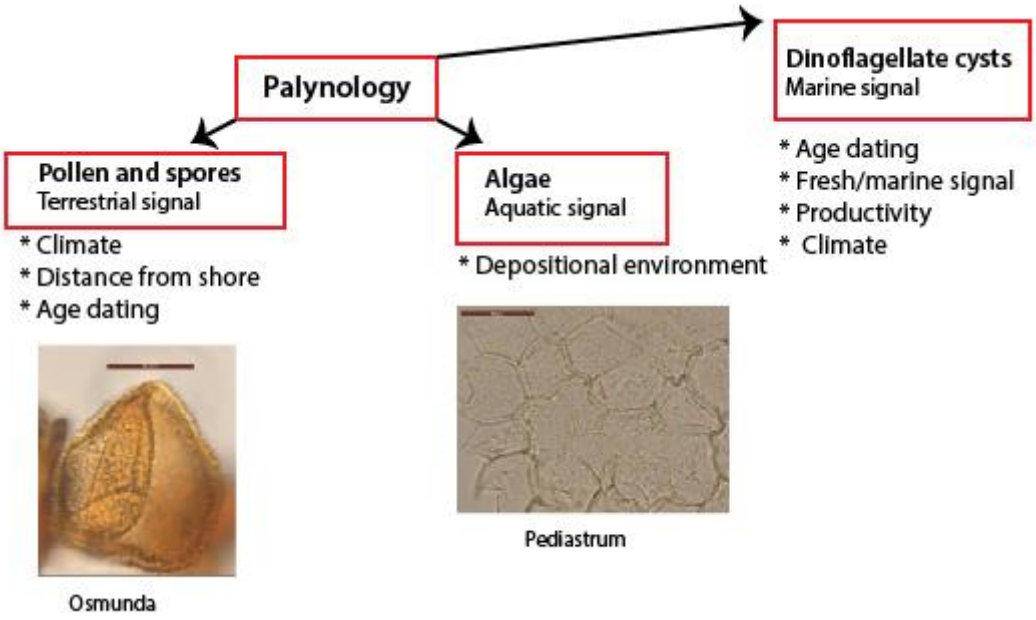

Figure 6 Subdivision of palynological analysis (Houben, 2019)

3.3 Stratigraphic relationships and climate reconstructions

The paleo-environment can be described using the recognised vegetation patterns and the occurrence of the marine palynomorphs. Marine palynomorphs and vegetation patterns are sensitive tracers of past climate changes. This core contain both tracers, which ensures to make a direct connection between both components.

The marine palynomorphs are characterised for their occurrence in a specific environment and can be used as a temperature tracer. The cold-water tracers are: *Filisphaera* spp., *Habibacysta tectata* and *Bitectatodinium tepikiense* (Donders et al., 2018; Zonneveld et al., 2013), warm-temperate tracers are *Operculodinium israelianum*, Achomosphaera *andalousiensis* and Lingulodinium *machaeophorum* (Versteegh and Zonneveld, 1994; Donders et al., 2009), heterotrophic conditions are marked by the Protoperidniacean family (Donders et al., 2018) and cosmopolitain conditions are observed by the presence of *Spiniferites* spp., *Operculodinium* spp (Versteegh and Zonneveld, 1994; Zonneveld et al., 2013).

Some intervals are marked by influxes of fresh water algae (*Pediastrum* and *Botryococcus*) indicating a strong riverine input (Donders et al., 2018). Together with the vegetation pattern and the patterns in the T/M – ratio this can be confirmed. *Dryopteris* – type (Wood fern) is one of the examples of riverine input, the genus grows very fast in disturbed areas.

It is known that the concentration of pollen and terrestrial spores in marine sediments decrease exponentially with distance offshore (Muller, 1959; Mudie, 1982; Rochon and De Vernal, 1994). For the bisaccates, their proportion gradually increases with distance from the shore (Abbink et al., 2004). This is called the Neves effect, the bisaccates are easily transported by the wind and can be used as indicator for the distance from the shore. A disadvantage of excluding the bisaccates is the low percentage arboreal pollen (Donders et al., 2007; Kothoff et al., 2014), however, this eliminates the signal due to direct effect of sea level changes (Donders et al., 2007; Kothoff et al., 2014).

For the vegetation, the most common cycle of vegetation succession is: open vegetation (steppe or tundra), dry open woodland, deciduous forest, mixed forest and conifer forest (*Picea*) reflecting climatic change from dry and cold, to warmer but still dry, to warm and humid, and finally cool and still humid (Leroy, 2007) (Figure 7). The subdivision of the terrestrial palynomorphs without bisaccates is based on environmental temperature characteristics. The subdivision is Ericaceae, Sphagnum, grasses, herbs, ferns, deciduous forest and Tsuga & Taxodium.

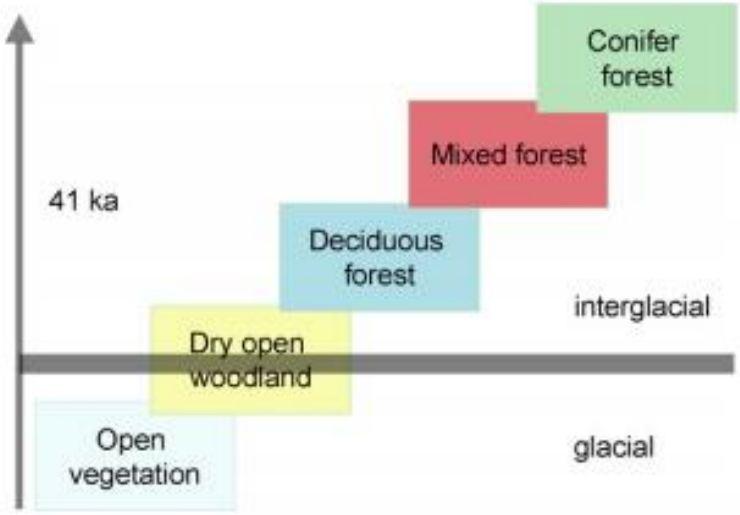

Figure 7 Most common cycle of vegetation succession for the glacial/interglacial cycle (Leroy, 2007)

The stratigraphic relationships can be drawn by using conventional range-based and range-top stratigraphy. Marine palynomorphs and terrestrial vegetation respond rapidly to changes in climate and sea-level, these changes can be used to establish stratigraphic correlations (Houben, 2019). The stratigraphic relationships are determined using absolute and percentage data of the samples. To calculate the absolute amount of pollen or dinoflagellate cysts, a known amount of *Lycopodium clavatum* is used.

For this equation, 19855 *Lycopodium clavatum* is added.

$$C = \frac{d_c * l_t * t}{l_c * w}$$

Equation 1

whereby;

C = absolute concentration
d_c = number of counted dinoflagellate cysts / pollen
l_t = number of *Lycopodium* spores in the tablet
t = number of tablets added to the sample
l_c = number of counted *Lycopodium* spores in the sample
w = weight of the dried sample (g)

The equations for the percentage pollen and dinoflagellate cysts are, the specified equations are presented in Appendix C:

$$\%Pollen = \frac{(Amount\ of\ pollen)}{Total\ sporomorph - bisaccates} * 100$$

Equation 2

$$\%Dinoflagellate\ cysts = \frac{(Amount\ of\ dinoflagellete\ cysts)}{Total\ Dinoflagellate\ cysts}$$

Equation 3

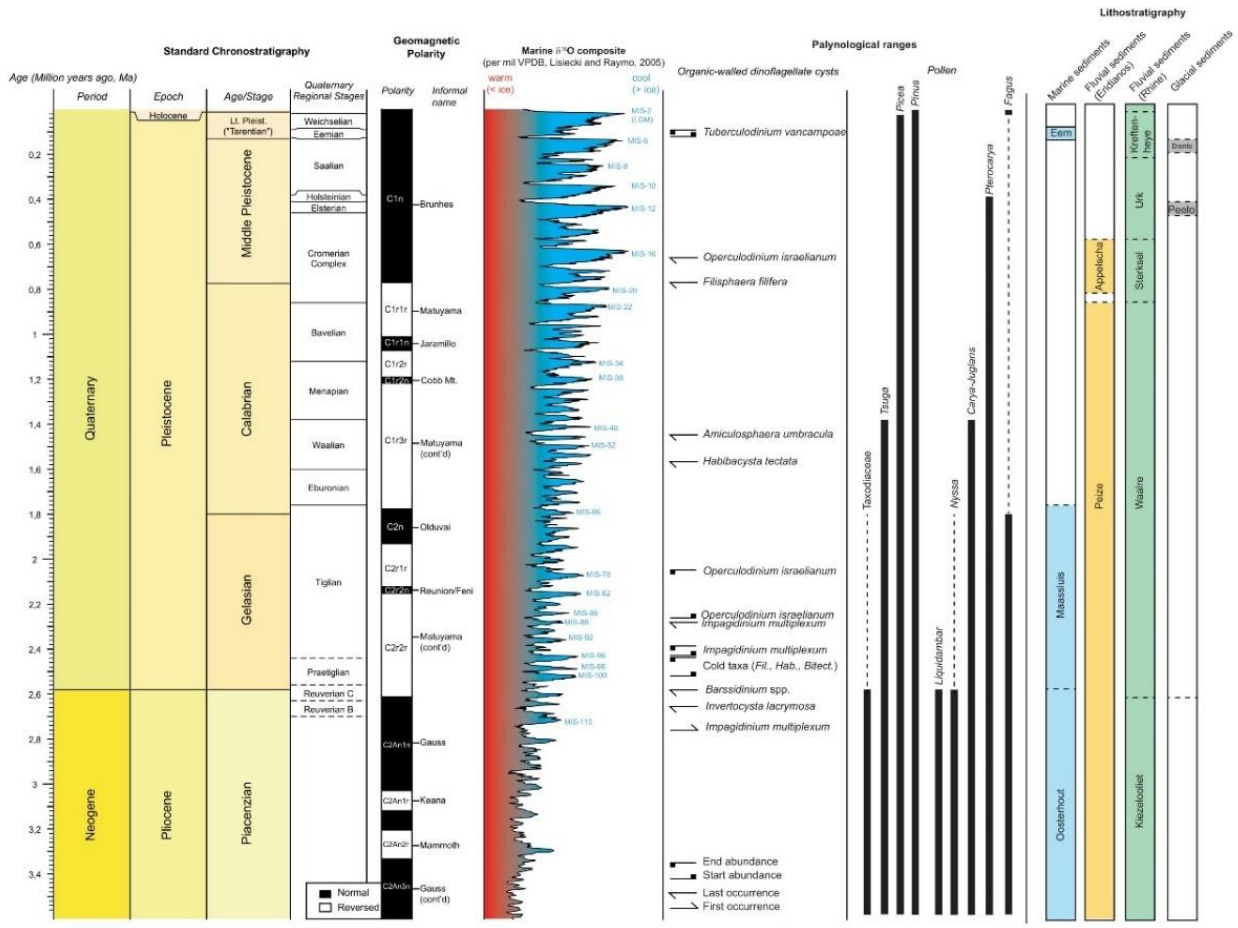

Figure 8 Standard chronostratigraphy, Geomagnetic polarity (Gradstein et al., 2012), Marine $\delta^{18}O$ composition (Lisiecki and Raymo, 2004), Organic walled dinoflagellate cyst distribution (Head et al., 2005; Kuhlmann et al., 2006; De Schepper and Head (2009), pollen distribution (Lang, 1994) and the lithostratigraphic subdivisions (TNO, 2013) made by Houben (2019)

The LO of the marine palynomorphs can be used to data specific samples. For this core, the *Amiculosphaera umbracula* (*A. umbracula*) is used, the dinoflagellate cyst had his last occurrence at a depth of 304.90 m near the top of the Gelasian (Kuhlmann et al., 2006; De Schepper and Head, 2009).

The absolute concentrations are used to support, together with the Terrestrial/Marine – ratio (T/M -ratio), the assumption of the environment. Closer to one indicates a dominance in terrestrial environment and close to zero indicates a dominance in marine environment.

$$T/M\ ratio\ = \frac{T}{(T+M)}$$

Equation 4

whereby;

T = sum of all sporomorph – bisaccates
M = sum of all dinoflagellate cysts

The T/M – ratio is an equation based on the most extreme end members of the environment, fully terrestrial or fully marine. The foraminifera are not included in the marine part because they indicate a brackish water influence.

Another method to correlate the core is the use of magneto-stratigraphy, as indicated by the second column in Figure 8. The correlation is done based on polarity, the core contains magnetic minerals, usually iron, which indicate the geomagnetic field. Houben (2019) presents magneto-stratigraphically data for the core. The section is pre-dominantly characterized by reversed polarity (white in Figure 8). A section of normal polarity was recorded between 357.12 – 321.70 m depth, which was by Houben (2019) tentatively interpreted as the C2n (Olduvai) Magnetochron. This would be placed the core in the Early Pleistocene, middle Gelasian (2.3 – 2.1 Ma).

To understand and describe local observations from the Petten core, a correlation with the $\delta^{18}O$ - stack of Lisiecki and Raymo (2005) is made. The relatively cold glacials (heavy $\delta^{18}O$) and warm interglacial (light $\delta^{18}O$) phases are often referred to as MISs with glacials having even numbers and interglacials having odd numbers (Hays et al., 1976). The $\delta^{18}O$ – stack of Lisiecki and Raymo (2005) can be compared with the T/M – ratio graph because this graph indicates the marine and terrestrial periods, so possible interglacial and glacial periods. However, this method can only be used if a complete core with a high preservation rate is observed.

3.4 Lithological and mineralogical data

The marine palynomorphs and vegetation patterns, together with the lithological data and the mineralogical data from the parallel thesis Ding (2020), indicate the paleo-environment. The lithological data is obtained by recording the core twice. First, the core is divided into smaller units based on lithology (sand, silt and clay) and colour, and next the dominant grain size ranges and colours were described visually. Element concentrations in the sediment provide more information about the sedimentary history. The data Ding (2020) generated from his samples are used in the results and discussion to generate a paleo-environment. To read the full methodological details of his analysis there is referred to the parallel thesis of Ding (2020).

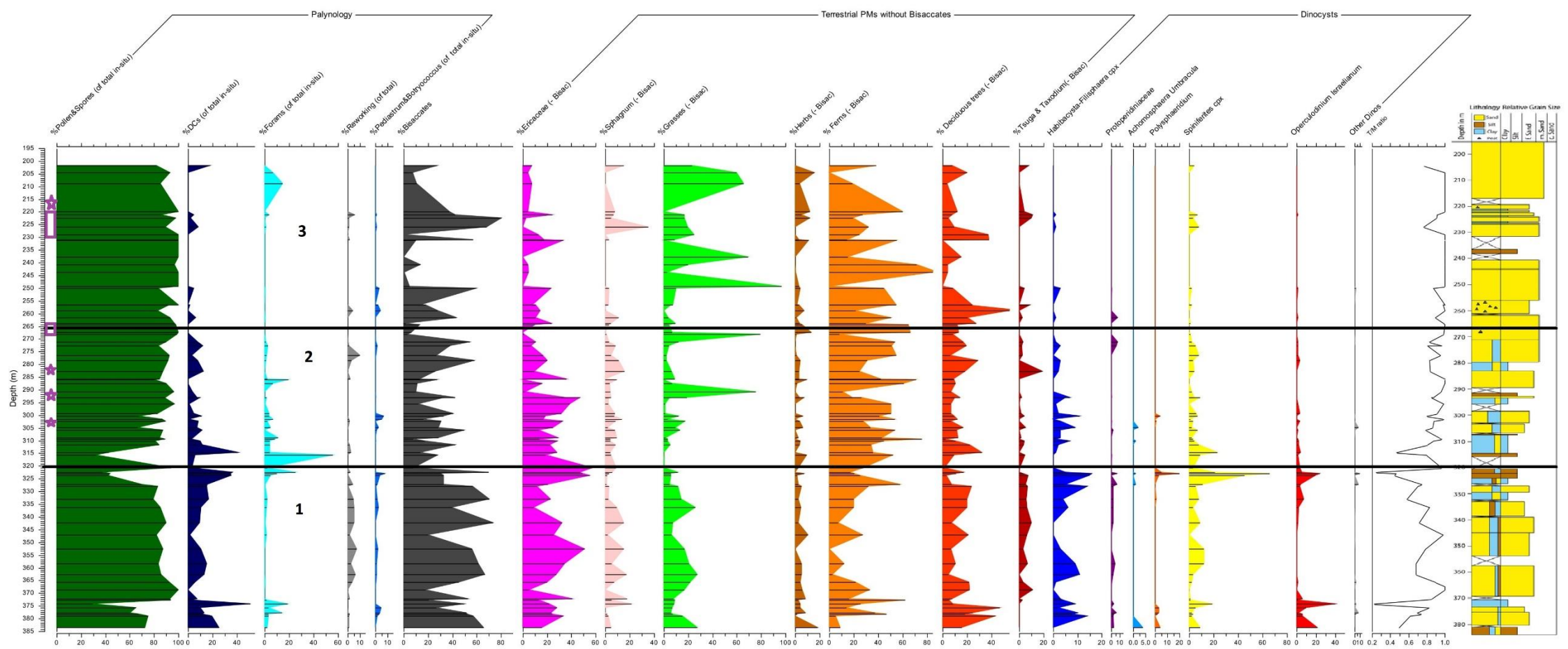

Figure 9 All counted data subdivided into three groups: Palynology, Terrestrial palynomorphs without bisaccates and dinoflagellate cysts. On the right side the T/M – ratio and the lithology is presented. The two red lines indicate the three different intervals. Possible hiatus are marked with a purple star or a purple square.

4. Results and Interpretation

Figure 9 indicates the percentages for all the data from 195 till 385 m, this figure is divided into three groups: Palynology, Terrestrial Palynomorphs without bisaccates and Dinoflagellate cysts. The samples numbers and depth are represented in Appendix A.

4.1 Composition of palynological associations

The interval below 200 m is characterized by shallow marine to estuarine conditions, indicated by the presence of dinoflagellate cysts and brackish to fresh-water tolerant algae like *Botryococcus* and *Pediastrum* (Houben, 2019).

The Palynology group is a 100% sum and includes Pollen&Spores, Dinoflagellate cysts, Forams, Reworking and Pediastrum&Botryococcus. The Pollen&Spores indicates the terrestrial pollen, the dinoflagellate cysts represent the marine environment, the foraminifera indicate the brackish environment, reworking explains something about influence of erosion, weathering or river incision and Pediastrum&Botryococcus indicates the fresh-water input. The first observation is the lack of dinoflagellate cyst near the top of the core, barely any dinoflagellate cysts is counted.

First, the absolute data is observed because the percentages indicates sometimes a distorted overview. The minimum of 200 palynomorphs is not reached for every sample, for some samples a very high percentage is indicated while just a few pollen or dinoflagellate cysts were counted. Not every sample is presented in the figure because for the samples, counted by Donders and Houben, the marker *Lycopodium clavatum* is unknown. Figure 10 shows a higher amount of terrestrial palynomorphs in comparison with marine palynomorphs for most of the samples. One explanation for the difference between the amount of material could be better preservation of the terrestrial palynomorphs. The dinoflagellate cysts do not preserve very well in sandy environments as indicated by the lithology. The highest concentrations for both are observed in silty and clayey environments. The silt and clay layers variating, which indicate that preservation and sedimentation rates as variables.

Figure 9 is subdivided into three intervals based on the Pollen&Spores and dinoflagellate cysts relative abundances. Interval 1, the lowest part of the core, has a dominance in marine palynomorphs. This interval has high percentages of dinoflagellate cysts in comparison with other parts of the core. Based on the lithology, the second interval is dominated by a tidal environment, a lot of variation in the lithology figure is observed. Also, the Pollen&Spores and Dinoflagellate cysts show a lot of variations. Another indicator of a tidal environment is the presence of foraminiferal linings, who live in shallow marine environments (Avnaim-Katav et al., 2013). The assumption of a tidal environment can be supported by the lithology, a lot of variation is observed in sediment size and material. The alternation between the sediment sizes and material indicates a high-energy system which is typical for a tidal environment. Interval 3 is dominated by Pollen&Spores > 85% and indicates a terrestrial environment, for this interval the dinoflagellate cysts are almost absent.

The next graphs are the Pediastrum&Botryococcus, *Pediastrum* and *Botryococcus* are indicators of fresh water input (Ranga Rao et al., 2007; Evitt, 1963). The highest dominance of these algae are observed in the lower (1) and middle (2) interval. This is also an indication for the lowest interval (1), it indicates not a fully dominance in marine environment, also terrestrial palynomorphs and fresh water input is present. The relative high presence of *Pediastrum* and *Botryococcus* for Interval 2 are a good indicator of fresh water input during a tidal environment.

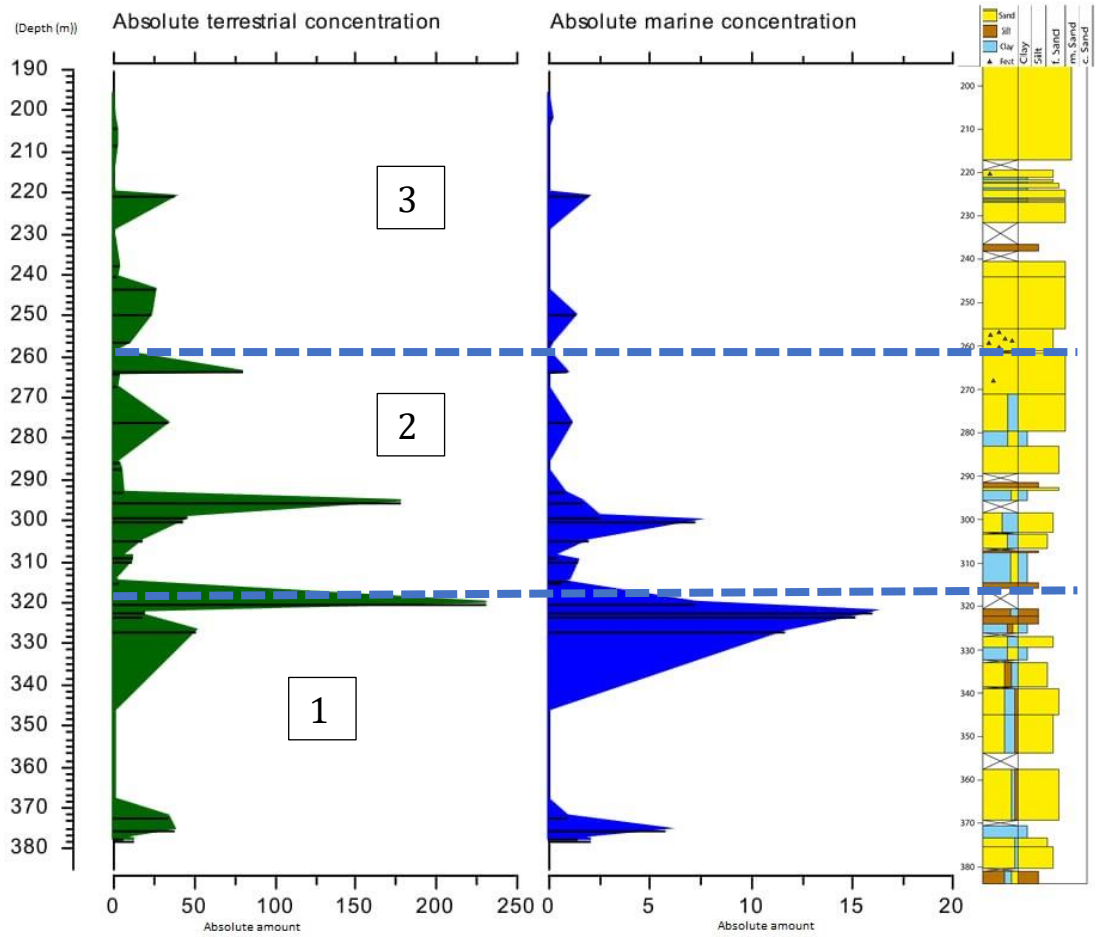

Figure 10 Absolute concentration of terrestrial and marine concentration. On the right side the lithology, the graph is subdivided into three intervals.

Reworked material is deposited by rivers, which incised into older layers. Most of the recognised reworked material is marine material. The highest percentages are observed in Interval 1, the lower part of the core. A possibility to distinguish the reworked material from other marine material is to their well-established timing of extinction (Houben, 2019). Most of the reworked material are from the Eocene – Oligocene period (e.g. Wetzeliella cpx and Homotryblium), however, older material from the Jurassic (*Callialasporites* spp., *Tasmanites* spp.) and the Carboniferous (*Denospora* and Crassispora *kosankei*) is also observed. Sometimes it is hard to distinguish in-situ and reworked material because several dinoflagellate cysts presented in Eocene – Oligocene period are still extant (*Brigantedinium* spp., *Lingulodinium* spp., *Operculodinium* spp., and *Spiniferites* spp.) (Houben, 2019).

It makes more sense to make a distinction between reworked and in-situ pollen. Only *Picea* and *Pinus* are observed as reworked material by their darker colour in comparison with in-situ material. However, several species are now absent from Europe, but have survived elsewhere, for example *Carya* in China and *Tsuga* in North America (Leroy, 2007). Figure 8 indicates the palynological ranges for *Taxodium*, *Tsuga*, *Nyssa* and *Carya*/*Juglans*. *Nyssa* and *Carya* extinct at the base of the Pleistocene (2.58 Ma) (Lang, 1994). For *Taxodium* is it hard to mention the exact timing of extinction. This data can help to make a distinction between reworked and in-situ material for the pollen.

4.2.1 Terrestrial/Marine – ratio

The T/M – ratio (Figure 9) is subdivided into the same three intervals according to the dominance of the terrestrial versus marine palynomorphs. Interval 1, the deepest part (385 –

320 m) has a low T/M – ratio, the marine component exceeds the terrestrial component. The second interval (320 – 265 m) indicates a lot of fluctuations between the marine and terrestrial component. A trend towards a more terrestrial dominance is observed. Interval 3 (265 – 195 m) is dominated by terrestrial palynomorphs, confirmed by the high T/M – ratio.

Two peaks (1 and 3) have extreme low values located at a depth of 374.15 and 322.45 m. After the first peak (1) a sharp increase is observed towards a more terrestrial dominance, however, directly after this incline a slowly decline is observed towards a more marine dominance. Peak 4 is the last peak with a very low T/M – ratio, located at a depth of 314.80 m. Going upwards in the core, the ratio remains relatively high, one specific peak (5) in the most upper part of the core is observed.

The T/M – ratio can also represent the glacial/interglacial – cycle, lower T/M – ratio indicates interglacial periods with marine conditions, while high T/M – ratio indicates glacial periods with a dominance in terrestrial palynomorphs and a lack in marine conditions.

4.2 Composition of pollen and spore assemblages

The second part of the graph (Figure 9) presents the terrestrial palynomorphs without bisaccates. The bisaccates are excluded from the percentage sum because of the Neves effect. The Neves effect means to counter effects of sea level change on the diverse transport capacity of pollen (Dearing Crampton-Flood, 2020). The terrestrial palynomorphs are subdivided into different groups (Table 4). These groups are sorted from cold to warm, left to right respectively.

Interval 1 shows very high percentages for Ericaceae, while for other groups at some depths a peak is observed. The grasses and ferns group indicate a cycle with very clear peaks and troughs. Another observation is the relative high percentage (~10%) of *Tsuga* and *Taxodium*. Interval 2 is mostly dominated by ferns, the whole interval a high percentage of ferns is observed. The *Ericaceae* are still high, however, a declining trend is observed. Two remarkable peaks are observed in the Grass graph, those two peaks are observed at a depth of 290.65 and 268.10 me. Those peaks in the grasses return four times during Interval 3, respectively at a depth of 250; 237.80; 229.10 and 208.70 m. The deciduous forest and ferns have also some peaks in the interval. The Tsuga&Taxodium is observed twice.

The pollen assemblages show some climatic patterns, with open landscapes during glacial periods and landscapes covered by vegetation during interglacial periods (Leroy, 2007). Overall, the pollen assemblages are dominated by fern pollen, particularly *Dryopteris*. The lower part has increasing proportions of Ericaceae and the upper part increasing proportions of grasses. The bisaccates assemblage (Figure 9) decreases in the upper part, with one large peak (222.40 m) near the top of the core.

Interval 1 and 2 shows gradual patterns, while going upwards the pattern become less gradual and abundance peaks are sharply delineated. The switch to another more dominance genus is more abrupt in the upper part in comparison with the lower part.

Table 4 Indication of different genus and family of the terrestrial palynomorphs

Group	**Genus**	**Family**
Ericaceae	*Ericales*	
Sphagnum	*Sphagnum*	
Grasses		*Cyperaceae, Poaceae*
Herbs	*Artemisia, Asteraceae, Caryophyllaceae, Chenopodiaceae, Liliaceae, Malvaceae, Nymphea, Succisa, Thalictrum, Urtica*	
Ferns	*Dryopteris, Lycopodium spp., Osmunda, Pilularia, Pteridium*	
Deciduous trees	*Abies, Acer, Alnus, Betula, Carpinus, Carya, Corylus, Fagus, Fraxinus, Juglans, Nyssa, Ostrya, Pterocarya, Quercus, Salix, Tilia, Ulmus*	
Tsuga and Taxodium	*Tsuga, Taxodium*	

4.2.1 Tree assemblages

The complete data of tree assemblages is presented in Appendix H. The most dominant tree species are: *Alnus*, *Betula* and *Quercus*. The Quercus is the dominant tree species for Interval 1, with percentages of 20%. *Corylus* (368.60 m) and *Alnus* (378.90;365.60 and 347.10 m) also have some distinct peaks. Interval 2 is again dominated by *Quercus* and *Betula*. Also, two small peaks in *Nyssa* (282.80 m) and *Taxodium* (282.80 m) are observed. Interval 3 can be subdivided into three parts, with a dominance in *Alnus* (256.60; 243.80 m), *Betula* (216.40 m) and *Quercus* (204.60 m). Also, a peak in *Corylus* (243.80 m) and *Carya* (243.80 m) is observed. Other observations are the small peaks in *Fagus* (263.82 m), *Ostrya* (375.60 m) and *Salix* (308.90 m).

Figure 11 indicates the differentiation in angiosperm (flowering plants) and gymnosperms (seed-producing plants). The angiosperms include: *Alnus, Betula, Carpinus, Carya, Corylus, Fagus, Fraxinus, Juglans, Nyssa, Ostrya, Pterocarya, Quercus, Salix* and *Ulmus*. The gymnosperms include *Juniperus, Picea, Pinus, Pinus* haploxylon type, *Taxodium* and *Tsuga*. The gymnosperms include the bisaccates, however, because of the high abundance in bisaccates, also a graph with gymnosperms without *Picea* and *Pinus* is presented. This graph indicates that most of the gymnosperms are *Picea* and *Pinus*. An overall increasing trend is observed in the angiosperms and during periods with a low total of trees a dominance in angiosperms. However, in comparison with the bisaccates, the angiosperms are relatively low in abundance.

The base of Interval 1 is dominated by angiosperms, but with decreasing dominance. *Picea* and *Pinus* have the highest occurrence during this period. One small peak in the gymnosperms is observed at a depth of 368.60 m. The next interval is again dominated by angiosperms, with one large peak in the gymnosperms at a depth of 282.80 m. The angiosperms have a higher abundance in comparison with Interval 1. Interval 3 is dominated by large peaks in the angiosperms and samples without *Picea* and *Pinus* (237.80 m). The gymnosperms do not have a relevant dominance during this interval.

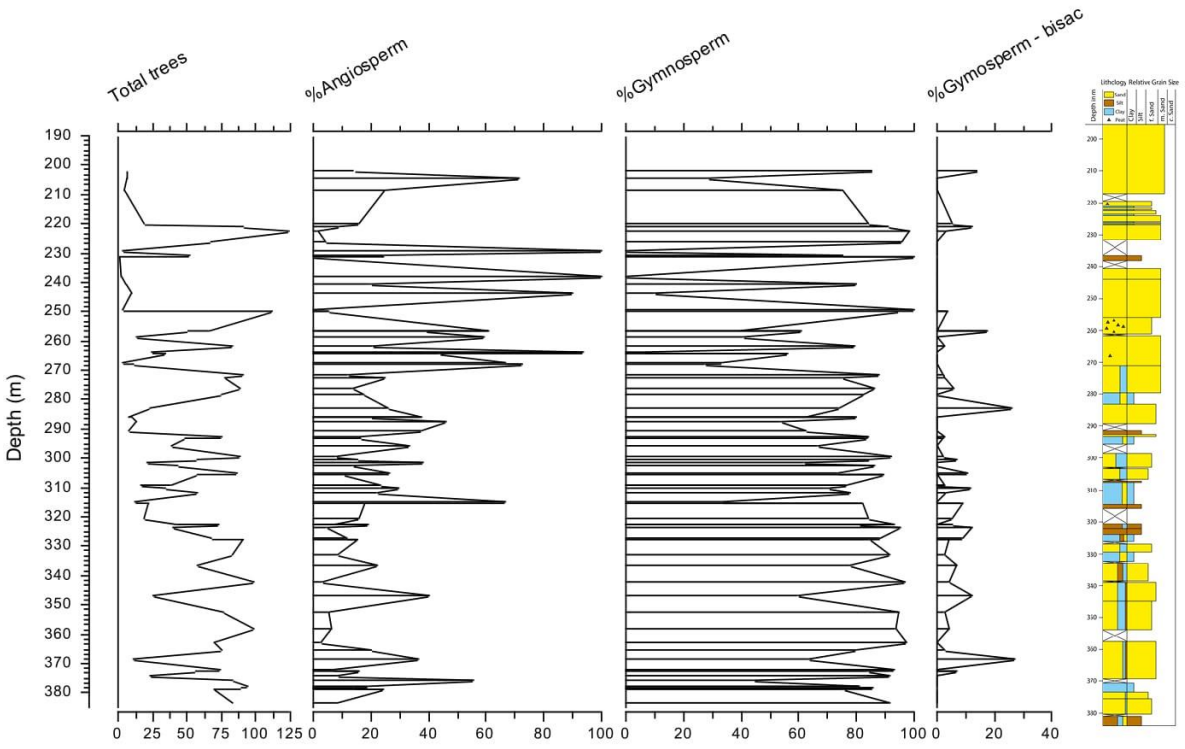

Figure 11 Indication of the angiosperms, gymnosperms and the gymnosperms without bisaccates (Picea and Pinus). On the left side the total trees is presented. The other values are presented in percentages.

4.3 Composition of organic walled dinoflagellate assemblages

The dinoflagellate cyst group is subdivided in cold and warm genera (Table 5, Table 6). Mainly in the upper part, not enough dinoflagellate cysts were counted to present a balanced overview of the environment. Therefore, the total amount of dinoflagellate cysts counted is presented instead of the percentages.

Table 5 Explanation of different dinoflagellate cyst groups

Group	**Genus**
Habibacysta-Filisphaera cpx	*Bitectatodinium tepikiensis*, *Filisphaera* cf, *Filisphaera* spp., *Habibacysta* spp.
Operculodinium israelianum	*Operculodinium israelianum*
Protoperidiniaceae	*Brigantedinium* spp., *Selenophemphix brevispinosum*
Spiniferites cpx	*Achomosphaera andalousiensis*, *Spiniferites* spp.
Other dino	Dino indet, Dino indet cold, Dino indet warm, *Lingulodinium machaeophorum*, *Operculodinium centrocarpum*, *Operculodinium eirikianum*, *Operculodinium tegillatum*

Interval 1 is dominated by marine palynomorphs and has the highest amount of dinoflagellate cysts for the whole core. Three peaks (378.90; 362.70 and 327.90 m) are observed for the *Habibacysta-Filisphaera* cpx, those peaks have a count of about 15 dinoflagellate cysts. The Protoperidiniaceae, *A. umbracula* and Polysphaeridium do not have distinct peaks with a maximum of 5 dinoflagellate cysts. Spiniferites cmx has four peaks (374.10; 358.30; 342.30 and 322.80 m) with different amounts (~20 – 70). *O. israelianum* has three distinct peaks (383.60;

374.10 and 322.80 m) with amounts of 40. The warmer species are more dominant for the first interval, however, between 370 and 335 m the *Habibacysta-Filisphaera* cpx is more dominant or only *Spiniferites* cpx is found.

For Interval 2, the marine dominance slowly decreasing, also indicated by Figure 9 where the amount of dinoflagellate cysts decreases going upwards in the core. Between 310 and 290 m, *Habibacysta-Filisphaera* cpx has a dominance with an amount of 10 dinoflagellate cysts. The A. *umbracula* has its last occurrence in this interval at a depth of 304.90 m. The *Spiniferites* cpx decreases in amount from a distinct peak at the border of the interval with almost 60 dinoflagellate cysts, to around 10 dinoflagellate cysts at the end of Interval 2. The *O*. *israelianum* does not have distinct peaks, an indication of going towards a colder environment. *O*. *israelianum* is a tropical species and like to live in equatorial regions (Zonneveld et al., 2013).

Interval 3 has just one peak in the *Spiniferites* cpx and a few small peaks in the *Habibacysta-Filisphaera* cpx. Almost no dinoflagellate cyst are counted for this interval.

Figure 12 presents the absolute concentration for the cold, warm and heterotrophic conditions. Between 330 and 320 m, a very high amount of warm – temperate dinoflagellate cysts are observed. Around this peak (323.70 and 300.30 m) high amounts of cool-indicating dinoflagellate cysts are observed. The heterotrophic dinoflagellate cysts have two distinct peaks (327.30 and 250.00 m). Heterotrophic dinoflagellate cysts are cosmopolitan in distribution and live in coastal waters (Jeong, 1999). High values of heterotrophic dinoflagellate cysts indicate high primary productivity, those peaks should agree with the peaks in Barium based on XRF data reported in Ding (2020).

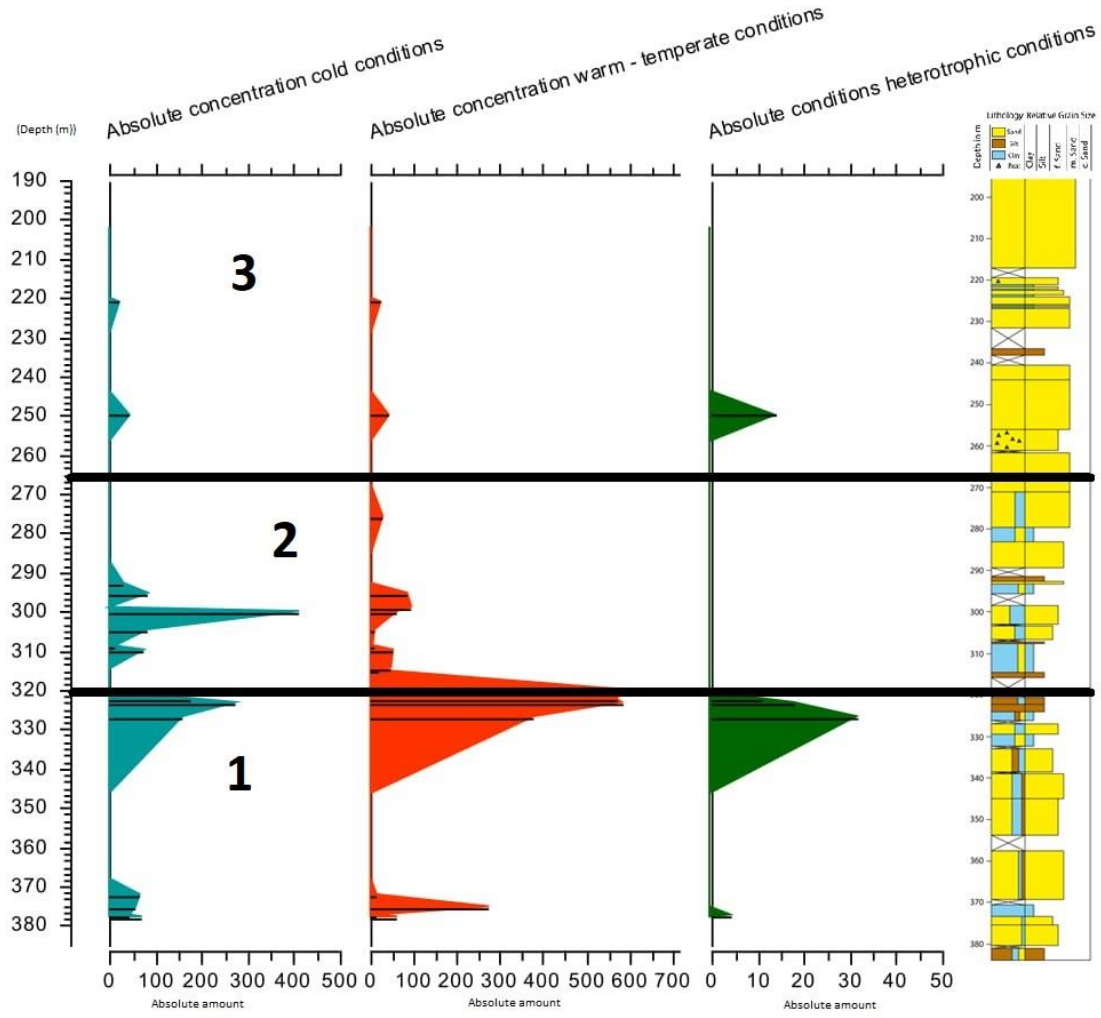

Figure 12 Absolute data cold, warm-temperate and heterotrophic conditions dinoflagellate cysts

Table 6 Indication of the environment based on dinoflagellate cysts

Depth (m)	Cold	Warm	Hetero trophic	Dinoflagellate cyst	Amount	Indication
221,20	1	1	0	*Bitectatdoinium tepikiensis* *Operculodinium israelianum*	1 1	Inconclusive
250,00	3	3	1	*Operculodinium israelianum* *Habibacysta* spp. *Achomosphaera andalousiensis* group *Operculodinium israelianum* *Protoperidinium* cpx	1 3 2 1 1	Inconclusive
276,40		2		*Operculodinium israelianum* *Achomosphaera andalousiensis* group	1 1	Inconclusive
295,55	1	1		*Operculodinium israelianum* *Bitectatdoinium tepikiensis*	1 1	Inconclusive
299,20		4		*Operculodinium israelianum* *Achomosphaera andalousiensis* group	3 1	Inconclusive
300,25	13	2		*Bitectatodinium tepikiensis* *Habibacysta* spp. *Achomosphaera andalousiensis* group	2 11 2	Cold
304,90	9	1		*Habibacysta* spp. *Achomosphaera andalousiensis* group	9 1	Cold
308,95	3	1		*Bitectatdoinium tepikiensis* *Achomosphaera andalousiensis group*	3 1	Inconclusive
309,30	1	1		*Operculodinium israelianum* *Habibacysta* spp.	1 1	Inconclusive
310,05	7	5		*Operculodinium israelianum* *Habibacysta* spp. *Achomosphaera andalousiensis* group	2 7 3	Inconclusive
314,75	1	12		*Operculodinium israelianum* *Bitectatdoinium tepikiensis* *Achomosphaera andalousiensis* group	4 1 8	Warm
315,55		3		*Operculodinium israelianum* *Achomosphaera andalousiensis* group	1 2	Inconclusive
320,75		5		*Operculodinium israelianum* *Achomosphaera andalousiensis* group	3 2	Inconclusive
322,80	16	52		*Operculodinium israelianum* *Filisphaera* spp. *Habibacysta* spp. *Achomosphaera andalousiensis* group *Lingulodinium machaeophorum* *Operculodinium centrocarpum* *Protoperidinium* cpx	24 2 14 25 1 2 1	Warm
323,70	15	32		*Operculodinium israelianum* *Filisphaera* cf *Filisphaera* spp. *Habibacysta* spp. *Achomosphaera andalousiensis* group *Protoperidinium* cpx	19 4 6 5 13 1	Warm
327,25	5	12	1	*Operculodinium israelianum* *Habibacysta* spp. *Achomosphaera andalousiensis* group	4 5 7	Warm

				Lingulodinium machaeophorum *Protoperidinium* cpx	1 1	
375,65	2	10		*Operculodinium israelianum* *Habibacysta* spp.	10 2	Warm
377,63	10	3	1	*Operculodinium israelianum* *Habibacysta* spp. *Achomosphaera andalousiensis* group *Protoperidinium* cpx	2 10 1 1	Cold
378,20	8	7		*Operculodinium israelianum* *Filisphaera* spp. *Habibacysta* spp. *Achomosphaera andalousiensis* group	6 3 5 1	Inconclusive

5. Discussion

The Terrestrial/Marine – ratio helps to indicate glacial/interglacial cycles and together with the bisaccates, indicates the relative distance from the shore. Bisaccate pollen are easily transported by the wind and their proportions gradually increase with distance from the shore, knows as the Neves effect. For other taxa, their proportions rapidly decrease when the distance of the shore increases. Donders et al., 2018 mentioned that bisaccate pollen are the component most sensitive to differential transport processes, yet regardless of whether it is included in the T/M – ratio the same patterns are recorded (Figure 15). During marine environments, the bisaccate pollen can be transported by the wind from the hinterland. Another possibility to explain a high amount of bisaccate pollen is transportation by rivers. During cold periods, a lot of bisaccate pollen are produced and they preserve very well. The rivers transport the bisaccate pollen into the area and deposit them at the mouth of the river. This could be an explanation of the high peak at a depth of 220 m, because no marine environment is observed. However, during very cold periods, like in the Late Pleistocene (Starnberger et al., 2013), the bisaccates also disappear and only open environments are present (Leroy, 2011). Based on the vegetation succession of Leroy (2007) five possible glacial/interglacial cycles are observed in Figure 13.

5.1 Terrestrial ecosystem change

Leroy (2007) describes the most common cycle of vegetation succession in glacial/interglacial – cycles for the 41 kyr world (Chapter 3.3). Interglacial cycles are characterised by the presence of Tertiary relics such as *Pterocarya*, *Tsuga* and *Carya* (Gibbard et al., 1991). Open environments are an indication of a glacial period (Leroy, 2011). Those open environments are dominated by grasslands and sometimes scattered trees (Leroy, 2011). The possible glacial/interglacial cycles are indicated in Figure 13 and are based on the information of Leroy (2007). Interval 2 does not have very well expressed cycles, the indication of the environment can explain this phenomena. During a tidal environment, indicated by the presence of foraminifera and an alternated T/M – ratio, it seems logical that more erosion is observed during this interval. A tidal environment is a high energy environment where a lot of erosion take place. Hypotheses that most of the glacial cycles are eroded during this interval. The erosion could be observed by higher amount of reworking in comparison with the other two intervals or incomplete vegetation cycles are observed.

5.1.1 Indication of glacial cycles

The grasses indicate the coldest periods (Leroy, 2011), two kinds of grasses are included in the grasses graph: *Poaceae* (Grass) and *Cyperaceae* (Sedges). The *Poaceae* is the most common grass for the whole core and occurs mainly in open areas like wetland and tundra areas, while *Cyperaceae* is more related to wetlands (Leroy, 2011). Near the top of the core (Interval 3), the peaks in the grasses became very sharp. Appendix K and L include the graph of all pollen and spores and show that the sharp peaks are *Poaceae*. The peaks in Interval 1 have a more gradual pattern in comparison with the peaks in Interval 3. The pattern in Interval 1 follows the same pattern as the T/M – ratio, going upwards to Interval 3 the patterns are not the same anymore. To investigate the sharp peaks in the grasses peak, the comparison between the lithology, sediment element concentration made by Ding (2020) and the amount of pollen and dinoflagellate cysts is made (Table 7). The samples at a depth of 237.75 and 229.05 m have a very low recovery of pollen. Most of the pollen observed in these two samples is *Poaceae*.

To indicate if erosion is a good explanation of the sharp peaks in the grass graph, it is important to go a step further into the glacial/interglacial – cycle. The next step is a warmer environment where the ferns take over. The two most important species for the ferns are *Dryopteris* and

Osmunda. *Dryopteris* is most common in temperate disturbed areas, like river-areas (Leroy, 2011). *Osmunda* prefer a warmer environment and indicate a next step in the glacial/interglacial – cycle. Assuming Leroy (2011), *Dryopteris* is the second step in the glacial/interglacial cycle.

Table 7 Comparison physical, chemical and palynological data for the sharp peaks in the grass graph

Depth (m)	**Physical**	**Chemical**	**Palynological**	
			Pollen	Dino's
208,70	Fine to medium sand, very low recovery sections	Small raise in Sr and Ba	26 of which 17 *Poaceae*	0
229,05	Fine to medium sand, continuous deposition	No special signals	8 of which 2 Poaceae	0
237,75	Sand with fine gravel, low recovery section	No sample taken	13 of which 9 *Poaceae*	0
249,30	Medium sand, continuous deposition, but relatively low recovery	No special signals	61 of which 59 *Poaceae*	0
268,12	Fine to medium sand, continuous deposition	No special signals	93 of which 74 *Poaceae*	1

Table 8 shows the vegetation patterns for the sharp peaks in the grasses graph, only at a depth of 249.30 m (Interval 2) an open field vegetation is preserved. These open field environments are indications of very cold glacial periods, with a very low sea level and a high amount of grasses (Leroy, 2011). These periods are the ideal situation for weathering and erosion, one possibility is that, the pollen preserved during these periods, are already eroded by the rivers or wind. The hypotheses is that the sharp peaks in the grasses are caused by erosion or weathering during very cold glacial periods. The coldest periods are not preserved, this indicates that the coldest periods are eroded and the next step in the glacial cycle is preserved, indicated by the presence of *Dryopteris* and *Betula*, the ferns and deciduous forest.

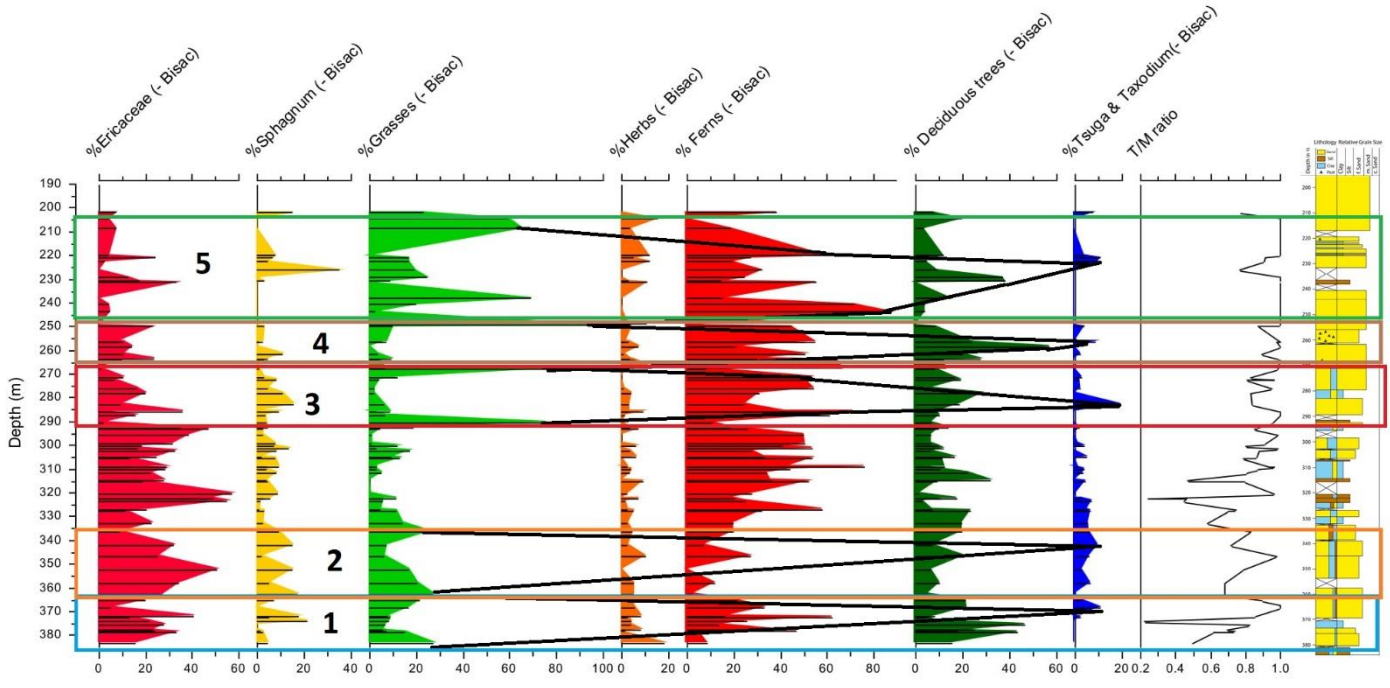

Figure 13 Indication of possible glacial/interglacial cycles found in the vegetation patterns. Each cycle has a different colour.

Table 9 shows the first peaks in *Dryopteris* just after the sharp peaks in the grasses. The second column indicates the amount of *Dryopteris* already present during the sharp peak. The third and the fourth column indicate the first peak in *Dryopteris* after the sharp peak and the amount of *Dryopteris* found in this peak. The last column is the sediment thickness between the two peaks. The table shows that not every possible glacial cycle is the same and not every glacial cycle is preserved that well. The depths with the high amount of *Dryopteris* (327.25; 264.25 and 243.85 m) are possible next steps in the glacial cycles. This indicates that at depth of 249.30 m a fully preserved glacial cycles starts.

The sediment thickness between the peaks is thicker in Interval 1 in comparison with Interval 2 and 3. One hypotheses is that more erosion took place in Interval 2 and 3, which could explain the thinner packages. Another hypotheses is the difference in sediment supply, this could be explained by the absolute amount of pollen. During periods with a high amount of pollen, a slow sediment supply is observed because relative a lot of pollen are found per gram. The highest peaks in absolute terrestrial concentrations are found at 320.80; 295.60;276.40; 264.80; 243.80 and 221.20 m. This could indicate, during the sharp peaks of 268.12 and 249.30 m, a slow sediment supply was observed. During the period of 268.12 till 243.85 m a very slow sediment supply was observed, however, not for every depth during this interval the slow sediment supply is the explanation, because for some samples the material is already eroded.

Table 8 Indication of the terrestrial environment during the sharp peaks in the grasses. The grey ones are from Interval 1, the green ones from Interval 2 and the yellow ones from Interval 3. (Cheno = Chenopodiaceae, Caryo = Caryophyllaceae)

Depth (m)	**Total**	**Ericaceae**		**Sphagnum**		**Herbs**		**Grasses**		**Ferns**		**Deciduous trees**		**Tsuga & Taxodium**	
208,70	26	*Ericales*	2	-	-	*Cheno*	1	*Poaceae*	17	*Dryopteris* *Osmunda*	4 1	*Quercus*	1	-	-
229,05	8	*Ericales*	1	-	-	-	-	*Poaceae*	2	*Dryopteris*	2	*Alnus*	2	-	-
237,75	13	-	-	-	-	-	-	*Poaceae*	9	*Dryopteris*	2	*Betula*	2	-	-
249,30	61	-	-	-	-	*Cheno*	2	*Poaceae*	59	-	-	-		-	-
268,12	93	*Ericales*	1	*Sphagnum*	1	*Artemisia*	1	*Poaceae*	74	*Dryopteris* *Osmunda*	7 1	*Alnus* *Betula* *Quercus*	2 3 1	-	-
290,65	45	*Ericales*		*Sphagnum*	2	-	-	*Cyperaceae* *Poacae*	1 33	*Dryopteris* *Osmunda*	4 1	*Alnus*	3	-	-
336,35	65	*Ericales*	6	*Sphagnum*	6	*Artemisia* *Asteraceae*	1 1	*Cyperaceae* *Poaceae*	2 15	*Dryopteris*	13	*Alnus* *Betula* *Carpinus* *Fagus* *Quercus*	5 2 1 1 2	*Tsuga* *Taxo*	2 2
362,70	40	*Ericales*	11	*Sphagnum*	7	*Caryo* *Cheno*	1 1	*Cyperaceae* *Poaceae*	2 9	*Osmunda*	1	*Corylus*	2	-	-
383,60	44	*Ericales*	7	*Sphagnum*	2	*Asteraceae* *Caryo* *Cheno*	2 3 3	*Cyperaceae* *Poaceae*	7 5	*Dryopteris* *Pteridium*	2 1	*Alnus* *Betula*	4 3	-	-

Table 9 Indication of the first peak in Dryopteris after the sharp peaks in the grasses. The grey ones are from Interval 1, the green ones from Interval 2 and the yellow ones from Interval 3.

Depth (m)	**Amount of *Dryopteris* for this depth**	**Depth of *Dryopteris* (m)**	**Amount of *Dryopteris***	**(m)**	
208,70	4	-	-	-	Erosion
229,05	2	221,20	21	7,85	Erosion
237,75	2	-	-	-	Erosion
249,30	0	243,85	177	5,45	Sed. Supply
268,12	7	264,25	76	3,87	Sed. Supply
290,65	4	287,45	33	3,20	Erosion
336,35	13	327,25	59	9,10	Erosion
362,70	0	347,05	11	14,65	Erosion
383,60	3	378,20	33	5,40	Erosion

5.1.2 Other vegetational patterns

Donders et al., (2018) describes that during interglacials the preservation of pollen increases, and more diverse tree pollen are observed, during glacials herb and heath pollen are indicative of open landscapes. The open environment is observed twice in the glacial/interglacial cycle, during very severe glacials and at the transition between glacials and interglacials (Leroy, 2011). Leroy (2011) mentioned that during the Early Pleistocene, open forests were observed. During glacial periods, the low temperatures were the limiting factors for the forests to grow (Leroy,2011). During the transitions to interglacials, also open forests were observed because trees needed time to grow (Leroy, 2011). During the Late Pleistocene, a complete open environment was observed (Zagwijn, 1989), during the Early Pleistocene, open environments are observed, however, during most of the time still some forest vegetation is presented.

The most common trees found in the samples are *Alnus*, *Betula* and *Quercus* (Figure 14). *Alnus* prefers wet sites and cannot react well to quick climate changes (Pliura, 2004). *Betula* has the lowest occurrence of the three dominant species, however, it is a pioneer tree in the glacial/interglacial cycle (Miller-Rushing and Primack, 2008). At a depth of 383.60; 336.35; 268.12 and 237.75 m the *Betula* is already observed. This could be another indication that the cycles preserved in this core are not the coldest ones. Hypotheses is that only 249.30 m is a very cold glacial, the others are glacial periods because of the presence of *Ericales* and *Sphagnum*, but not the very cold ones because of the presence of the *Betula* and the *Alnus*. For the depth 336.35 m, already *Tsuga* and *Taxodium* are observed, indicates the end of a glacial cycle, so possibly almost the transition towards an interglacial.

Hypotheses for the vegetational patterns is that the glacial cycles are eroded, proved by the thinner packages, especially for Interval 2 and 3. Only one fully glacial cycle is observed, others are not completely preserved indicated by the presence of *Dryopteris* and *Betula*.

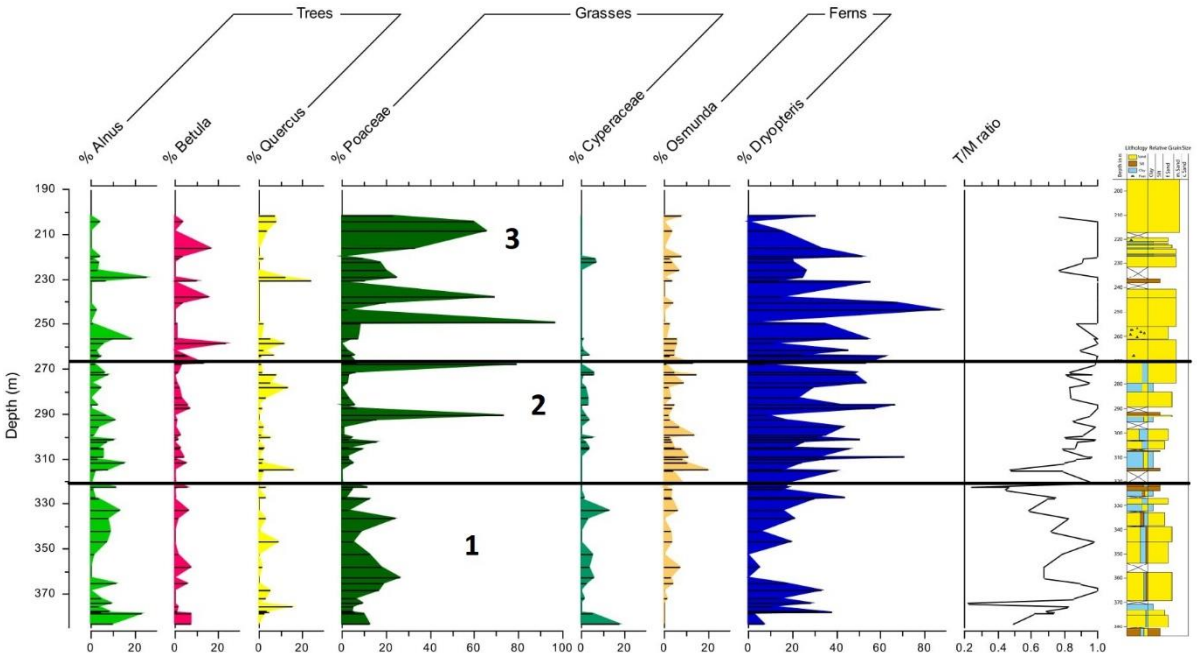

Figure 14 Most important species for the trees, grasses and ferns. Presented together with the T/M – ratio and the lithology.

5.2 Marine ecosystem change

The dinoflagellate cysts indicate the surface temperature of the marine-environment, the data of the dinoflagellate cysts is presented in Appendix I and J and Figure 15. Table 6 shows the amount of dinoflagellate cysts per depth and the indication of the environment based on the differentiation in cold and warm species. For some depths it is hard to interpret the environment because not enough dinoflagellate cysts are counted, or the abundance of warm and cold taxa are almost equal. Observed is a warmer period in Interval 1 and a colder and inconclusive for Interval 2 and 3. The higher number of inconclusive samples for Interval 2 and 3 could be explained by the fact of higher marine influence in Interval 1 in comparison with Interval 2 and 3.

In the upper part of Interval 1, a very high amount of warm dinoflagellate cysts is observed, which agrees with the further distance from the shore indicated from the bisaccates. Interval 2 starts with a colder period, which is also in line with the theory of a decreasing distance from the shore going upwards in the core.

5.2.1 Water depth indications

Ding (2020) have made an indication of the water depth based on the lithology and the geochemistry. The water depth is compared with the T/M – ratio and the amount of pollen and grass peaks (Figure 15). The two orange arrows indicate the same water depth based on both data sets. A very low ~0.2 T/M – ratio together with a high amount of warm – temperate dinoflagellate cysts (*Operculodinium israelianum (O. israelianum*)) and bisaccate pollen are observed. The *O. israelianum* occurs in warm subtropical regions and is restricted to full-marine regions (Zonneveld et al., 2013).

For the other indicated water depths, some inequalities are found between the palynological data, T/M – ratio and water depth. The yellow dotted box (~325 m), has a very low T/M – ratio of 0.23. The low ratio is caused by the high amount of dinoflagellate cysts found in this sample. However, most of the dinoflagellate cysts found in the core are *Spiniferites* cpx and *Protoperidinium* cpx. Two species of the Spiniferites are counted: *Spiniferites mirabilis* is found

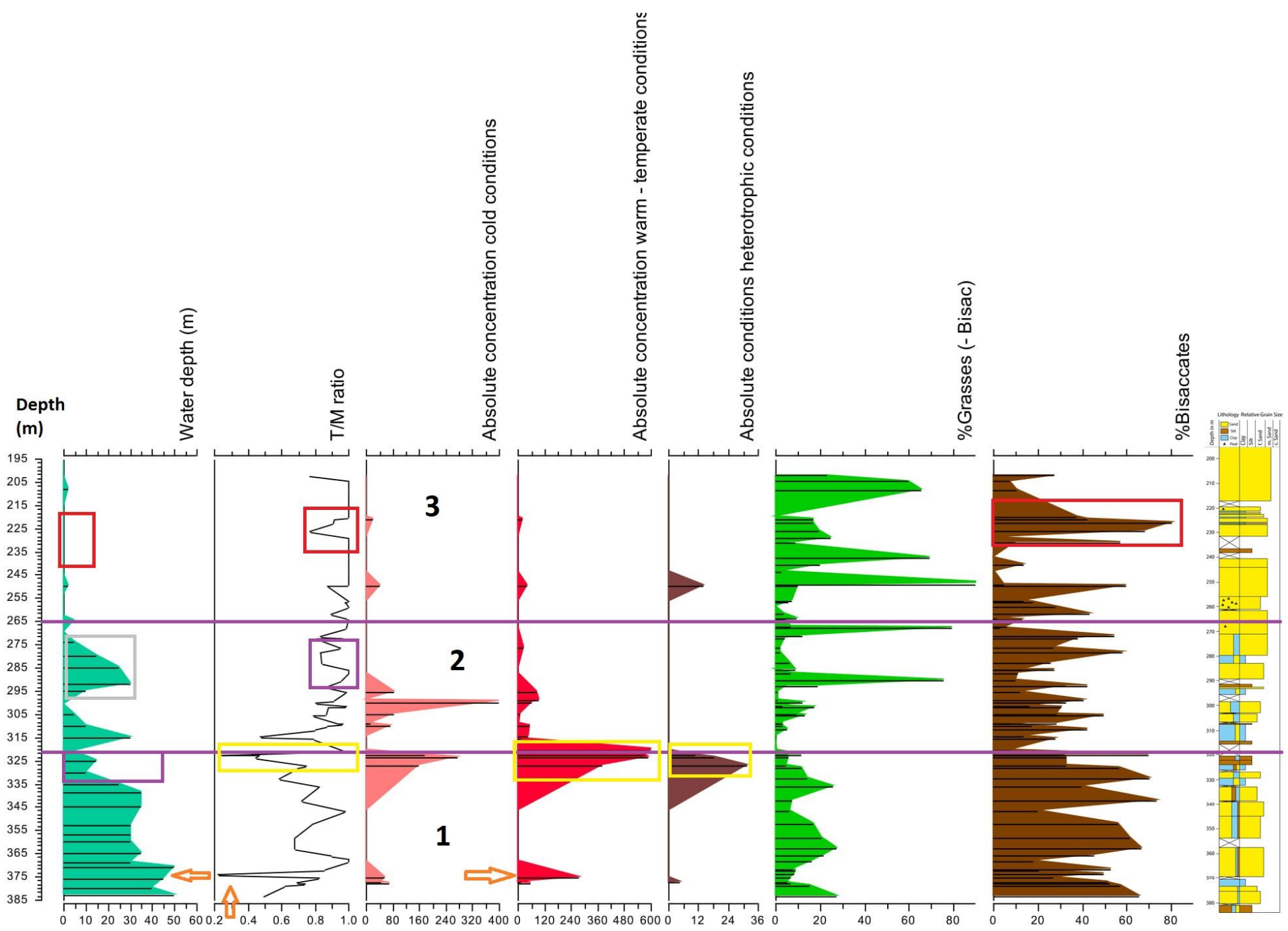

Figure 15 Comparison water depth with T/M - ratio, absolute amount of cold, warm-temperate and heterotrophic conditions and percentage grasses and bisaccates. On the right side the lithology is presented. The different squares are explained in paragraph5.2.1.

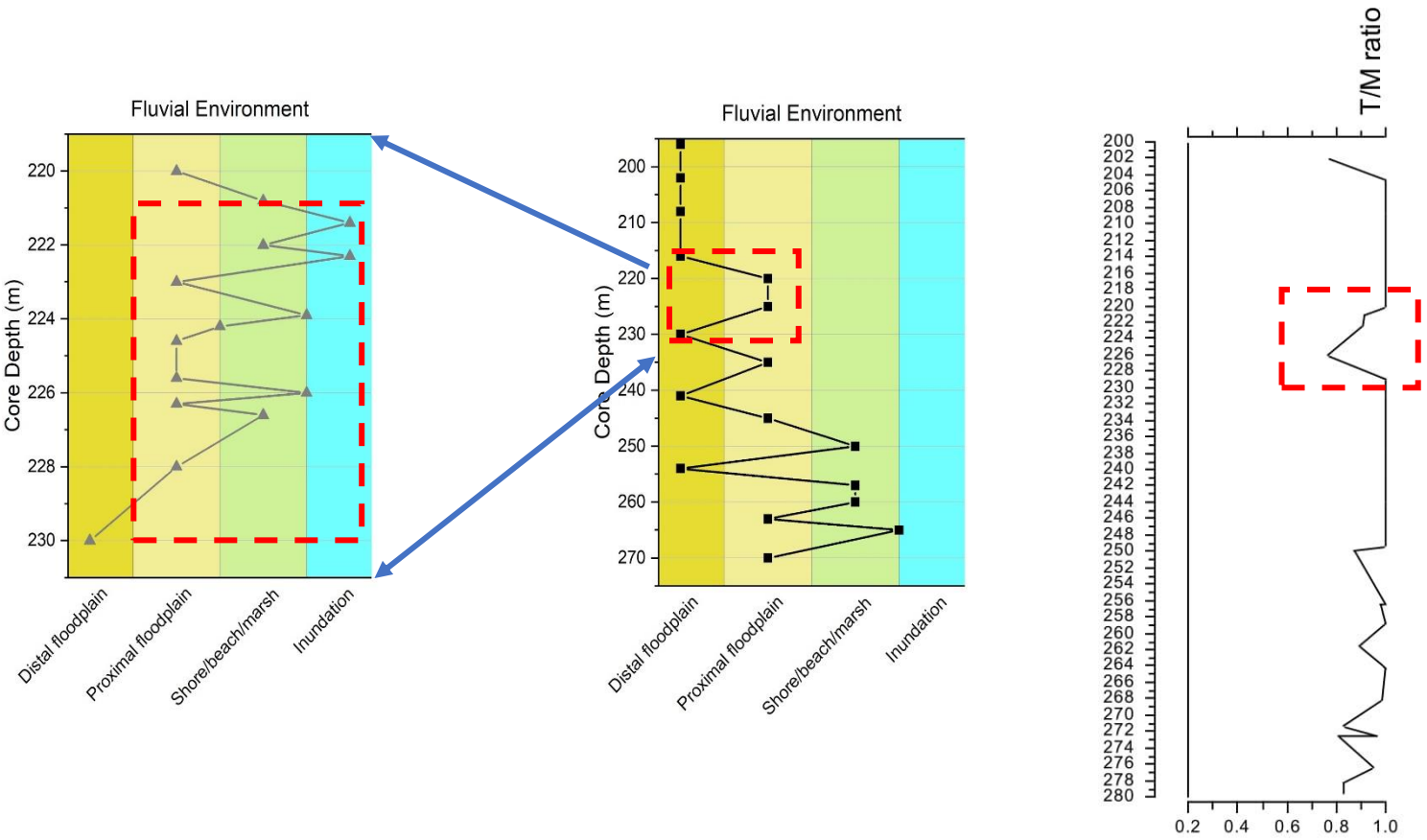

Figure 16 Water depth indication for Interval 3 (265 - 200 m)

in temperate to equatorial regions in coastal to open regions (Zonneveld et al., 2013) and *Spiniferites ramosus* is observed in sub-polar to equatorial regions with the polar front forming roughly the margins of its distribution in both hemispheres (Zonneveld et al., 2013). *Spiniferites* is not a good genus to indicate the environmental temperature because it was hard to distinguish the reworked and in-situ ones. For this sample, also a high number of foraminifera are observed (37), an indication of shallow marine environment. It is hard to conclude a water depth for this sample because an indication of deep open water environment and a high number of foraminifera are observed. The lithology indicates a silty environment, which is an indicator for a shallower water depth. The dinoflagellate cysts are possible deposited or reworked, as mentioned earlier, it is very hard to distinguish reworked and in-situ *Spiniferites*.

The purple dotted box (~280 m) indicates a deep water moment with a relative high T/M – ratio (0.83). The palynology indicates a high amount of pollen (85) and 12 dinoflagellate cysts, whereby most of the dinoflagellate cysts are *Filisphaera* spp., a cold-water genus. The lithology indicates a lot of alternation between sand, silt and clay, which can indicate a lot of variation in sea level. The palynological data contains a lot of *Dryopteris* and *Ericaceae*, an indication of colder environment. Considering this information, the deep water seems incorrect, a colder environment is more likely with a lower water level.

The most upper red dotted box (~226 m) has a T/M – ratio of 0.76 which is not in agreement with a water depth of almost zero indicated by Ding (2020). Ding (2020) had made a new water depth for the most upper part (Figure 16). The specific sample with the 0.76 ratio contains a high amount of bisaccate pollen, an indication of further distance from the coast. However, in combination with the explanation in paragraph 5.1.1 about the possible colder environments in the hinterland and the low amount of dinoflagellate cysts (9), a more terrestrial environment is suspected. The dinoflagellate cysts found in this sample are *Spiniferites* spp., which, mentioned before, the dinoflagellate cysts cannot give a good indication of the temperature. The most dominant pollen taxon for this depth, except the bisaccates, is *Sphagnum*, an indicator of a colder environment. Most of the observations indicate a colder terrestrial environment, the *Spiniferites*

are possibly deposited during a short inundation event more inland. The overall indication of proximal floodplain made by Ding (2020) seems supported by the palynology.

5.3 Correlation with Marine Isotopic Stages

The $\delta^{18}O$ – curve made by Lisiecki and Raymo (2005) is presented together with the T/M – ratio, to attempt to make a correlation between the BH-1 core and the MISs (Figure 19). The initial correlation is made by the age – indication of the Olduvai event. For this correlation, assumed is that the dating of the Olduvai is correct. Four glacial-interglacial cycles should be found between 355 and 322 m. The four cycles are not observed in the core, however, three cycles are found in the T/M -ratio. This indicates a sediment rate of:

$$Sedimentation\ rate = \frac{357.12 - 321.70\ (m)}{1.94 - 1.78\ (Ma)} = \frac{35.42(m)}{0.16\ (Ma)} = 221.375\ m/Ma$$

The sedimentation rate per year:

$$221.375\frac{m}{Ma} = 0.0002214\frac{m}{year} = 0.02\frac{cm}{year}$$

Donders et al., (2018) made an age model for the Early Pleistocene and found a sedimentation rate of 0.07 cm/year. The research area of Donders et al., (2018) is located more to the north in the Southern North Sea. Two hypotheses could be made based on those numbers:

1) The core used for this thesis had a lower sedimentation rate in comparison with the core Donders et al., (2018) used.
2) Due to erosion the sedimentation rate seems lower, the erosion removed a lot of material which was preserved earlier

The research area of Donders et al., (2018) is in the middle of the North Sea Basin, this area had not the influence of tidal systems and full terrestrial environments. As mentioned above, erosion is used as explanation for the missing glacial/interglacial cycles in the core used for this thesis. The erosion rate was possibly higher in this thesis' area, however due to the tidal systems and the terrestrial areas a lot of material disappeared. Hypothesis 2 seems the most logical hypotheses because of the erosion events observed above, however, it is not reasonable that hypothesis 1 is not true. It is hard to indicate the sedimentation rate without erosion, because it is not known what is missing. The red dotted box (Figure 19) could explain more about the erosion events observed in between the grass peaks. The $\delta^{18}O$ – data in this square is very heavy in comparison with other glacial periods. Supposed that the erosion between the grass peaks are caused by very severe glacials, possible those severe glacials are indicated by the red box. This is another prove for hypothesis 2, that an erosion event had removed a lot of material and lowered the calculated sedimentation rate.

Four cycles were observed in the MISs stack, three complete cycles are observed in the T/M – ratio. Possibly, the coldest one is eroded and not preserved in the core. However, between 355 – 322 m only one vegetation glacial/interglacial cycle is observed. Because more cycles are observed in the T/M – ratio graph, the smaller cycles are not observed in the vegetation cycle. This could be an indication that in the vegetation patterns only the large cycles indicate and not the smaller ones.

Another possibility is that the Reunion/Feni sub-chron is observed instead of the Olduvai event. The Reunion/Feni sub-chron started 2.2 Ma and has a duration of 0.38 Ma (Singer et al., 2014) (Figure 17). Five large glacial/interglacial cycles are observed in this period, however, during those cycles also a lot of colder periods are observed with heavier $\delta^{18}O$ – values are observed.

During the colder periods, again a lot of material could be eroded, which can explain that less than five glacial/interglacial cycles are observed in the data.

For further research, it is interesting to indicate the exact timing of the core, to indicate precise the missing glacial/interglacial cycles. With the known data, it is hard to make an exact correlation between the $\delta^{18}O$ – graph and the T/M – ratio.

5.4 Erosion and reworking events

To investigate possible erosion events, a link to the parallel thesis of Ding (2020) is made (Figure 18). He has assumed possible hiatus contacts based on the lithology in the core. The possible hiatus are also marked in Figure 9. Some erosion events might by simply resulted from sea level fluctuations, while others are from open field erosion. For a more extended explanation there is referred to the thesis of Ding (2020). Those depths are:

- 216.90 m
    - Contact shows the change from pure clay to medium sand given in fluvial sediment
    - Sample is taken in a very poorly recovered interval
    - Hypotheses: Very large erosion event
- 220 – 229 m
    - Regular pattern of sand and clay, each time when the lithology changes, erosion could occur
    - Amount of pollen changed from 8 (220 m) to 99 (228 m)
    - Hypotheses: Sand/clay pattern could be formed by sea level fluctuations, no indication of a large erosion event
- 264.60 – 267.45 m
    - Significant geochemistry change (highest S, Sr and Ba)
    - T/M – ratio is one
    - High Sr indicates a high marine productivity, however, a low amount of dinoflagellate cysts is observed
    - Exact at the dividing line between Interval 2 and 3
    - Hypotheses: Open field erosion or reworking
- 282.70 m
    - Abrupt change from pure clay to silt
    - Hypotheses: Storm, which could rework the deposition and only the relatively coarser grains were re-deposited again
- 293.05 m
    - Lithology changes abruptly from clay to fine sand
    - Hypotheses: Fluvial erosion due to sea level down
    - Abruptly after first sharp peak in grasses graph

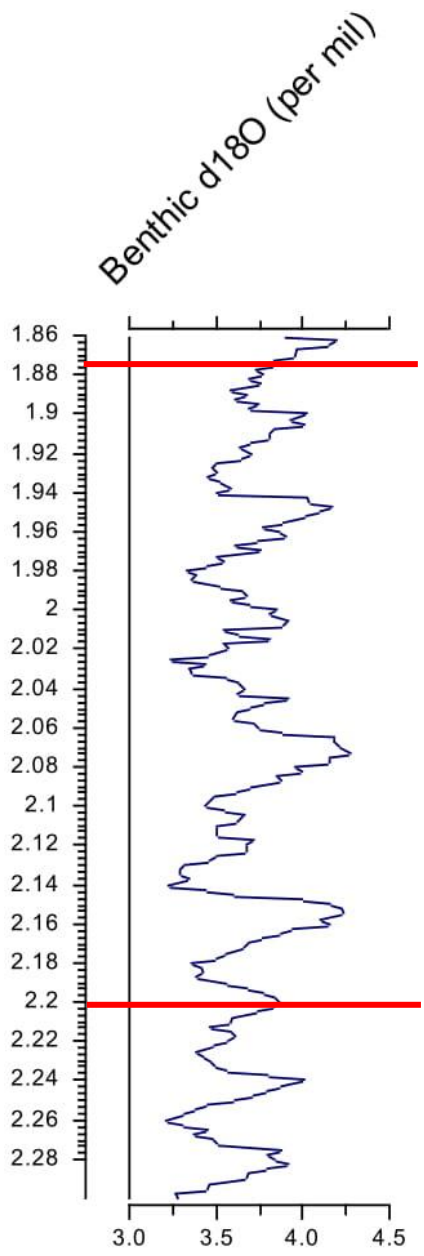

Figure 17 Benthic d18O for the Reunion event

- 302.70 m
    - Change from clay to fine sand, the clay section contains thin alternations with sand, formed in an intertidal environment and the fine sand is regarded as fluvial depositions
    - Hypotheses: Fluvial erosion

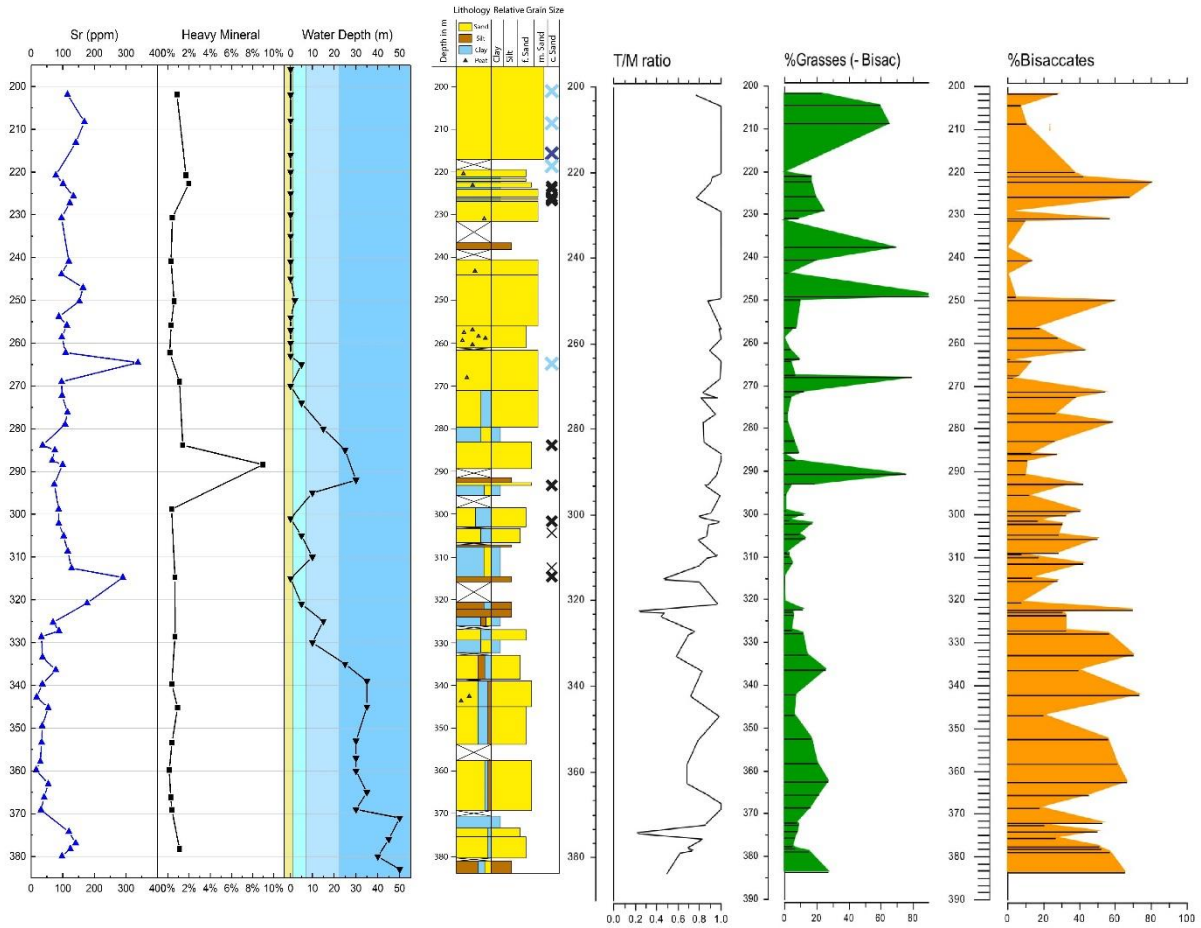

Figure 18 Combined figure with data from the parallel thesis of Ding (2020), Br, Heavy minerals and water depth. On the right side the T/M - ratio, percentage grasses and bisaccates

5.5 Pollen-based stratigraphy

The chronostratigraphic subdivision of Zagwijn (1992) was derived from short sections with only some biostratigraphy and (unreliable) palaeomagnetism and the presence of absence of some pollen taxa considered as chrono-stratigraphical markers (Westerhoff, 1998). The assumption is made that the subdivision is right, however, some remarkable findings are found in this core.

The Tiglian stage is located near the top of the Olduvai event and lasts from 2.40 – 1.80 Ma (van den Bergh and Kasse, 1989). If the Olduvai event recorded at Petten is right, it seems reasonable that the TC is present in the core. Figure 20 indicates the pollen species important for the different pollen zones, *Fagus*, *Artemisia*, *Ericales* and *Pterocarya*. The first observation is the peak in *Pterocarya* at the base of the core, this could be an indication of TC. In the upper part of the core (258,80 m) another peak in *Pterocarya* is observed, is the dating is consistent with an Olduvai age (including near absence of *Fagus*), it seems impossible that the upper peak is from the TC stage. However, it is not impossible that *Pterocarya* is in-situ present in the core because it goes extinct regionally after the Holstein interglacial (Sauer, 1988).

The second observation is the presence of the *Fagus* at a depth of 263.82; 327.95 and 336.35 m. Zagwijn had mentioned *Fagus* did not occur in the Netherlands after TA until the Holocene (Zagwijn, 1957). Only at a depth of 336.35 m, a high reworking event is observed, for the sample at this depth it seems reasonable that it is reworked. For the other two depths, just one or two pollen grains are found, which could also indicate that the *Fagus* pollen are reworked. Only for the 327.95 m, a reworked dinoflagellate cysts is observed, for the other depth no other reworked material was found. An explanation for the *Fagus* pollen at these two depths could be the observed shallow water depth. During these periods, a more terrestrial environment with rivers is present. The rivers could bring the reworked pollen to the research area. Another observation is the occurrence of both *Fagus* and *Pterocarya* at the same depth. As Westerhoff (1998) mentioned, the *Fagus* did not occur in the Netherlands until the Holocene, it seems not reasonable that both are in-situ.

5.5.1 Reworking events

Some pollen species are now absent in the Netherlands and Europe. For example, *Carya* and *Tsuga* completely disappear in the Netherlands during the Early Pleistocene (Leroy, 2007) (Figure 8). *Carya* is counted in 6 times in total in the core, not much than one time per sample. This could be an indication of reworking because, one pollen is not enough to assume that the tree has grown in the area. However, it is not completely sure if the *Carya* was darker or had a different colour, so it is not completely sure reworked.

At a depth of 267.40 m, a high amount of reworked *Picea* and *Pinus* is observed. These pollen were dark-brown and a very clear-distinction between in-situ and reworked *Picea* and *Pinus* could be made due to the colour differences.

Taxodium goes extinct at the basis of the Pleistocene (~2.58 Ma) (Donders et al., 2018) and *Tsuga* is present until Bavelian (~0.9 Ma) (Zagwijn, 1992). *Fagus* did not occur in the Netherlands until the Holocene (Westerhoff, 1998), but did not extinct completely in Europe in the Early Pleistocene. As indicated by Figure 9, both have a significant occurrence in the core. It is hard to mark if the pollen are in-situ or reworked, because no colour change was found in the different sample. An explanation of the high reworking is the presence of both pollen in the hinterland and deposited by the rivers.

Most reworked material is found in the dinoflagellate cysts (Appendix I), some dinoflagellate cyst originates from the Jura (210.30 – 145.00 Ma) or Cretaceous (145.00 – 66.00 Ma). The reworking is caused by the rivers that incised in older layers. For further research, it is interesting to investigate the origin of the reworked material. Known from the data of Ding (2020), the upper part is dominated by material from the Eridanos paleo-river, for the lower part it is unknown. The source of the Eridanos paleo-river is far north, so it had a very long transport road and can take a lot of material with it.

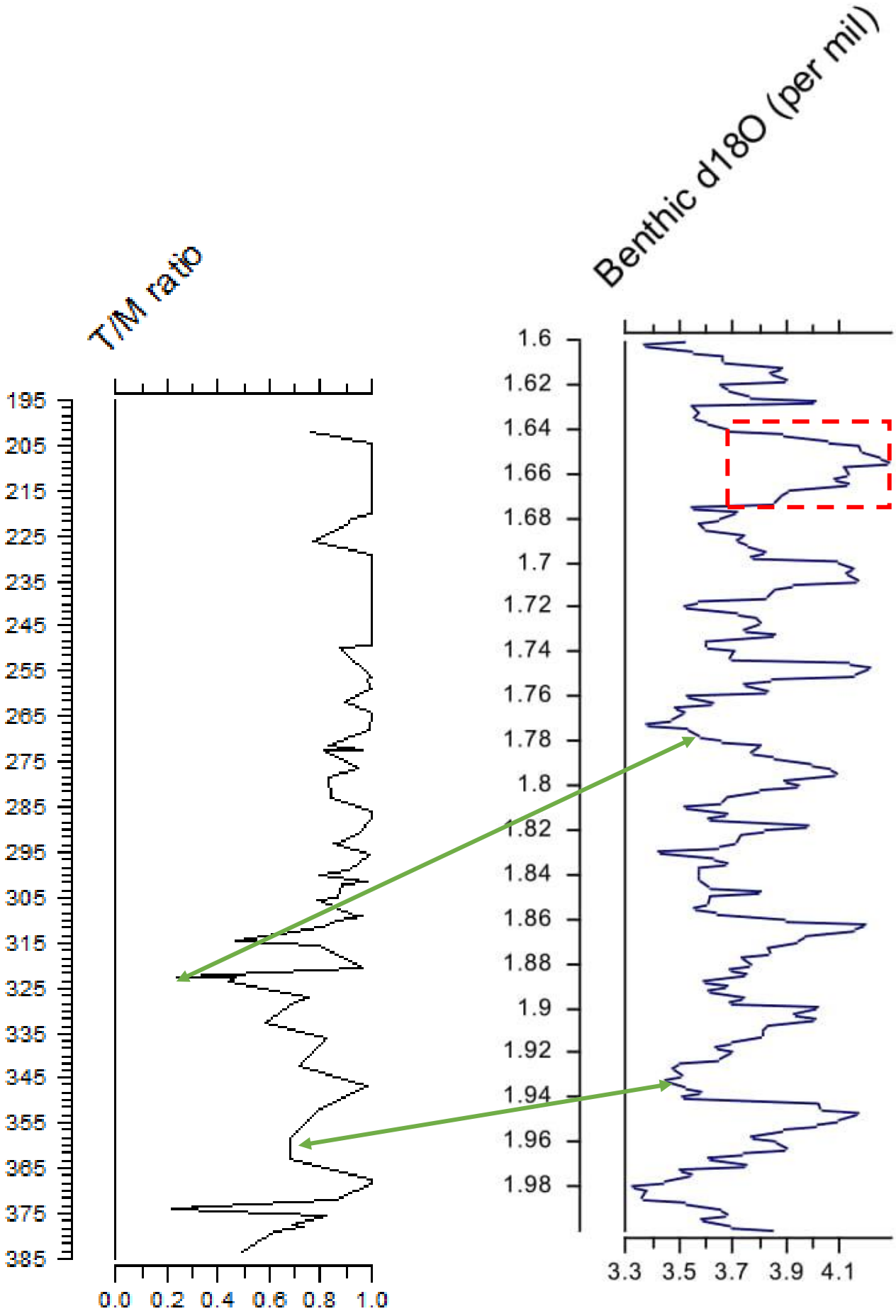

Figure 19 T/M - ratio presented together with the d18O - stack of Lisiecki and Raymo (2005). The two greens arrows are the known ages of the Olduvai - event. The red box on XX m is an indication of a severe glacial which can explain the erosion event

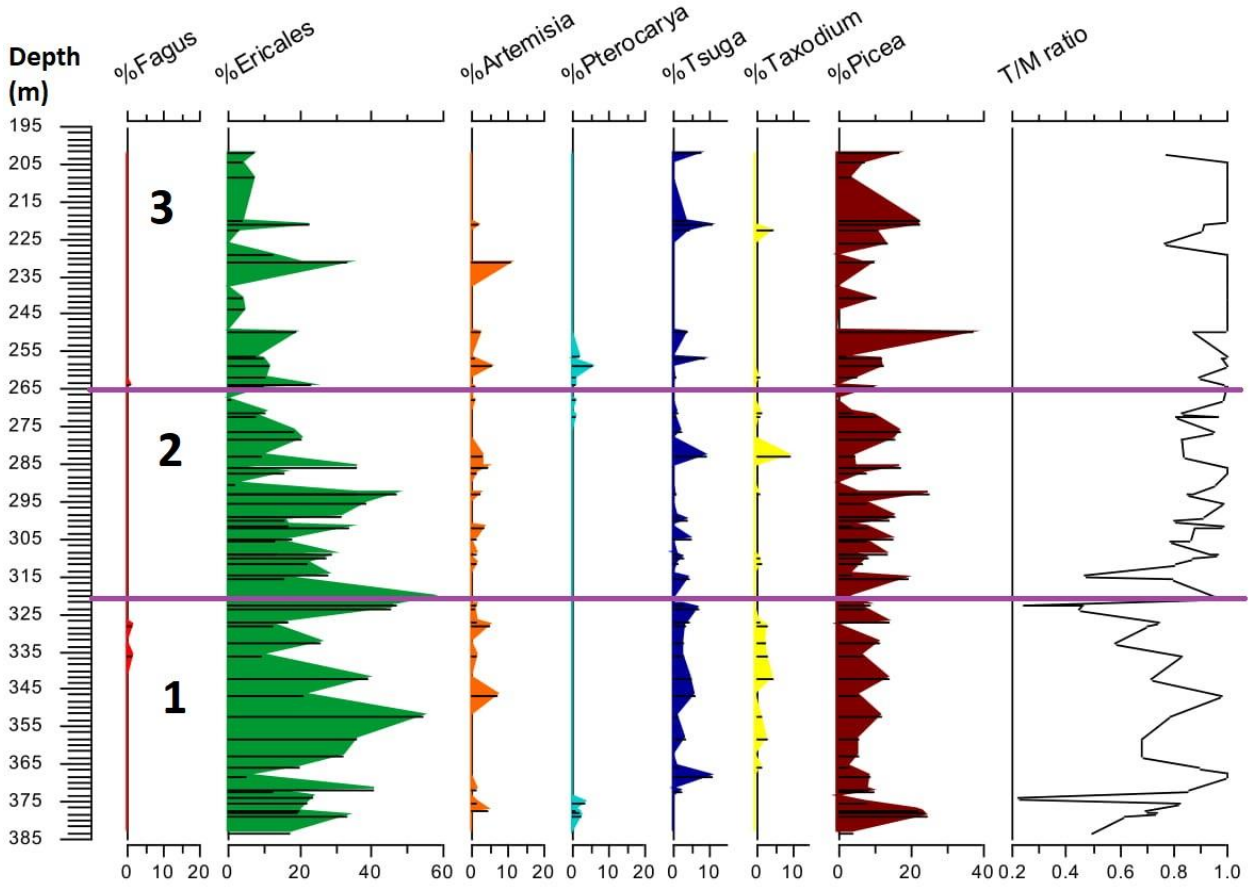

Figure 20 Import pollen for the subdivision of the Tiglian

Table 10 Amount of Fagus and Pterocarya

Depth (m)	Fagus	Pterocarya
256,55		3
259,80		1
261,65		1
263,82	1	1
268,12		1
272,65		1
327,95	1	
336,35	1	
375,65		5
377,63		1
378,20		2
378,90		1

6. Conclusions

The aim of this thesis was to reconstruct paleo-environmental changes and the alternation of the terrestrial and marine environments during the Early Pleistocene in the Southern North Sea. The paleo-environmental changes are based on vegetational patterns and ratios between terrestrial and marine components. The core is subdivided into three intervals, based on the T/M – ratio, percentages pollen and spores and percentages dinoflagellate cysts. The first interval (385 – 320 m) is dominated by marine palynomorphs and a low T/M – ratio. The second interval (320 -265 m) is dominated by a tidal environment indicated by the presence of a high number of foraminifera. The third interval (265 – 195 m) is dominated by terrestrial palynomorphs with a T/M – ratio of almost one.

Five glacial/interglacial cycles are observed in the vegetational data, the glacial cycles start with a high amount of grasses and some forest vegetation, an indication of an open field environment, typical for a glacial environment. However, different with the environment during the Late Pleistocene, where forest vegetation almost not occur during very severe glacials. Changing to an interglacial, the vegetation changes to fern, deciduous forest and Tsuga&Taxodium domination. The dinoflagellate cysts are almost not observed in Interval 3, for Interval 1 they are used to indicate warmer and colder periods. Interval 1 is dominated by a high amount of warm dinoflagellate cysts, Interval 2 has more alternation between the different species but is overall dominated by cold water dinoflagellate cysts. This is in line with the trend to a more terrestrial and colder environment.

The T/M – ratio is compared with the $\delta^{18}O$ – stack of Lisiecki and Raymo (2005) to correlate the glacial cycles with the MISs. Two possible correlations are made based on the known ages of the Olduvai event, found by Houben (2019). If these correlations are correct, for the lower part of sedimentation rate of 0.02 cm/year is observed. It is impossible to find the change from a 40 to a 100 kyr world, because of the high number of erosion events in Interval 2 and 3.

It is hard to recognise hiatus in the core, however, together with the lithological and geochemical data from the parallel thesis of Ding (2020), some hiatus and erosion events are observed. For Interval 1, the sedimentation seems continuous with some short-term reworking, while for the other two intervals a lot of erosion events are observed with quite some reworking. The erosion events are recognised by the sharp peaks in the grass graph in Interval 3.

A lot of reworking is observed for Interval 1, these reworking peaks are mostly dominated by dinoflagellate cysts from the Jura, Eocene or Cretaceous. An implication to find reworked dinoflagellate cysts is that some dinoflagellate cyst can be in-situ or reworked, because they have a long stratigraphic range. Most of the time they have the same colour of the reworked dinoflagellate cysts, so it was hard to distinguish for these dinoflagellate cysts the reworked and the in-situ ones. For the pollen data, it was hard to recognise reworking because they have a very long range and for a lot of pollen the exact extinction time is unknown. For further research it is interesting to indicate the origin of the reworked material. Some older layers are very close to the surface, so seems to be possible locations where the rivers incised into the older layers and deposited it into the basin.

For further research it seems interesting to investigate the dominance of the rivers. To investigate the material and to recognise the source of the material. Sampling on higher resolutions results in more detail in the glacial/interglacial cycles and a better correlation with the MISs.

References

Abbink, O.A., van Konijnenburg-van Cittert, J.H.A., Visscher, H. (2004) *A sporomorph ecogroup model for the Northwest European Jurassic Lower Cretaceousi: concepts and framework*. Netherlands Journal of Geosciences/Geologie en Mijnbouw 83 (1), 17 – 38.

Arz, H.W., Lamy, F., Ganopolski, A., Nowaczyk, N., Pätzold, J. (2007) *Dominant Northern Hemisphere climate control over millennial-scale glacial sea-level variability*. Quaternary Sceince Reviews 26, 312 – 321.

Avnaim-Katav, S., Almogi-Labin, A., Sandler, A., Sivan,D. (2013) *Benthic foraminifera as palaeonvironmental indicators during the last million years in the eastern Mediterranean inner shelf*. Paleogeography, Paleoclimatology, Palaeoecology Vol. 386, 512 – 530.

Birks, H.J.B., Birks, H.H., (1980). *Quaternary Palaeoecology.* Edward Arnold, London. 289 pp.

Busschers, F.S., Kasse, C., van Balen, R.T., Vandenberghe, J., Cohen, K.M., Weerts, H.J.T., Wallinga, J., Johns, C., Cleveringa, P., Bunnik, F.P.M. (2007) *Late Pleistocene evolution of the Rhine-Meuse system in the southern North Sea Basin: imprints of climate change, sea-level oscillation and glacio-isostacy*. Quaternary Science Reviews 26, 3216 – 3248.

Clark, P.U., Pollard, D. (1998) *Origin of the middle Pleistocene transition by ice sheet erosion of regolith*. Paleoceaongraphy, Vol. 13, No.1, pp 1- 9.

de Schepper, S., Head, M.J. (2009) *Pliocene and Pleistocene dinoflagellate cyst and acritarch zonation of DSDP hole 610a, Eastern North Atlantic*. Palynology, Vol. 33, 179 – 218.

de Vernal, A., Eynaud, F., Henry, M., Hillaire-Marcel, C., Londeix, L., Mangin, S., Matthiessen, J., Marret, F., Radi, T., Rochon, A., Solignac, S., Turon, J.-L., (2005*). Reconstruction of sea-surface conditions at middle to high latitudes of the Northern Hemisphere during the Last Glacial Maximum (LGM) based on dinoflagellate cyst assemblages*. Quat. Sci. Rev. 24, 897–924.

Dearing Crampton-Flood, E., Noorbergen, L.J., Smits, D., Christine Boschman, R., Donders, T.H., Munsterman, D.K., ten Veen, J., Peterse, F., Lourens, L., Sinninghe Damsté, J.S. (2020) *A new age model for the Pliocene of the southern North Sea basin: a multi-proxy climate reconstruction*. Clim. Past, 16, 523 – 541.

Drees, M. (2005) *An evaluation of the Early Pleistocene chronology of The Netherlands*. Vertebrate palaeontology, 1, 1.

Donders, T.H., Kloosterboer-van Hoeve, M.L., Westerhoff, W., Verreussel, R.M.C.H., Lotter, A.F. (2007) *Late Neogene continental stages in NW Europe revisited*. Earth-Science Reviews, 3 – 4, 161 – 186.

Donders, T.H., van Helmond, N.A.G.M, Verreussel, R., Munsterman, D., ten Veen, J., Speijer, R.P., Weijers,s J.W.H., Sangiorgi, F., Peterse, F., Reichart, G., Sinninghe Damsté, J.S., Lourens, L., Kuhlmann, G., Brinkhuis, H. (2018) *Land-sea coupling of early Pleistocene glacial cycles in the Southern North Sea exhibit dominant Northern Hemisphere forcing*. Climate of the Past, 14, 397-411.

Dodweswell, J.A., Ottesen, D., Rise, L. (2010) *Rates of sediment delivery from the Fennoscandian Ice sheet through an ice age*. Geology, V. 38, p 3 – 6.

Evitt, W.R. (1963) *Occurrence of freshwater alga Pediastrum in Cretaceous marine sediments*. American Journal of Science, Vol. 261. 890 – 893.

Gibbard, P.L. (1988) *The history of the great northwest European rivers during the past three million years*. Phil. Trans. R. Soc. Lond. B 318, 559 – 602.

Gibbard, P.L., West, R.G., Zagwijn, W.H., Balson, P.S., Burger, A.W., Funnell, B.M., Jeffery, D.H., de Jong, J., van Kolfschoten, T., Lister, A.M., Meijer, T., Norton, P.E.P., Preece, R.C., Rose, J., Stuart, A.J., Whiteman, C.A., Zalasieqicz, J.A. (1991) *Early and Early Middle Pleistocene correlations in the southern north sea basin*. Quaternary Science Reviews, Vol. 10, pp 23 -52.

Gibbard, P.L., Cohen, K.M. (2008) *Global chronostratigraphical correlation table for the last 2.7 Million years.* Episodes, Vol. 31, no. 2, pp 243 – 247.

Gradstein, F.M., Ogg, J.G., Schmitz, M., Ogg, G. (2012) *The geologic timescale 2012*. Elsevier

Graham, A.G.C., Stoker, M.S., Lonergan, L., Bradwell, T., Stewart, M.A. (2010) *The Pleistocene glaciations of the North Sea Basin*. Quaternary Glaciations, Extend and chronology, 2n edition.

Hays, J.D., Imbrie, J., Shackleton, N.J. (1976) *Variations in the Earth's Orbit: Pacemaker of the ice ages*. Science, Vol. 194, pp. 1121 – 1132.

Head, M. J. (1996) *Modern dinoflagellate cysts and their biological affinities*, in: Palynology: Principles and Application, Vol. 3, edited by: Jansonius, J. and McGregor, D. C., American Association of Stratigraphic Palynologists Foundation, College Station, Texas, USA, 1197–1248.

Head, M.J., Riding, J.B., Eidvin, T., Andrew Chadwick, R. (2004) *Palynological and foraminiferal biostratigraphy of (Upper Pliocene) Nordland Group mudstones at Sleipner, northern North Sea*. Marine and Petroleum Geology 21, 277 – 297.

Head, M.J., Seidenkrantz, M.S., Janczyk-Kopikowa, Z., Marks, L., Gibbard, P.L. (2005) *Last interglacial (Eemian) hydrographic conditions in the southeastern Baltic Sea, NE Europe, based on dinoflagellate cysts.* Quaternary International, 130(1), 3 – 30.

Heusser, LE.. (1983). *Pollen distribution in the bottom sediments o[" the western North Atlantic Ocean.* Mar. Micropaleontol. s. 77 88.

Hijma, M.P., Cohen, K.M., Roebroeks, W., Westerhoff, W.E., Busschers, F.S. (2012) *Pleistocene Rhine-Thames landscapes: geological background for hominin occupation of the southern North Sea region.* Journal of Quaternary Science 27: 17 -39.

Houben, S. (2019) *Palyno- and magnetostratigraphic constraints and correlation of two sediment cores near the Pallas site in Petten, the Netherlandsi*. TNO report.

Huuse, M., Lykke-Andersen, H., Michelsen, O. (2001) *Cenozoic evolution of the eastern Danish North sea*. Marine Geology 177, 243 – 269.

Jeong, H.J. (1999) *The ecological roles of heterotrophic dinoflagellates in marine planktonic community*. J. Eukaryot, Microbiol, 46(4), 390 – 396.

Kooi, H., Hettema, M., Cloetingh, S. (1991) *Lithospheric dynamics and the rapid Pliocene-Quaternary subsidence phase in the southern North Sea basin*. Tectonophysics 192, 245 – 259.

Kotthoff, U., Greenwood, D. R., McCarthy, F. M. G., Müller-Navarra, K., Prader, S., & Hesselbo, S. P. (2014). *Late Eocene to middle Miocene (33 to 13 million years ago) vegetation and climate development on the North American Atlantic Coastal Plain* (IODP Expedition 313, Site M0027).

Kuhlmann, G., Pedersen, R.B., de Boer, P., Wong, T.E. (2004) *Provenance of Pliocene sediments and paleo-environmental change in the southern North Sea region using Sm/Nd (samarium-neodymium) provenance ages and clay mineralogy.* Sediment, Geol., 171, 205-226.

Kuhlmann, G., Langereis, C.G., Munsterman, D., van Leeuwen, R.-J., Verreussel, R., Meulenkamp, J.E., Wong, Th.E. (2006) *Integrated chronostratigraphy of the Pliocene-Pleistocene interval and its relation to the regional stratigraphical stages in the southern North Sea region*. Netherlands Journal of Geosciences, 85-1, 19-35.

Lamb, R.M., Huuse, M., Stewart, M. (2016) *Early Quaternary sedimentary processes and paleoenvironments in the Central North Sea*. Journal of Quaternary Science, 32(2). 127 – 144.

Lamb, R.M., Harding, R., Huuds, M., Stewart, M., Brocklehurst, S.H. (2018) *The early Quaternary North Sea Basin*. Journal of the Geological Society, 175 (2). 274 – 290.

Lang, G. (1994) *Quatäre Vegetationsgestichte Europas,* Gustav Fischer Verlag.

Lang, G. (2004) *Quartaire Vegetationsgeschichte Europas: Methoden und Ergebnisse.* G. Fischer, Jena.

Leroy, S.A.G. (2007) *Progress in palynology of the Gelasian-Calabrian stages in Europe: Ten messages*. Revue de micropaléontologie 50, 293 – 308.

Leroy, S.A.G., Arpe, K., Mikolajewicz, U. (2011) *Vegetation context and climatic limits of the Early Pleistocene hominin dispersal in Europe*. Quaternary Science Reviews 30, 1448 – 1463.

Lisiecki, L.E., Raymo, M.E. (2005) *A Pliocene-Pleistocene stack of 57 globally distributed benthic $\delta^{18}O$ records.* Paleoceanography, Vol. 20, PA 1003.

Maslin, M.A., Brierley, C.M. (2015) *The role of orbital forcing in the Early Middle Pleistocene Transition*. Quaternary International 289, 47 – 55.

McCarthy, F.M.G., Mudie, P.J. (1998) *Oceanic pollen transport and pollen: dinocyst ratios as markers of Late Cenozoic sea level change and sediment transport*. Paleogeography, Paleoclimatology, Paleoecology, 138, pp 187 -206.

McMillan, A.A., Hamblin, R.J.O., Merritt, J.W. (2005) *An overview of the lithostratigraphical framework for the Quaternary and Neogene deposits of Great Britain (onshore)*, Britisch Geological Survey Research Report, RR/04/04.

Meijer, T., Cleveringa, P., Munsterman, D.K., Verreussel, R.M.C.H. (2006) *The Early Pleistocene Praetiglian and Ludhamian pollen stages in the North Sea Basin and their relationship to the marine isotope record*. Journal of Quaternary Science 21(3), 307 – 310.

Mertens, K.N., Verhoeven, K., Verleye, T., Louwye, S., Amorim, A., Ribeiro, S., Deaf, A.S., Harding, I.C., de Schepper, S., González, C., Kodrans-Nsiah, M., de Vernal, A., Henry, M., Radi, T., Dybkjaer, K., Poulsen, N.E., Feist-Burkhardt, S., Chitolie, J., Heilmann-Clausen, C., Londeix, L., Turon, J., Marret, F., Matthiessen, J., McCarthy, F.M.G., Prasad, v., Pospelova, V., Kyffin Hughes, J.E., Riding, J.B., Rochon, A., Sangiorgi, F., Welters, N., Sinclair, N., Thun, C., Soliman, A., van Nieuwenhove, N., Vink, A., Young, M. (2009) *Determining the absolute abundance of dinoflagellate cysts in recent marine sediments: the Lycopodium marker-grain method put to the test*. Review of Paleobotany and Palynology 157, 238 – 252.

Miller, K., Mountain, G., Wright, J et al., (2011) *A 180 million year record of sea level and ice volume variations from continental margin and deep-sea isotopic records*. Oceanography 24, 40 - 53.

Miller-Rushing, A.J., Primack, R.B. (2008) *Effects of winter temperature on two birch (Betula) species*. Tree Physiology 28, 659 – 664.

Morzadec-Kerfourn, M.T. (1997) *Dinoflagellate cysts and the paleoenvironment of Late-Pliocene Early-Pleistocene deposits of Brittany, North-West France*. Quaternary Science Reviews, Vol. 16, pp 883-898.

Mudie, P.J., (1982). *Pollen distribution in recent marine sediments, Eastern Canada.* Can. J. Earth Sci. 19, 729 747.

Mudie, P.J. (1989) *Palynology and dinocyst biostratrigraphy of the Late Miocene to Pleistocene, Norwegian Sea: ODP Leg 104, Sites 642 to 644*. Proc, ODP Sci Results 104, 587 – 610.

Mudie, P.J., McCarthy, F.M.G., (1994). *Pollen transport processes in the western North Atlantic: evidence from crossmargin and north-south transects.* Mar. Geol. 118, 79 105.

Muller, J., (1959). *Palynology of Recent Orinoco Delta and shelf sediments*. Micropaleontology 5, 1 32

Noorbergen, L.J., Lourens, J.J., Munsterman, D.K et al., (2015) *Stable isotope stratigraphy of the early Quaternary of borehole Noordwijk, southern North Sea Quaternary.* Internationaal 386, 148 – 157.

Ottensen, D., Batchelor, C.L., Dowdeswell, J.A., Loseth, H. (2018) *Morphology of Quaternary sedimentation in the North Sea Basin (52 - 62°N)*. Marine and Petroleum Geology 98, 836-859.

Overeem, I., Weltje, G.J., Bishop-Kay, C., Kroonenberg, S.B. (2001) *The Late Cenozoic Eridanos delta system in the Southern North Sea Basin: a climate signal in sediment supply*. Basin Research, 13. 293-312.

Patrono, S., Scisciani, V., Helland-Hansen, W., D'Intino, N., Reid, W., Pellegrini, C. (2018) *Upslope-climbing shelf-edge clinoforms and the stepwise evolution of the northern European glaciations (lower Pleistocene Eridanos Delta system, U.K. North Sea): When sediment supply overwhelms accommodation*. Basin Research, 2019: 00: 1-16.

Pliura, A. (2004) *Possibilities for adaptations of Alnus glutinosa to changing environment*. Biologija, Nr. 1. P. 6 – 12.

Radi, T., de Vernal, A., (2008). *Dinocysts as proxy of primary productivity in mid–high latitudes of the Northern Hemisphere.* Mar. Micropaleontol. 68, 84–114.

Ranga Rao, A., Dayananda, C., Sarada, R., Shamala, T.R., Ravishankar, G.A. (2007) *Effect of salinity on growth of green alga Botryococcus braunii and its constituents*. Bioresource Technology 98, 560 – 564.

Rochon, A., De Vernal, A., (1994). *Palynomorph distribution in Recent sediments from the Labrador Sea*. Can. J. Earth Sci. 31, 115-127.

Rose, J. (2009) *Early and Middle Pleistocene landscapes of eastern England*. Proceedings of the Geologists, Assocation 120: 3 – 33.

Ruddiman, W.F. *Earth's climate: Past and Future*. W.H.Freeman & Co Ltd, 2014.

Sauer, Jonathan D. *Plant Migration: The Dynamics of Geographic Patterning in Seed Plant Species.* Berkeley: University of California Press, c1988 1988. http://ark.cdlib.org/ark:/13030/ft196n99v8/

Scott, D.B., Mudie, P.J., Vilks, P.J., Younger, D.C. (1984) *Latest Pleistocene Holocene paleoceanographc trends on the continental margin of eastern Canada: foraminiferal, dinoflagellate and pollen evidence*. Mar, Micropaleontol. 9. 181 – 218.

Stockmarr, J. (1971) *Tablets with spores used in absolute pollen analysis*. Pollen et spores 13, 615 – 621.

Starnberger, R., Drescher – Schneider, R., Reitner, J.M., Rodnight, H., Reimer, P.J., Spötl, C. (2013) *Late Pleistocene climate change and landscape dynamics in the Eastern Alps: the innter-alpine Unterangerberg record (Austria)*. Quaternary Science Review, May 15; 68; 17 – 42.

TNO (2013) Lithostratigrafische Nomenclator van de Ondiepe Ondergrond. Retrieved from www.dinoloket,nl/nomenclator

Van den Berghe, J., Kasse, C. (1989) *Periglacial environments during the Early Pleistocene in Southern Netherlands and Northern Belgium*. Paleogeography, Paleoclimatology, Paleoecology, 72, 133 – 139.

Van Nieuwenhove, N., Bauch, H.A., Matthiessen, J., (2008). *Last interglacial surface water conditions in the eastern Nordic seas inferred from dinocyst and foraminiferal assemblages*. Mar. Micropaleontol. 66, 247–263.

Verleye, T., Louwye, S., (2010*). Late Quaternary environmental changes and latitudinal shifts of the Antarctic Circumpolar Current as recorded by dinoflagellate cysts from offshore Chile (41°S)*. Quat. Sci. Rev. 29, 1025–1039

Versteegh, G.J.M. (1994) *Recognition of cyclic and non-cyclic changes in the Mediterranean Pleistocene a palynological approach*. Mar. Micropaleontol, 23, 147 – 183.

Westerhoff, W.E., (2009) *Stratigraphy and sedimentary evolution: The Lower Rhine-Meuse system during the Late Pliocene and Early Pleistocene (southern North Sea Basin).* Rotterdam: TNO Built Environment and Geosciences

Westerhoff, W.E., Cleveringa, P., Meijer, T., van Kolfschoten, T., Zagwijn, W.H. (1998) *The lower Pleistocene fluvial (clay) deposits in the Maalbeek pit near Tegelen, The Netherlands*. Mededelingen Nederlands Instituut voor Toegepaste Geowetenschappen TNO, Nr. 60.

Zagwijn, W.H. (1992) *The beginning of the ice age in Europe and its major subdivisions*. Quaternary Science Reviews, Vol. 11, pp 583 – 5991.

Zagwijn, W.H., (1957). *Vegetation, climate and time-correlations in the early Pleistocene of Europe*. Geologie en Mijnbouw 19, 233–244

Zagwijn, W.H., (1960). *Aspects of the Pliocene and early Pleistocene vegetation in The Netherlands*. Mededelingen van de Geologische Stichting, Serie C III-1–5, 1–78

Zagwijn, W.H., (1963). *Pollen-analytical investigations in the Tiglian of The Netherlands.* Mededelingen van de Geologische Stichting. Nieuwe Serie 16, 49–71.

Zonneveld, K.A.F. (1996) *Reconstruction of the last deglaciation (18 ka BP – 8 Ka BP) in the Adriatic Sea region: a land sea correlation based on palynological evidence.* Paleogeogr. Paleoclimatol, Paleoecol 122, 89 – 106.

Zonneveld, K.A.F., Marret, F., Versteegh, G.J.M., Bogus, K., Bonnet, S., Bouimearhan, I., Crouch, E., de Vernal, A., Elshanawany, R., Edwards, L., Esper, O., Forke, S., Grosfjeld, K., Henry, M., Holzwarth, U., Kielt, JF., Kim, SY., Ladouceur, S., Ledu, D., Chen, L., Limoges, A.,

Londeix, L., Lu, SH., Mahmoud, M.S., Marino, G., Matsouka, K., Matthiessen, J., Mildenhal, D.C., Mudie, P., Neil, H.L., Pospelova, V., Qi, Y., Radi, T., Richerol, T., Rochon, A., Snagiorgi, F., Solignac, s., Turon, JL., Verleye, T., Wang, Y., Wang, Z., Young, M. (2013) *Atlas of modern dinoflagellate cyst distribution based on 2405 data points*. Review of Palaeobotany and Palynology 191, 1- 197.

List with figures

Figures:

15. Absolute amount of Cyperaceae and Poaceae, presented together with the percentage of grasses and the T/M - ratio
16. Absolute amount of Dryopteris and Osmunda, presented with the percentage ferns and T/M - ratio
17. Absolute amount of Alnus, Betula and Quercus, presented with the T/M - ratio
18. Comparison water depth with T/M - ratio, absolute amount of cold, warm-temperate and heterotrophic conditions and percentage grasses and bisaccates
19. Upper part of the water depth indication, together with the T/M – ratio
20. Comparison between the percentage bisaccates and T/M - ratio
21. T/M - ratio together with the δ18O values of Lisiecki and Raymo (2005)
22. Presence of the pollen important for the subdivision of the Tiglian

Tables:

1. Division of the Pliocene and Pleistocene described by Zagwijn (1957,1960, 1963)
2. Subdivision Tiglian with corresponding pollen
3. Subdivision of the terrestrial palynomorphs
4. Subdivision of the dinoflagellate cysts
5. Summary of the mineralogical data
6. Peak indication of the absolute amount of dinoflagellate cysts
7. Indications of the absolute peaks for the Pediastrum and Botryococcus and Foraminifera
8. Peaks in the tree assemblages
9. Comparison physical, chemical and palynological information for the spikey grass pattern
10. Amount of Dryopteris found in the samples above the spikey grass peaks
11. Amount of pollen for every spikey grass peak observed in Figure 14
12. Indication of the temperature by the amount of dinoflagellate cysts
13. Amount of Fagus and Pterocarya

Appendix A: Sample numbers

Sample number	Depth (m)	Analyser	Sample number	Depth (m)	Analyser
	383.60	SHOU		285.60	SHOU
	378.90	SHOU		285.40	SHOU
4	378.20	LKR		283.65	SHOU
8	377.63	LKR		282.83	SHOU
7	375.65	LKR	17	280.85	LKR
	374.15	SHOU		278.35	SHOU
13	372.60	LKR	37	276.40	LKR
	372.10	SHOU		272.65	TDO
26	368.85	LKR		271.25	SHOU
	366.86			268.12	TDO
	365.65		41	267.50	LKR
	362.70		40	264.25	LKR
	358.30		18	263.82	LKR
	352.50			261.65	SHOU
5	349.50	LKR	**25**	**258.80**	**LKR**
6	347.05	LKR	**15**	**258.80**	**LKR**
	342.30	SHOU	12	256.60	LKR
	336.35	SHOU		256.55	TDO
	332.90	SHOU	21	250.00	LKR
	327.95	SHOU		249.30	SHOU
3	327.25	LKR	20	243.85	LKR
2	323.70	LKR	43	240.65	LKR
1	322.80	LKR	42	237.75	LKR
	322.45	SHOU	32	231.30	LKR
48	320.75	LKR		231.00	TDO
23	315.55	LKR	44	229.05	LKR
29	314.75	LKR		226.00	SHOU
	311.60	SHOU		222.45	TDO
10	310.05	LKR	24	221.20	LKR
47	309.30	LKR	33	220.00	LKR
28	308.95	LKR	45	216.45	LKR
	305.80	SHOU	35	208.70	LKR
11	304.90	LKR	34	204.60	LKR
	302.25	SHOU		204.40	SHOU
	301.50	SHOU	36	201.85	LKR
9	300.25	LKR	46	195.85	LKR
31	299.20	LKR		192.30	SHOU
30	298.80	LKR		183.40	SHOU
49	295.55	LKR		171.40	SHOU
22	293.00	LKR		163.90	SHOU
	292.90	SHOU		143.00	SHOU
	290.65	SHOU		133.40	SHOU
38	287.45	LKR		129.40	SHOU
39	286.05	LKR			

Appendix B: Rough data

Depth (m)	Abies	Acer	Alnus	Artemisia	Asteraceae	Betula	Carpinus	Carya	Caryophyllaceae	Chenopodiaceae	Corylus	Cyperaceae	Dryopteris	Ericales	Fagus	Fraxinus	Juglans	Juniperus	Liliaceae	Lycopodium spp.	Malvaceae	Nymphea	Nyssa	Osmunda	Ostrya	Picea	Picea reworked	Pilularia	Pinus	Pinus reworked	Pinus haploxylon type	Poaceae	Pteridium	Pterocarya	Quercus	Salix	Sphagnum	Succisa	Taxodium	Thalictrum	Trilete kemmerk indet	Tropische plant	Tilia	Tsuga	Ulmus	Urtica
201,85													4	1										1		3			2			3			1		2								1		
204,60			1			1				4	1			1												2						15			2											
208,70										1			4	2												1									1											
220,00			1		2	1			1		1		13	1										2		9			6								2						1			
221,20			1	2	2	2	3			1		7	21	24										3		39			34			10	3		2		7					11		2		
222,45			1		5						1	2	6	1										1		16			90		12	5	1				2					2				
226,00			1				2						8											2		13			50		1	6				11									
229,05			2										2	1																		2			1										
231,00			2			1	3						4	6										1		5			29		5	3			7		1						1		
231,30				1									5	3												1																			
237,75						2							2																			9													
240,65						1							17	1										1		3			1			5													
243,85	0	0	5	0	1	0	0	1	0	0	3	0	177	10	0	0	0							1	0	1			0			5			0	0	0					0	0	0	
249,30										2																0			3			59													
250,00			1	2		1				1			29	16			1	1						2		64			38			7			2							3			
256,55			30		3	2	1				1		88	13										2		4			20		2	12		3	2								1		
256,60			11	1	1	1	2		1			1	46	11										6		15			7			5			6		1					9			
258,80			1	1		4							2	2										1		3			3					1	2										
261,65			2		1		9				3	1	38	9										4		8			56			2		1	2		9	1			1				
263,82			3			4	6		1	1	1	3	21	20	1									4					2			5		1	6		4		1				1			
264,25			6	1	2	7				4	1		76	12										3		14			5			5			1		4								
267,50						2				2			8											2					1																
268,12			2	1		3	1						7	1										1		0			3			74		1	1		1								
271,25			4				5					4	32	7										3		6			72			4			1		2			1				
272,65			7				2					1	44	7										4		15			33		8	3	2	1	7		8			1		2		
276,40			1		2	2							89	31										15		45	9		26	14		4					9			5				
278,35			2			1		1	1	1	2	1	13	9									1	1		17			44		1				6		5							
282,83				1		1	1	1				1	7	3									1	1		2			8			1	1		1		5		3			3	1		
285,80			1	1		2						1	14	12										1		2			3			2												
286,05				1		1				1	1		14											1		5			3								2							
287,45				1		4			1		1		33	9										2		5			2			4			1		2							
290,65			3									1	4	1										1		0			5			33					2							
292,90			9		3	1						3	14	30										2		9			50		2	13					4		1		1	2		
293,00			5	2	3	2	1			1			21	38												30			10			4					2					1			
295,55			7			1					1		81	72										13		17			9			2			4		5							
299,20			2			3					1	1	41	37						2				16		30,5			49,5			1			1		9			1	2			
300,25					2	1	2			3		6	34	17						1	1			3		20			26			5			6		7			4				
301,50			7			1							33	11										2		3			10			2					9							
302,25			6	3								2	21	28										3		10			25		2	13					7							
304,90	0	0	7	3	0	5	4		0	1	2	7	37	34		0	0	2	1			3		9	0	29			26			6	0	0	5	0	3	1			0	7	0		
305,80			3			1					1	2	24	7										4		8			44			5			1		4							
308,95			4	1		3				1	1		23	21										8		14			15			1				1	7			1				
309,30			2			1							107	21										8		5			8			5			1		6							

310,05			3			1	3						34	27							1	3		8		10			11			3			2		4		1					3	1	
311,60			9	1	1	3							14	13										6		7			36			3			1		5		1					1		
314,75			2								2		4	7										5		1			3						4		1									
315,55			1		1		2			3			20	8										2		12			5						1		2							2		
320,75			1		3	1				2			32	101						2				15		6			9			1			1		16							1		
322,45			2			1							3	8												5			34			2					1									
322,80	0	0	2	2	7	2	5		0	0	1	0	25	62	0	0	0							1	0	14			42			7	0	0	4	0	4						0	4	0	
323,70	0	0	1	1	0	0	0		0	0	1	0	13	37	0	0	0							3	0	8			26			4	1	0	0	0	1						0	5	0	
327,25	0	0	3	2	1	1	0		0	0	0	2	59	23	0	0	0							4	0	23		1	31			3	0	0	4	0	1		1				0	5	0	
327,95			2	3			1				6		17	7	1									2		0			70		3	7					2		2					2	4	
332,90			4		1	2						4	5	8										2		12			58		4	1					1		1					1	1	
336,35			5	1	2	1	1					2	13	6	1											7			31		3	15			2		6		2					2	3	
342,30			3		1								2	13										1		18			67		7	3					6		2					2		
347,05	0	0	4	4	0	0	1		0	1	0	0	11	12	0	0	0							2	0	4			9			3	0	0	5	0	1						0	3	0	
352,50			1			1		2				3		30												15			51		4	7					9		1					1		
358,30					3	4					1	2	3	20										4		8			77		3	10			1		3		2					2		
362,70									1	1	2	2		11										1		6			56		6	9					7									
365,65			8		3	4						2	12	14										3		4			54			13					5		1					1	3	
368,65										1	3		6	1				1								2			2			3			1									2		
372,10			3	1	2				1	1		1	9	25										1		11			58			4			2		11									
372,60			3			1	3				2	10	79	22								2		25		21			22			5					9			2				4		
374,15			2		1								6	5												0			19		2	2					5									
375,65	0	1	5	2	0	2	7		0	2	6	0	14	28	0	0	0							0	1	11			26			7	0	5	20	0	0						0	0	0	
377,63	0	0	7	4	1	1	1		0	0	4	0	27	17	0	0	0	0						0	0	33			43			4	0	1	3	0	0						0	0	1	1
378,20			4			1	1		0	0	0	0	33	17	0	0	1	0						0	0	35			42			5	0	2	4	0	1			1			0	0	0	
378,90			9			3					2	2	1	13						1						23			30			4		1	1		1								1	
383,60			4		2	3			3	3		7	3	7												5			67		4	5	1				2									

Depth (m)	Foram	Botryococcus	Pediastrum	Broken forams	Arcitarch	Arcitarch 1	Arcitarch 2	Cymatiosphera	Glyptosperma	Depth (m)	Foram	Botryococcus	Pediastrum	Broken forams	Arcitarch	Arcitarch 1	Arcitarch 2	Cymatiosphera	Glyptosperma
201,85										314,75	3				8				
204,60	2									**315,55**	7			94	1				2
208,70	5									**320,75**	4				2				
220,00										322,45	37								
221,20	7	2	0		2					**322,80**	8	30	3	34	0	0	3	1	2
222,45										**323,70**	0	9	0	11	18	0	0	0	0
226,00	1	1								**327,25**	0	4	0	1	0	1	3	0	0
229,05										327,95	1	1							
231,00										332,90	3		2						
231,30										336,35			3	2					
237,75										342,30	1								
240,65					1					**347,05**	0	0	0	1	1	0	1	0	0
243,85	0	0	0	0	0	0	0	0	0	352,50		2	1						
249,30										358,30		2							
250,00	1	5	2	0		1				362,70		1							
256,55										365,65			1	1					
256,60		3								368,65									
258,80			1							372,10									
261,65				1						**372,60**	3				2				
263,82										374,15	7			20					
264,25					3					**375,65**	0	9	1	7	7	0	0	1	0
267,50										**377,63**	0	8	1	35	0	1	4	1	0
268,12										**378,20**	0	7	0	7	0	0	7	4	4
271,25	1	1		1						378,90		1	1	4					
272,65	5		3							383,60				3					
276,40	4		1		7					378,90									
278,35	1									383,60									
282,83																			
285,80	1				6														
286,05	7																		
287,45	5				2														
290,65																			
292,90		1			4														
293,00	2																		
295,55	1				4														
299,20	9		1		19														
300,25	3	11	3	4		2	3	1	1										
301,50	1	1	4	5															
302,25	3																		
304,90	5	7	1	8	0	1	0	2	0										
305,80		1																	
308,95	13																		
309,30	16																		
310,05	6	1			2														
311,60	5																		

Appendix C: Equations

$$Bisaccates = Abies + Picea + Pinus\ haploxylone\ type + Pinus$$

$$\%Grasses = \frac{(Cyperaceae + Poaceae)}{Total\ sporomorph - bisaccates} * 100$$

$$\%Herbs = \frac{\begin{matrix}(Artemisia + Asteraceae + Caryophyllaceae + Chenopodiaceae \\ +Liliaceae + \\ Malvaceae + Nymphea + Succisia + Thalictrum + Urtica)\end{matrix}}{Total\ sporomorph - bisaccates} * 100$$

$$\%Ferns = \frac{(Dryopteris + Lycopodium\ spp. + Osmunda + Pilularia + Pteridium)}{Total\ sporomorph - bisaccates} * 100$$

$$\%Deciduous\ trees = \frac{\begin{matrix}(Acer + Alnus + Betula + Carpinus + Carya + Corylus + \\ Fagus + Fraxinus + \\ Juglans + Nyssa + Ostrya \\ + Pterocarya + Quercus + Salix + Tilia + Ulmus)\end{matrix}}{Total\ sporomorph - bisaccates} * 100$$

$$\%Habibacysta/Filisphaera\ cpx = \frac{\begin{matrix}(Bitectadonium\ tepikiensis + Filisphaera\ cf \\ + Filisphaera\ spp. + Habibacysta\ spp.\end{matrix}}{Total\ amount\ of\ dinocysts} * 100$$

$$\%Protoperidiniaceae = \frac{(Brigantedinium\ spp. + Selenopemphix\ brevispinosum)}{Total\ amount\ of\ dinocysts} * 100$$

$$\%Polysphaeridium = \frac{Polysphaeridium\ zoharyi}{Total\ amount\ of\ dinocysts} * 100$$

$$\%Spiniferites\ cpx = \frac{(Achomosphaera\ andalousiensis + Spiniferites\ cpx)}{Total\ amount\ of\ dinocysts} * 100$$

$$\%Other\ dinos = \frac{\begin{matrix}(Dino\ indet + Dino\ indet\ cold + Dino\ indet\ warm + \\ Lingolodinium\ machaeophorum + Operculodinium \\ centrocarpum + Operculodinium\ eirikianum + \\ Operculodinium\ tegillatum)\end{matrix}}{Total\ amount\ of\ dinocysts} * 100$$

Appendix D: Weight of the samples

Depth (m)	$D_{c\ (marinel)}$	$D_{c\ (terrestrial)}$	L_t	L_C	W (g)
201,85	4	18	19855	376	10,4617
204,60	0	27	19855	205	10,7037
208,70	0	29	19855	207	10,3005
220,00	0	40	19855	609	10,0743
221,20	9	171	19855	87	10,0975
229,05	0	8	19855	306	9,9952
231,30	0	10	19855	203	10,1754
237,75	0	13	19855	71	9,7359
240,65	0	29	19855	235	10,3125
243,85	0	204	19855	153	10,0949
250,00	10	171	19855	135	10,4373
256,60	2	124	19855	228	10,0000
258,80	0	20	19855	335	9,6334
263,82	1	85	19855	20	10,4547
264,25	0	141	19855	594	10,3171
267,50	0	16	19855	155	9,9082
276,50	9	261	19855	151	9,8999
285,80	0	38	19855	429	10,2345
286,05	0	29	19855	162	10,5605
287,45	0	64	19855	225	9,738
295,55	2	212	19855	24	9,7887
299,20	11	196	19855	80	10,6218
300,25	23	137	19855	60	10,0000
304,90	21	192	19855	203	10,0000
308,95	5	101	19855	421	10,1739
309,30	5	164	19855	269	9,9513
310,05	14	114	19855	186	10,0000
314,75	28	29	19855	517	9,7807
315,55	11	59	19855	340	10,1908
320,75	6	191	19855	16	10,2151
322,80	145	182	19855	178	10,0000
323,70	83	100	19855	108	10,0000
327,25	37	164	19855	61	10,0000
347,05	1	59	19855	699	10,0000
368,65	0	22	19855	366	10,2184
375,65	21	137	19855	72	10,0000
377,63	32	148	19855	430	10,0200
378,20	25	147	19855	225	10,0000

Appendix E: Absolute amount

Depth (m)	Absolute terrestrial concentration	Absolute marine concentration	Absolute Pediastrum	Absoluto Botryococcus	Absolute Foraminifera	Absolute concentration cold conditions	Absolute concentration warm - temperate conditions	Absolute conditions heterotrophic conditions
195,85	0,47	0	0	0	0	0	0	0
201,85	0,91	0,2	0	0	0	0	0	0
204,60	2,44	0	0	0	18,1	0	0	0
208,70	2,7	0	0	0	46,56	0	0	0
216,45	0,59	0	0	0	0	0	0	0
220,00	1,29	0	0	0	0	0	0	0
221,20	38,6	2,03	0	45,2	158,2	22,6	22,6	0
229,05	0,52	0	0	0	0	0	0	0
231,30	0,96	0	0	0	0	0	0	0
237,75	3,73	0	0	0	0	0	0	0
240,65	2,38	0	0	0	0	0	0	0
243,85	26,2	0	0	0	0	0	0	0
250,00	24,1	1,41	28,18	70,46	14,09	42,27	42,27	14,09
256,60	10,6	0,17	0	25,72	0	0	0	0
258,80	1,23	0	6,152	0	0	0	0	0
263,82	80,7	0,95	0	0	0	0	0	0
264,25	4,57	0	0	0	0	0	0	0
267,50	2,07	0	0	0	0	0	0	0
276,40	34,7	1,2	13,28	0	53,13	0	26,56	0
285,80	1,72	0	0	0	4,522	0	0	0
286,05	3,37	0	0	0	81,24	0	0	0
287,45	5,8	0	0	0	45,31	0	0	0
293,00	7,21	0,84	0	0	12,01	30,03	0	0
295,55	179	1,69	0	0	84,51	84,51	84,51	0
299,20	45,8	2,57	23,37	0	210,3	0	93,46	0
300,25	43,6	7,31	95,37	349,7	222,5	413,3	63,58	0
304,90	18,4	2,01	9,572	67	124,4	86,15	9,572	0
308,95	4,68	0,23	0	0	60,26	13,91	4,636	0
309,30	12,2	0,37	0	0	118,7	7,417	7,417	0
310,05	12,1	1,49	0	10,63	63,81	74,44	53,17	0
314,75	1,14	1,1	0	0	11,78	3,927	47,12	0
315,55	3,38	0,63	0	0	578,8	0	17,19	0
320,75	232	7,29	0	0	485,9	0	607,4	0
322,80	20,1	16	33,2	332	464,8	177,1	575,5	11,07
323,70	18,4	15,2	0	165,2	201,9	275,4	587,4	18,36
327,25	51,9	11,7	0	126,6	0	158,3	379,8	31,65

347,05	1,63	0,03	0	0	2,767	0	0	0
368,65	1,17	0	0	0	0	0	0	0
372,60	34,4	0,98	0	0	49,18	65,58	16,39	0
375,65	37,9	5,81	27,67	249,1	193,7	55,34	276,7	0
377,63	6,82	1,47	4,608	36,87	161,3	46,08	13,82	4,608
378,20	12,7	2,16	0	60,48	60,48	69,11	60,48	0

- *Absolute amount is divided by 100*

Appendix F: Terrestrial / Marine – ratio

Depth (m)	Sporomorph	Dinocyst	Total sporomorph + dinocyst	T/M ratio	M/T ratio	Depth (m)	Sporomorph	Dinocyst	Total sporomorph + dinocyst	T/M ratio	M/T ratio
201,85	13	4	17	0,7647	0,2353	308,95	72	5	77	0,9351	0,06494
204,60	25	0	25	1	0	309,30	151	5	156	0,9679	0,03205
208,70	26	0	26	1	0	**310,05**	94	14	108	0,8704	0,12963
220,00	25	0	25	1	0	311,60	58	14	72	0,8056	0,19444
221,20	99	9	108	0,9167	0,0833	314,75	25	28	53	0,4717	0,5283
222,45	29	3	32	0,9063	0,0938	**315,55**	42	11	53	0,7925	0,20755
226,00	30	9	39	0,7692	0,2308	**320,75**	176	6	182	0,967	0,03297
229,05	8	0	8	1	0	322,45	17	54	71	0,2394	0,76056
231,00	29	0	29	1	0	**322,80**	126	145	271	0,4649	0,53506
231,30	9	0	9	1	0	**323,70**	67	83	150	0,4467	0,55333
237,75	13	0	13	1	0	**327,25**	110	37	147	0,7483	0,2517
240,65	25	0	25	1	0	327,95	56	24	80	0,7	0,3
243,85	203	0	203	1	0	332,90	31	22	53	0,5849	0,41509
249,30	61	0	61	1	0	336,35	62	13	75	0,8267	0,17333
250,00	69	10	79	0,8734	0,1266	342,30	33	13	46	0,7174	0,28261
256,55	162	0	162	1	0	**347,05**	47	1	48	0,9792	0,02083
256,60	102	2	104	0,9808	0,0192	352,50	55	15	70	0,7857	0,21429
258,80	14	0	14	1	0	358,30	55	26	81	0,679	0,32099
261,65	83	10	93	0,8925	0,1075	362,70	34	16	50	0,68	0,32
263,82	83	1	84	0,9881	0,0119	365,65	69	8	77	0,8961	0,1039
264,25	122	0	122	1	0	367,50	15	0	15	1	0
268,12	93	1	94	0,9894	0,0106	368,65	18	0	18	1	0
271,25	65	13	78	0,8333	0,1667	372,10	61	10	71	0,8592	0,14085
272,60	167	6	173	0,9653	0,0347	374,15	21	73	94	0,2234	0,7766
272,65	90	21	111	0,8108	0,1892	**375,65**	100	21	121	0,8264	0,17355
276,40	167	9	176	0,9489	0,0511	**377,63**	72	32	104	0,6923	0,30769
278,35	44	9	53	0,8302	0,1698	**378,20**	70	25	95	0,7368	0,26316
282,83	31	6	37	0,8378	0,1622	378,90	39	24	63	0,619	0,38095
285,80	33	0	33	1	0	383,60	40	41	81	0,4938	0,50617
286,05	21	0	21	1	0						
287,45	57	0	57	1	0						
290,65	45	2	47	0,9574	0,0426						
292,90	83	12	95	0,8737	0,1263						
293,00	80	14	94	0,8511	0,1489						
295,55	186	2	188	0,9894	0,0106						
299,20	116	11	127	0,9134	0,0866						
300,25	92	23	115	0,8	0,2						
301,50	65	1	66	0,9848	0,0152						
302,25	83	11	94	0,883	0,117						
304,90	137	21	158	0,8671	0,1329						
305,80	52	14	66	0,7879	0,2121						

Appendix G: Mineralogical data

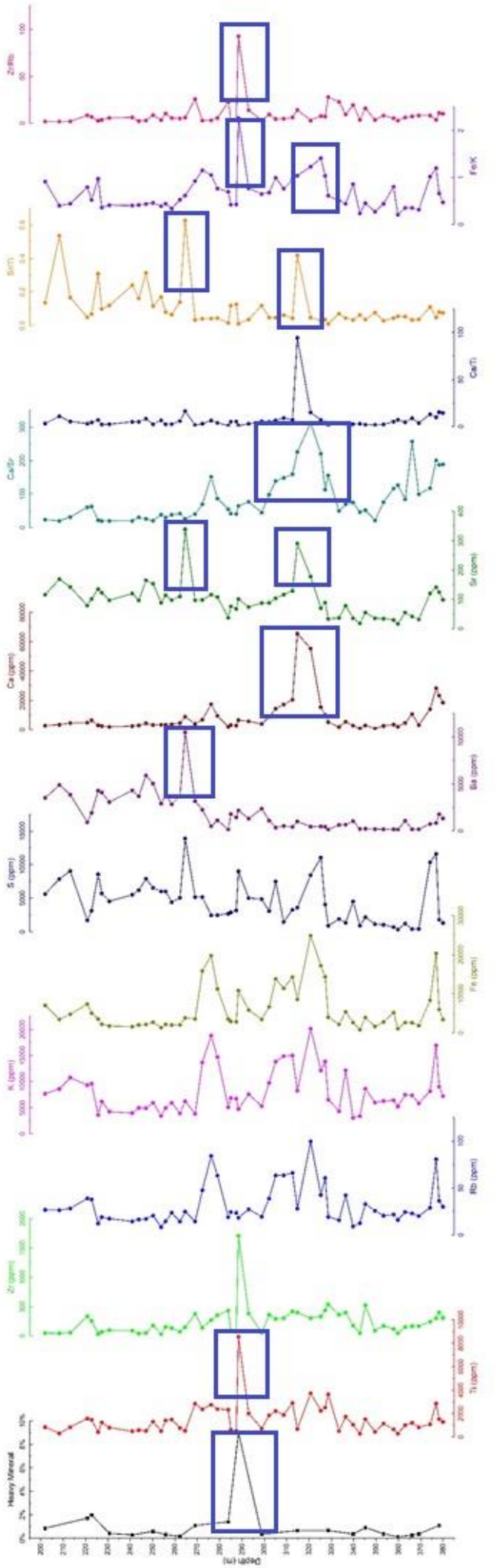

Appendix H: Tree assemblage

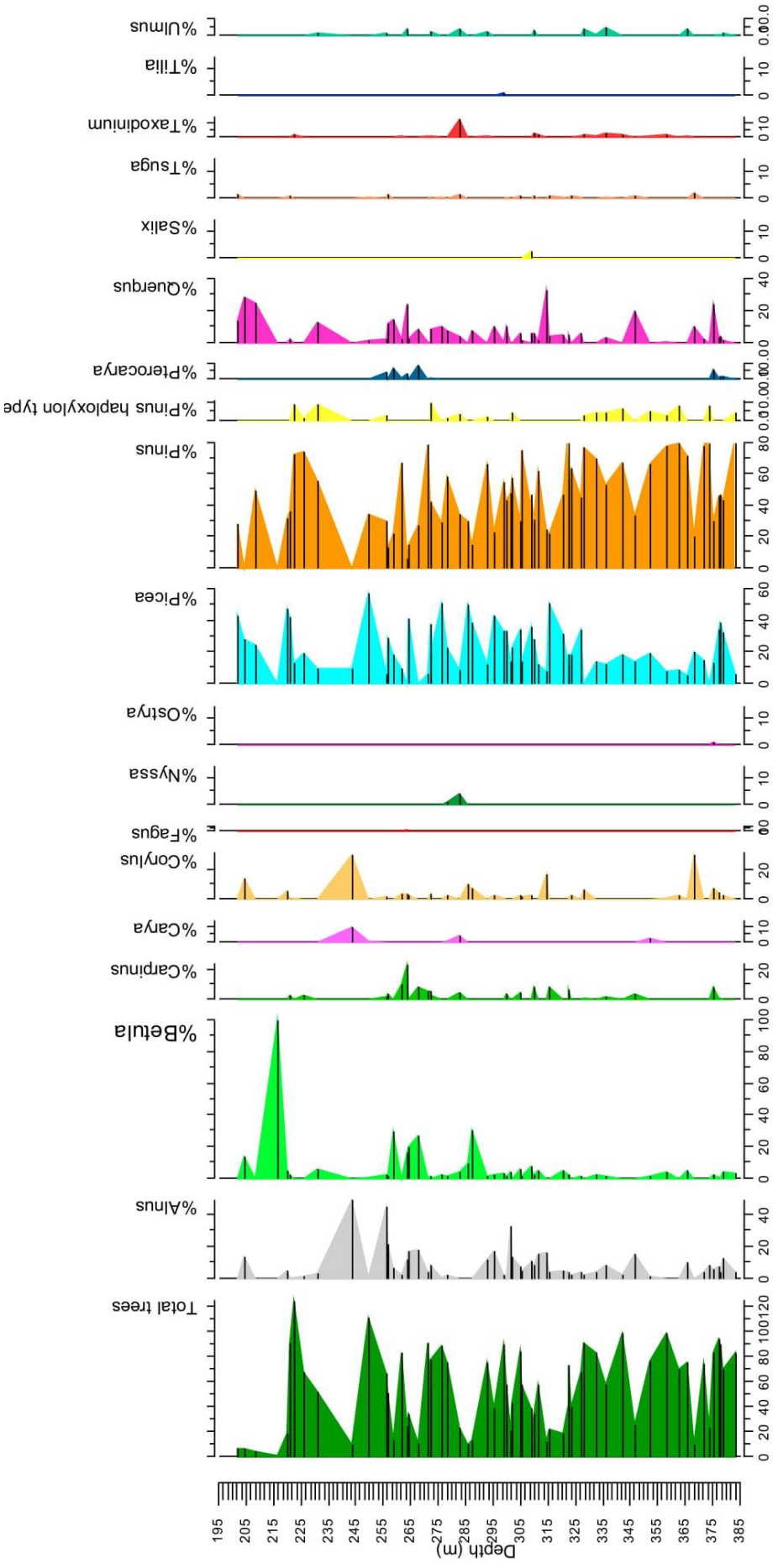

Appendix I: Reworked dinoflagellates

Species	Depth (m)	Amount
Areosphaerdium *diktyoplokum* (Paleogene)	352.50 365.65	1 2
Callialasporites (Jura)	221.20 285.80 327.25	1 1 1
Cerebrocysta spp. (Paleogene)	221.20	1
Cerebropollenites spp. (Mesozoic)	352.50	1
Cereodinium spp. (Cretaceous – Paleogene)	358.30	1
Chiropteridium spp. (Oligocene)	276.40 302.25 311.60 336.35	1 1 1 1
Classopollis spp. (Mesozoic)	222.45 276.65 336.35 342,30 358,30 372,10	2 1 3 2 1 2
Cleistosphaeridium *placacanthum* (Paleogene – Neogene)	221,20	1
Cordosphaeridium spp. (Paleogene)	221,20 226,00 278,35 342,30 352,50 362,70 365,65	1 1 1 2 2 1 1
Cordosphaeridium *fibrospinosum* (Paleogene)	327,25	1
Crassispora *kosankei* (Carboniferous)	221,20	1
Cribroperidinium spp. (Paleogene)	332,90 362,70	1 1
Denospora spp. (Carboniferous)	322,80	1
Dracodinium (Paleogene)	327,25	1
Diphyes (Paleogene)	276,40 327,25	3 1
Eocene dino	276,40 304,90 314,75	1 1 1
Deflandrea spp. (Paleogene)	272,65 332,90 358,30	1 1 2
Distatodinium *ellipticum* (Paleogene)	352,50	2
Distatodinium *paradoxum* (Paleogene)	322,45	1
Enneadocysta *arcuata* (Paleogene)	322,45	1
Glaphyrocysta spp. (Paleogene)	322,45	1
Heteraulacacysta porosa (Paleogene)	332,90	1
Homotrybilium (Paleogene)	221,20 314,75 327,25	1 1 1

	377,63 378,20	1 3
Hystrichokolporna *rigaudiae* (Paleogene – Neogene)	231,00 258,80 327,25 336,35 342,30 362,70 378,90	1 1 1 1 1 1 1
Lejeunecysta (*Protoperidinium*)	327,25	1
Melitasphaeridium *choanophorum* (Paleogene – Neogene)	327,95 332,90 352,50	1 1 1
Michrystridium (Paleozoic – Cenozoic)	322,80 383,60	1 1
Nannoceratopsis spp. (Jurassic)	352,50	1
Oligocene/Miocene dinoflagellate cyst	327,25	1
Pentadinium spp. (Paleogene)	278,35 302,25	1 1
Prasinophyte (Jurassic)	221,20	1
Pterospermella (Likely Jurassic)	221,20	2
Spiniferities pseudo furaactus	327,25	1
Subtilisphaera spp. (Jurassic)	365,65	1
Surculosphaeridium spp. (Jurassic)	365,65	1
Systematophora ancyrea (Paleogene)	221,20 271,25 278,35 301,50 311,60 327,25 332,90 336,36 342,30 352,50 358,30 362,70	1 1 2 1 1 2 3 1 2 2 1 4
Tasmanites	221,20 322,80 336,35 342,30 352,50 383,60	1 1 1 1 1 1
Wetzeliella cpx (Paleogene)	276,40 304,90 347,05	1 1 1

Appendix J: Dinoflagellate cysts data

Depth (m)	*Achomosphaera andalousiensis* group	*Amiculosphaera umbracula*	*Bitectatodinium tepikiensis*	Brigantedinium spp.	Dino indet	Dino indet cold	Dino indet warm	*Filisphaera* cf	*Filisphaera* spp.	*Habibacysta* spp.	*Lingulodinium machaeophorum*	*Operculodinium centrocarpum*	*Operculodinium eirikianum*	*Operculodinium israelianum*	*Operculodinium tegillatum*	*Polysphaeridium zoharyi*	*Protoperidinium* cpx	*Selenopemphix brevispinosum*	*Spiniferites* spp.
201,85																			4
204,60																			
208,70																			
220,00																			
221,20			1											1					7
222,45																			3
226,00									1										8
229,05																			
231,00																			
231,30																			
237,75																			
240,65																			
243,85																			
249,30																			
250,00	**2**					**2**				**3**				**1**			**1**	**1**	
256,55																			
256,60																			2
258,80																			
261,65				8					1					1					
263,82																			1
264,25																			
267,50																			
268,12																			1
271,25				8						1		1		1					2
272,65				6					3					1			6		5
276,40	1													1					7
278,35										3				3					3
282,83			1						1										4
285,80																			
286,05																			
287,45																			
290,65																			2
292,90	1			1					5	2									3
293,00			3							2									9
295,55			1											1					
299,20	1		2											3					5
300,25	2					1				11						4			5

301,50																			1
302,25				1						3				3		1			3
304,90	1	2			4	4				9									1
305,80	3			2					3			1		1					4
308,95	1		3																1
309,30										1				1					3
310,05	3	1								7				2					1
311,60										2				2			2		8
314,75	8		1											4					15
315,55	2			1										1					7
320,75	2													3					1
322,45									3	2				5		5	18		21
322,80	25	1		7	4	3			2	14	1	2		24		20	1		41
323,70	13							4	6	5				19		3	1		32
327,25	7	1		6	3	4				5	1			4			1	1	4
327,95	4			2					2	12				3					1
332,90				2						4				7		1			8
336,35				2						6				2					3
342,30				2								1		1					9
347,05						1													0
352,50									1	2									12
358,30	1		1	5					1	7									11
362,70				2					2	9									3
365,65				1						1		3		1					2
368,65																			
372,10			1							2				6					1
372,60										4				1					1
374,15	10		6	3						3		2		40					9
375,65							1			2				10		3			5
377,63	1			6	2	6				10				2		3	1		1
378,20	1			3	2	1			3	5				6		2			2
378,90				2					5	9				6					2
383,60		4		3										21		4			9

Appendix K: Pollen diagram

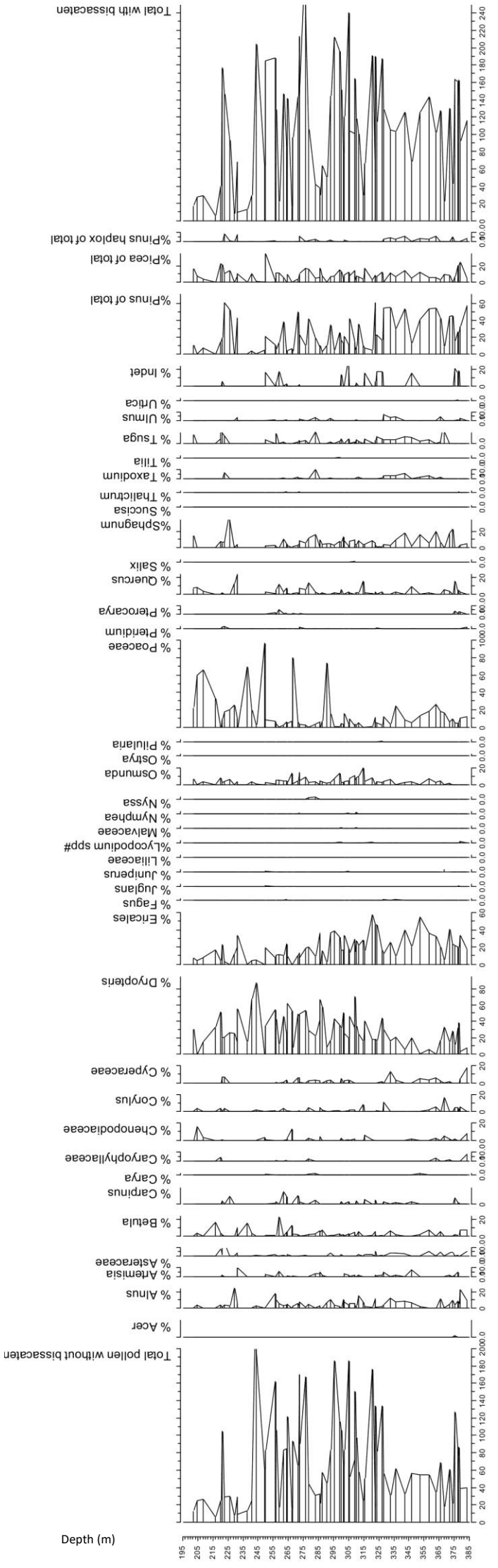

Appendix L: Pictures pollen and spores

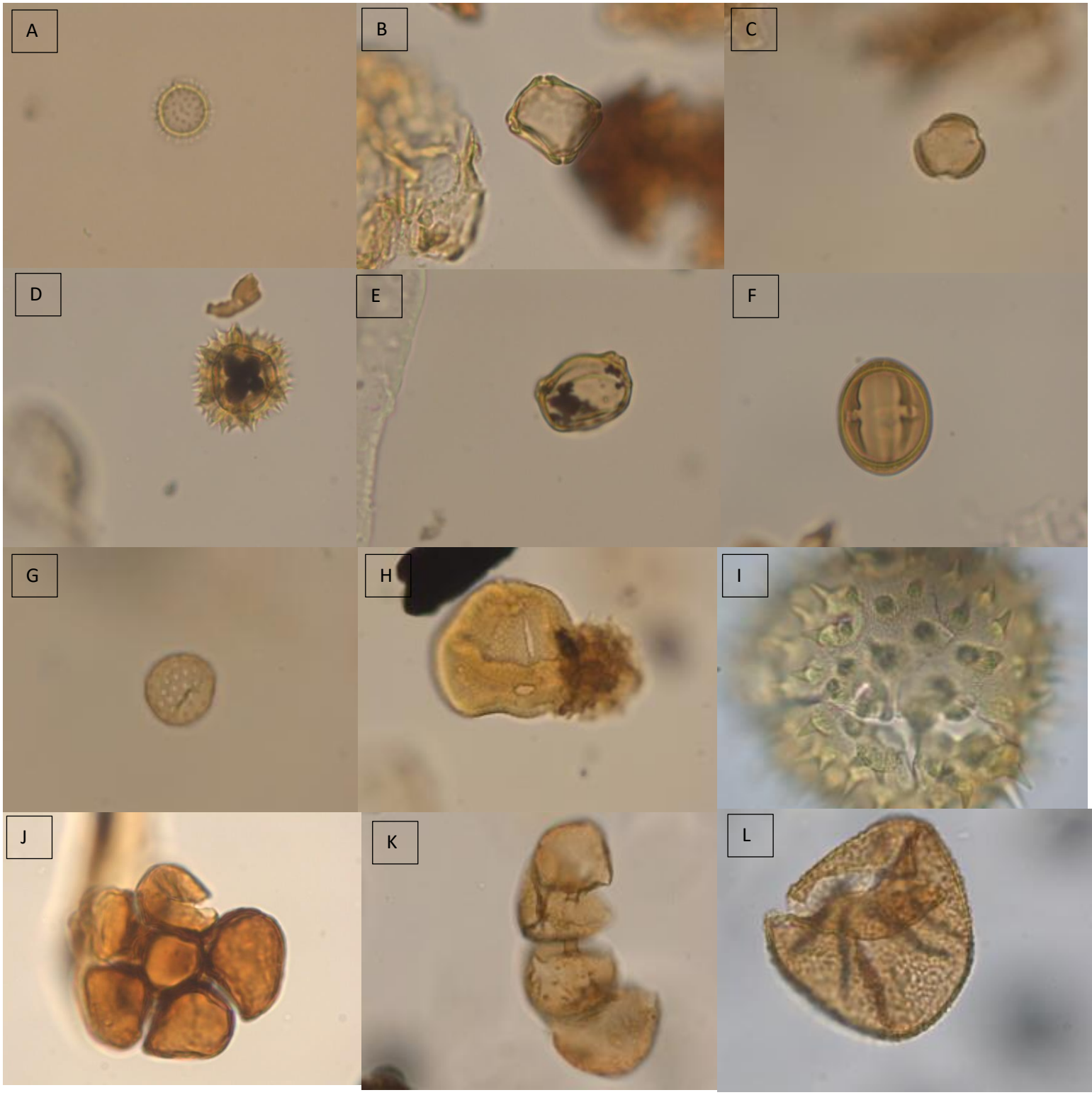

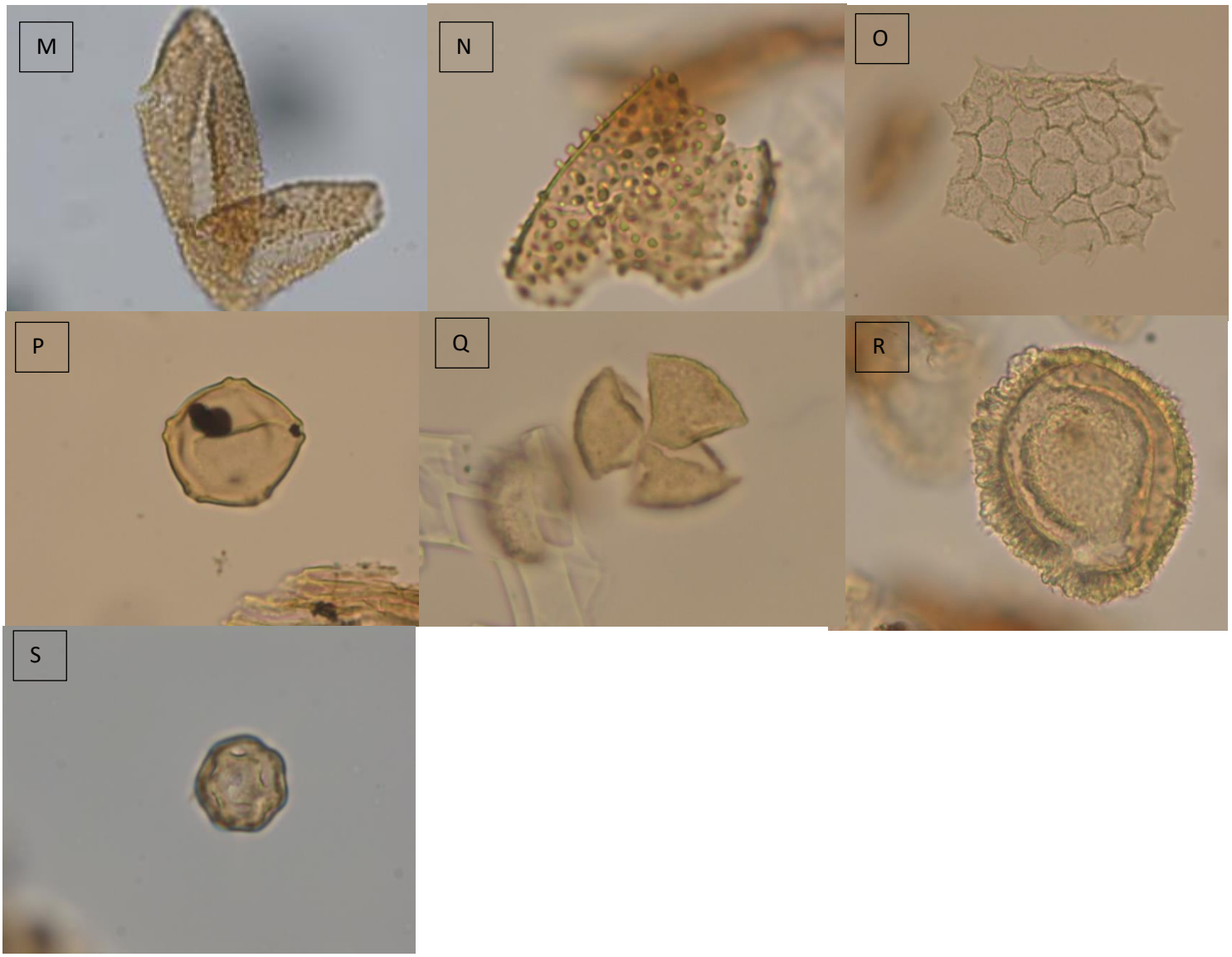

A) Arcitarch; B) *Alnus*; C) *Artemisia*; D) *Asteraceae*; E) *Betula*; F) *Centaurea*; G) *Chenopodiaceae*; H) Foraminifera; I) *Malvaceae*; J) Organic lining of benthic foraminifera; K) Organic lining of benthic foraminifera; L/M/N) *Osmunda*; O) Pediastrum; P) *Pterocarya*; Q) *Quercus*; R) *Tsuga*; S) *Thalictrum*

Appendix M: Pictures of dinoflagellate cysts

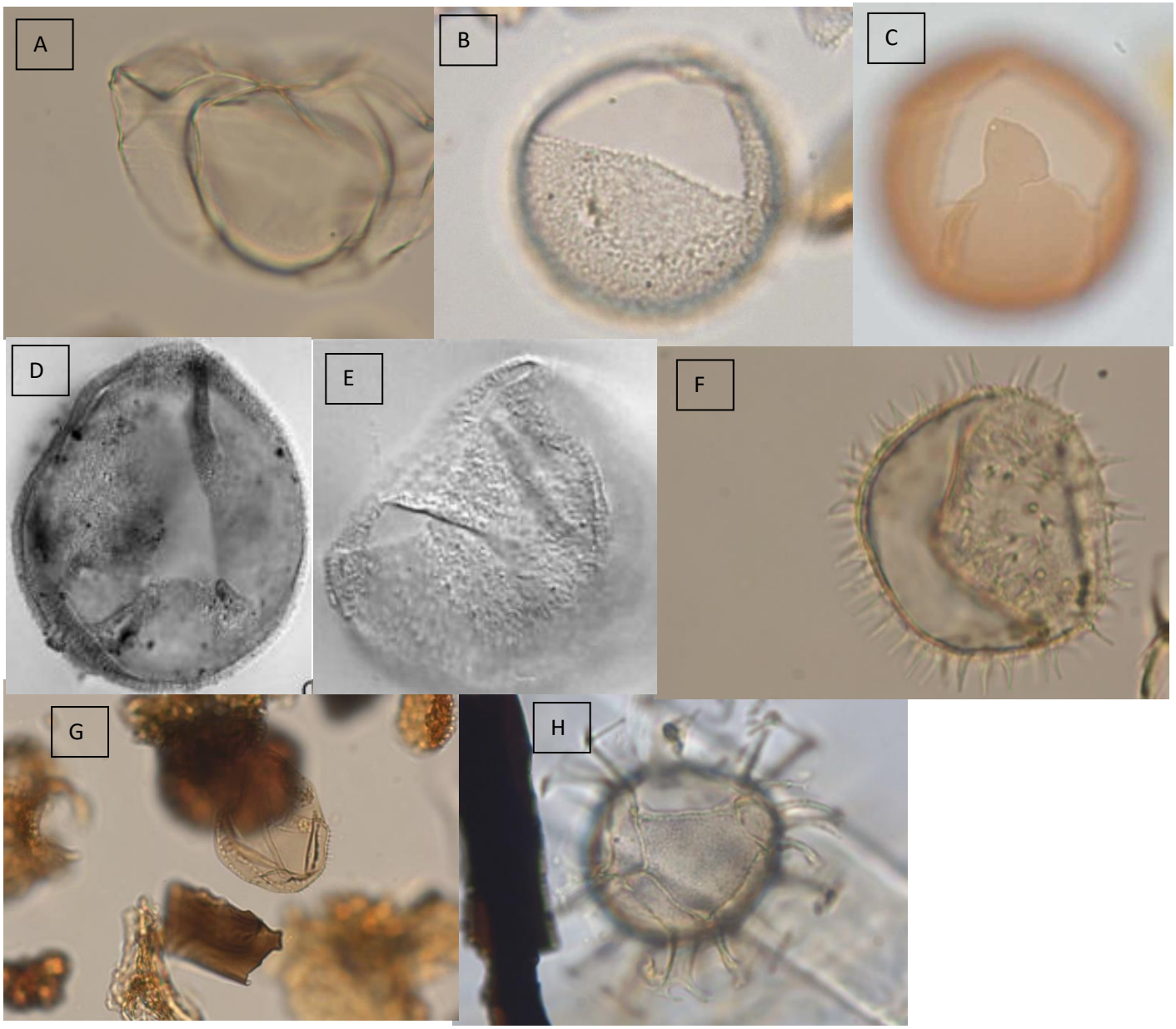

A) *A. umbracula*; B) *Bitectatodinium tepikiensis*; C) *Brigantedinium* spp.,; D) *Filisphaera* spp., (Head et al., 2004); E) *Habibacysta* spp., (Head et al., 2004); F) *O. israelianum*; G) *Selenopemphix selenoides*/*Brevispinosium*; H) *Spiniferites* spp.

Appendix N: Pictures of reworked material

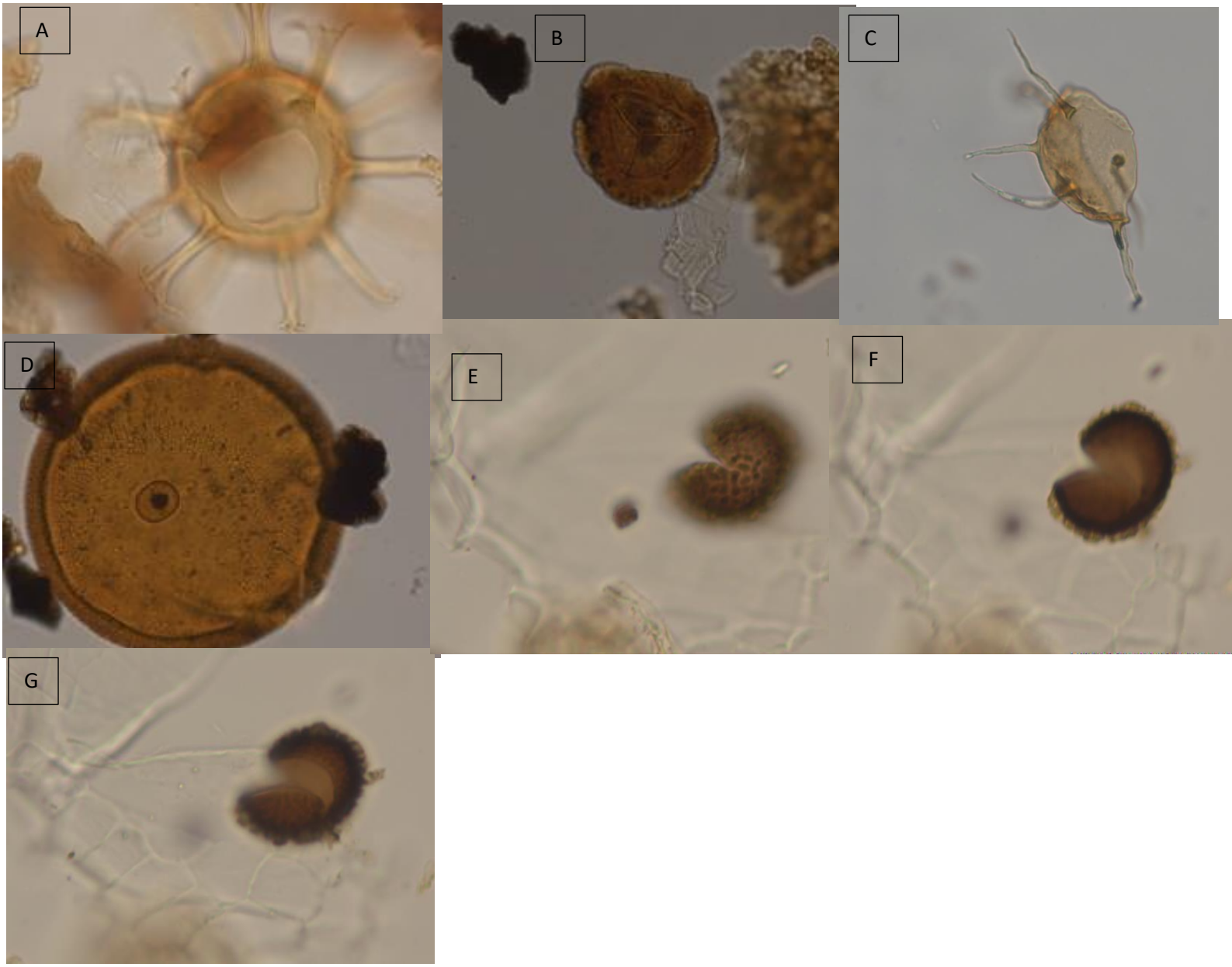

A) *Cordosphaeridium fibrospinosum*; B) Denospora spore (Carboniferous); C) Michrystridium (reworked acritarch); D) Likely reworked Tasmanites spp.; E/F/G) Unknown